

**SIMULATION AIDED INVESTIGATIONS ON NON-COAL
APPLICATIONS OF HEAVY MEDIUM CYCLONE**

**AĞIR ORTAM SİKLONLARININ KÖMÜR DIŐI
UYGULAMALARININ SİMÜLASYON YARDIMIYLA
İNCELENMESİ**

AHAD AGHLMANDI HARZANAGH

PROF. DR. ŐEVKET LEVENT ERGÜN

Supervisor

Submitted to Institute of Science of Hacettepe University
as a Partial Fulfilment to the Requirements
for the Award of Degree of Master of Science
in MINING ENGINEERING

2014

This worked named “**SIMULATION AIDED INVESTIGATIONS ON NON-COAL APPLICATIONS OF HEAVY MEDIUM CYCLONE**” by **AHAD AGHLMANDI HARZANAGH** has been approved as a thesis for the Degree of **MASTER OF SCIENCE IN MINING ENGINEERING** by the below mentioned Examining Committee Members.

Prof. Dr. M. Ümit ATALAY

Head

.....

Prof. Dr. Ş. Levent ERGÜN

Supervisor

.....

Prof. Dr. Özcan GÜLSOY

Member

.....

Assist. Prof. Dr. N. Metin CAN

Member

.....

Dr. E. Caner. ORHAN

Member

.....

This Thesis has been approved as a thesis for the Degree of **MASTER OF SCIENCE IN MINING ENGINEERING** by Board of Directors of the Institute for Graduated Student in Science and Engineering.

Prof. Dr. Fatma SEVİN DÜZ

Director of the Institute of
Graduate Studies in Science

ETHICS

In this thesis study, prepared in according with the spelling rules of the Institute of Graduate Studies in Science of Hacettepe University,

I declare that

- All the information and documents have been obtained in the base of the academic rules
- All audio-visual and written information and results have been presented according to the rules of scientific ethics
- In case of using others Works, related studies have been cited in accordance whit the scientific standards
- All cited studies have been fully referenced
- I did not do any distortion in the data set
- And any part of this thesis has not been presented as another thesis study at this or any other university.

18/07/2014

AHAD AGHLMANDI HARZANAGH

ABSTRACT

SIMULATION AIDED INVESTIGATIONS ON NON-COAL APPLICATIONS OF HEAVY MEDIUM CYCLONE

Ahad Aghlmandi Harzanagh

Master of Science, Department of Mining Engineering

Supervisor: Prof. Dr. Ş. Levent Ergün

July 2014, 119 pages

The aim of the thesis is to investigate the possibility of using heavy medium cyclone separation method for the concentration of problematic ores, of which the enrichment is difficult using other gravity methods like jigs and shaking tables. Samples of iron, manganese, zinc and chromite ores were selected and after determining physical and mineralogical properties of the samples, all of them were prepared in appropriate size fractions for sink-float tests. Combination of sodium polytungstate (SPT) and tungsten carbide powder (TC) were used to prepare a non-toxic heavy suspension with up to 3.5 gr/cm³ density.

Using sink-float test results and existing empirical models for high density HMC plants, simulations were performed. The results of the simulations showed that:

For the -9.5+0.5mm iron ore, a concentrate having 55% Fe was obtained with 80% Fe recovery. Separation density was 3.1 gr/cm³.

For the -16+0.5mm manganese ore, a concentrate having 38% Mn was obtained with 92% Mn recovery. Separation density was 2.9 gr/cm³.

For the -1.8+0.2 mm chromite ore, a concentrate having 45% Cr₂O₃ was obtained with 52% Cr₂O₃ recovery. Separation density was 3.5 gr/cm³. It seems that low degree of liberation is the major reason for low recovery.

Finally, using the data for iron ore, the process flowsheet including drain and rinse screens, magnetic separator etc. was developed and the dimensions of all equipment were calculated.

Keywords: Heavy medium cyclone, ferrosilicon, heavy liquid, simulation, iron ore, manganese ore, chromite ore.

ÖZET

AĞIR ORTAM SIKLONLARININ KÖMÜR DIŐI UYGULAMALARININ SİMÜLASYON YARDIMIYLA İNCELENMESİ

Ahad Aghlmandi Harzanagh

Yüksek lisans, Maden Mühendisliđi Bölümü

Tez danışmanı: Prof. Dr. Ő. Levent Ergün

Temmuz 2014, 119 sayfa

Ađır ortam siklonları 1950'lerin baŐında geliŐtirilmiŐ ve günümüzde kömür hazırlamada en yaygın olarak kullanılan yüksek verimli zenginleŐtirme ekipmanlarıdır. Ađır ortam siklonlarında basınçla yapılan beslemeyle sađlanan merkezkaç kuvvetinin yardımıyla ince tanelerin verimli olarak ayrıŐmasını sađlamaktadır. Ađır ortam oluŐturmak üzere 1.9 g/cm^3 'e kadar kömür uygulamalarında manyetit ve 2.6 g/cm^3 'ün üzerindeki yođunluklarda ferrosilikon, bunların arasında ferrosilikon - manyetit karıŐımı kullanılmaktadır.

Türkiye'de ađır ortam siklonları kömür yıkamada yaygın olarak uygulanmasına rađmen, kömür dıŐındaki minerallerin zenginleŐtirmesinde herhangi bir uygulaması bulunmamaktadır.

Bu çalıŐmanın amacı, jig ve sallantılı masa gibi diđer yerçekimiyle zenginleŐtirme ekipmanlarıyla zenginleŐtirilemeyen sorunlu cevherlerin zenginleŐtirilmesinde ađır ortam siklonlarının kullanım olanaklarının araŐtırılmasıdır.

Demir, mangan, çınko ve kromit cevherlerinin fiziksel ve mineralojik özellikleri belirlendikten sonra, ađır sıvı testi için uygun boyut fraksiyonlarında hazırlanmıŐlardır. 3.5

g/cm³ yoğunlukta ağır süspansiyon hazırlamak için sodyum politungstat ve tungsten karbit tozu karışımı kullanılmıştır.

Ağır sıvı test sonuçları ve yüksek yoğunluklu ağır ortam siklonu tesisleri için geliştirilmiş ampirik modeller kullanılarak simülasyonlar yapılmıştır. Sonuç olarak;

-9.5+0.5mm demir cevheri için, %55 Fe içeren bir konsantre %80 Fe verimiyle elde edilmiştir. Ayırım yoğunluğu 3.1 g/cm³ olarak belirlenmiştir.

-16+0.5mm demir cevheri için, %38 Mn içeren bir konsantre %92 Mn verimiyle elde edilmiştir. Ayırım yoğunluğu 2.9 g/cm³ olarak belirlenmiştir.

-1.8+0.2mm kromit cevheri için, %45 Cr₂O₃ içeren bir konsantre %52 Cr₂O₃ verimiyle elde edilmiştir. Ayırım yoğunluğu 3.5 g/cm³ olarak belirlenmiştir. Yetersiz serbestleşme düşük verimin en önemli nedeni olarak görünmektedir.

Son olarak, demir cevheri sonuçları kullanılarak yıkama-durulama elekleri ve manyetik ayırıcılar vd. içerecek şekilde süreç akımşeması geliştirilmiş ve tüm ekipmanların boyutları belirlenmiştir.

Anahtar kelimeler: ağır ortam siklonu, ferrosilikon, ağır sıvı, benzetme, demir cevheri, mangan cevheri, krom cevheri.

ACKNOWLEDGEMENTS

I kindly would like to express my sincere thanks and appreciation to my supervisor, Prof. Dr. Ş. Levent Ergün for his supervision, guidance, criticism, advice, support and encouragement throughout thesis study.

I also want to thank Dr. E. Caner Orhan for his patient and effective advices and helps during this research.

I am indebted to my colleagues in the department, especially to Ata Bahrami, Hojjat Hoseinzadeh, Ergin Gülcan and Elif Özdemir for their helps.

Lastly but not least, fond acknowledgement should go to my wife, Aysa Sapchi who endured this long process with me, always offering support and love.

Table of Contents

	<u>Page</u>
ABSTRACT.....	i
ÖZET.....	iii
ACKNOWLEDGEMENTS.....	v
Table of Contents.....	vi
Table of Figures.....	viii
Legend of Figures.....	xii
1 INTRODUCTION.....	1
1.1 GENERAL INFORMATION.....	1
1.2 OBJECTIVE OF THE THESIS.....	4
2 LITERATURE REVIEW.....	6
2.1 HEAVY MEDIUM SEPARATION.....	6
2.1.1 History of dense medium separation.....	6
2.1.2 Heavy Medium: Types and Features.....	8
2.1.3 Heavy Medium Separators.....	21
2.1.4 Dense Medium Separation Circuits.....	21
2.2 HEAVY MEDIUM CYCLONE.....	25
2.2.1 Operating Principle of HMCs.....	26
2.2.2 Theory of Separation in Dense Medium Cyclones.....	26
2.2.3 The Practical Medium Flow Regime.....	29
2.2.4 Heavy Medium Cyclone Geometry.....	33
2.2.5 DM Cyclone Efficiency, Models and Simulation Method.....	42
2.2.6 Applications.....	50
3 EXPERIMENTAL STUDIES AND RESULTS.....	63
3.1 FEED CHARACTERISTICS.....	63
3.1.1 Iron Ore.....	63
3.1.2 Manganese Ore.....	64
3.1.3 Chromite ore.....	65
3.1.4 Zinc Ore.....	68

3.2	METHODOLOGY	69
3.2.1	Background	69
3.2.2	Organic Heavy Liquids	69
3.2.3	Inorganic heavy liquids.....	69
3.2.4	Heavy suspensions.....	70
3.3	RESULTS.....	73
3.3.1	Iron Ore.....	73
3.3.2	Manganese Ore.....	76
3.3.3	Chromite Ore.....	78
3.3.4	Zinc ore	80
4	SIMULATION STUDIES AND RESULTS	81
4.1	SIMULATION STUDY FOR IRON ORE SAMPLE AND RESULTS	82
4.2	SIMULATION STUDY FOR MANGANESE ORE SAMPLE AND RESULTS	85
4.3	SIMULATION STUDY FOR CHROMITE ORE AND RESULTS.....	88
5	DISCUSSION OF THE RESULTS	92
6	CONCLUSIONS AND FUTURE WORK	98
6.1	CONCLUSIONS.....	98
6.2	FUTURE WORK	98
	REFERENCES.....	99
	CURRICULUM VITAE.....	103

Table of Figures

Figure 1.1 Typical DMS flowsheet [2]	2
Figure 1.2. Scope of the thesis.....	5
Figure 2.1 Achievable densities with both magnetite and ferrosilicon suspensions in water[13]	9
Figure 2.2. Medium Density VS. Ferrosilicon Mass Percentage[13]	11
Figure 2.3 Scanning electron micrograph from milled ferrosilicon [13]	12
Figure 2.4 Scanning electron micrograph from steam atomized ferrosilicon [13].....	14
Figure 2.5 Scanning electron micrograph from gas atomized ferrosilicon [13].....	15
Figure 2.6 Possible density ranges for ferrosilicon types[13]	17
Figure 2.7 Viscosity vs. specific gravity for milled and atomized ferrosilicon [14]	18
Figure 2.8 Relationship between medium density and medium stability in different slime contents [17]	19
Figure 2.9. Typical dense medium vessel circuit [20]	22
Figure 2.10. Cyclone geometry [24]	26
Figure 2.11. The effects of particle size and medium viscosity on the terminal settling velocity of particles within a 400mm dense medium cyclone [27]	31
Figure 2.12.The complex inter-relationship between the variables [32]	34
Figure 2.13. Cyclone layout [32].....	35
Figure 2.14. Cyclone straight section “run-in”	36
Figure 2.15. Different types of meeting between inlet nozzle and cyclone body [32]	37
Figure 2.16. Cyclone diameter vs. centrifugal acceleration [36].....	38
Figure 2.17. Breakaway size vs. Cyclone diameter [32].....	39
Figure 2.18. Spigot / vortex finder relationship [32]	41
Figure 2.19. The effects of adding a barrel extension on efficiency [32]	42
Figure 2.20. Partition curve and main parameters [40].....	43
Figure 2.21. the partition phenomenon in ideal and real conditions [40]	44

Figure 2.22. Logic flow in the Wood dense medium cyclone model [41].....	49
Figure 2.23. Schematic flowsheet of heavy media plant in ISCOR's Sishen iron mine[46]	51
Figure 2.24. Argyle process plant - block flowsheet[47].....	53
Figure 2.25. Schematic flowsheet of Mount-Isa pre-concentration plant[27]	54
Figure 2.26. Schematic flowsheet of Troodos chromite mine, Cyprus[49]	59
Figure 2.27. Crushing and pre-concentration at Buffalo Fluorspar Mine, South Africa[50]	60
Figure 2.28. Schematic flowsheet at Groote Eylandt Mining Co. Australia[53]	60
Figure 2.29. The Barroca Grande pre-concentrator of Beralt Tin & Wolfram, Portugal[44]	61
Figure 2.30. Andalusite treatment at a South African plant[56]	62
Figure 3.1. Schematic illustration of magnetic separation process	63
Figure 3.2. Size distribution analysis of iron ore sample	64
Figure 3.3. Particle size distribution of crushed manganese ore sample	65
Figure 3.4. Particle size distribution of chromite ore sample.....	65
Figure 3.5. Photomicrographs of four different size fractions of chromium sample	67
Figure 3.6. XRD pattern for chromite ore.....	68
Figure 3.7. Particle size distribution for two Zinc samples.....	68
Figure 3.8. Illustration of preparing TC-SPT suspension in laboratory	71
Figure 3.9. Modified separation funnel.....	72
Figure 3.10. Schematic illustration of sink-float test.....	72
Figure 3.11. Heavy liquid density vs Fe grade (%), Fe recovery (%) and weight of the sink products (%) for -9.5mm+4.75mm size fraction	73
Figure 3.12. Heavy liquid density vs Fe grade (%), Fe recovery (%) and weight of the sink products (%) for -4.75mm+1.18mm size fraction	75
Figure 3.13. Heavy liquid density vs Fe grade (%), Fe recovery (%) and weight of the sink products (%) for -1.18mm+0.212mm size fraction	75

Figure 3.14. . Heavy liquid density vs Mn grade (%), Mn recovery (%) and weight of the sink products (%) for -16mm+5mm size fraction.....	77
Figure 3.15. Heavy liquid density vs Mn grade (%), Mn recovery (%) and weight of the sink products (%) for -5.0mm+1.0mm size fraction.....	77
Figure 3.16. Heavy liquid density vs Mn grade (%), Mn recovery (%) and weight of sink products (%) for -1.0mm+0.2mm size fraction	78
Figure 3.17. Heavy liquid density vs Cr ₂ O ₃ grade (%), Cr ₂ O ₃ recovery (%) and weight of sink products (%) for -1.18mm+0.425mm size fraction.....	78
Figure 3.18. . Heavy liquid density vs Cr ₂ O ₃ grade (%), Cr ₂ O ₃ recovery (%) and weight of sink products (%) for -0.425mm+0.212mm size fraction	79
Figure 4.1. Principle of working with Lave 1.0 separator	82
Figure 4.2. Grade-recovery relationship for iron ore sample	83
Figure 4.3. Grade, recovery and concentrate weight for different separation densities	84
Figure 4.4. Schematic flowsheet of HMC plant for iron ore in separation density of 3.1 gr/cm ³	84
Figure 4.5. Partition curves used in the simulation of the heavy medium cyclone plant of the iron ore with the separation density of 3.1 g/cm ³ (based on simulated data)	85
Figure 4.6. The relationship between Mn grade an recovery for manganese ore.....	86
Figure 4.7. Effect of separation density in grade, recovery and concentrate weight of manganese ore sample (based on simulated data)	87
Figure 4.8. Schematic flowsheet of HMC plant for manganese ore.....	87
Figure 4.9. Partition curves used in the simulation of the heavy medium cyclone plant of the manganese ore with the separation density of 2.9 g/cm ³	88
Figure 4.10. The relationship between Cr ₂ O ₃ grade and recovery for chromite ore	89
Figure 4.11. Effect of separation density in grade, recovery and concentrate weight of chromite ore sample (based on simulated data).....	90
Figure 4.12. Schematic flowsheet of HMC plant for chromite ore	90
Figure 4.13. Partition curves used in the simulation of the heavy medium cyclone plant of the chromite ore with the separation density of 2.9 g/cm ³	91

Figure 5.1. Schematic flowsheet of designed HMC plant for iron ore97

Legend of Tables

Table 1.1 Selecting separation method with respect to near gravity content [4].....	3
Table 1.2. The comparison of HMS and Jigging for iron ore [5].....	4
Table 2.1 Heavy liquids used in laboratories	10
Table 2.2. Specifications for milled ferrosilicon 14-16 percent silicon (size analysis)[14].	13
Table 2.3. Chemical and Physical Specifications of Milled Ferrosilicon[14].....	13
Table 2.4 Specifications for atomized ferrosilicon 14-16 percent silicon (size analysis)[14]	15
Table 2.5 Physicochemical specifications of atomized ferrosilicon [14]	16
Table 2.6 Chemical specifications of atomized ferrosilicon [14].....	16
Table 2.7. Heavy media cyclone diameter and maximum particle size [20]	24
Table 2.8. Heavy media cyclone diameter and capacity [20]	24
Table 2.9. Approximate velocities and accelerations within a 400mm dense medium cyclone [27].....	32
Table 2.10. Particle Reynolds number [27].....	33
Table 2.11. Capacity comparasion in various inlet types.....	38
Table 2.12. Typical Heavy medium separation of Iron ores	50
Table 2.13. Historical and technical information about African Diamond plants[21]	52
Table 2.14 Efficiency features of Argyle diamond DMC plant[47].....	54
Table 2.15. Metallurgical features of pre-concentration plant in Mount-Isa [27].....	55
Table 2.16. Feed density distribution and partition curve parameters of Mount-Isa HMS plant in different pulp densities[27]	56
Table 3.1. Degree of liberation for different size fractions of Sivişli chromite ore	66
Table 3.2. Cr ₂ O ₃ content of different size fractions of chromite ore sample	67
Table 3.3. Sink-float results for three coarse size fractions of iron ore sample	74
Table 3.4. Sink-float results for three coarse size fractions of iron manganese sample	76
Table 3.5. Sink-float results for three coarse size fractions of chromite ore sample.....	79

Table3.6. Sink-float results for Zinc ore sample1	80
Table 3.7. Sink-float results for zinc ore sample2	80
Table 4.1. Calculated E_p values for different size fractions	83
Table 4.2. Calculated E_p values for different size fractions of manganese ore	86
Table 4.3. Calculated E_p values for different size fractions of chromite ore	89
Table 5.1. The amount of near gravity particles for different ores	93
Table 5.2. Required information for plant design	93

1 Introduction

1.1 General Information

Heavy medium separation (HMS), also called dense medium or float-sink separation, is one of the newer forms of gravity concentration [1]. Though the concept can be traced back to the 19th century, the process has enjoyed its major growth since 1940. Heavy liquid separation is a mutation. The heavy media process is used extensively to clean coal and for the concentration of a wide variety of ores such as those of iron, lead-zinc, chrome, manganese, tin, tungsten, fluorspar, magnesite, sylvite, garnet, diamonds, gravel, etc. It may be used where ever a significant density difference occurs between two minerals, and commercial separations are typically made in the range of 1.3 to 3.8 sp gr. The particle size range is wide enough to cover feeds in 200-0.1mm intervals. The flowsheet of a typical heavy media process, in this case one using a ferrous medium, is shown in Figure 1.1. In essence, the process consists of:

- Preparation of the feed usually by wet screening to remove undesired fines.
- Heavy medium separation.
- Removal and recovery of the medium from the separated products.

Many mutations of the basic scheme are possible and numerous options are possible.

The process may be used to produce a finished concentrate, two finished concentrates, or a concentrate and a middling of differing quality, or a pre-concentrate by rejection of unwanted gangue. It is an ideal method for the re-processing of coarse waste dumps. The greatest use for the process lies in coal cleaning and in the pre-concentration of ores. The relatively inexpensive heavy media process may be used advantageously to reject large quantities of coarsely crushed gangue. When used in this way, the process will allow:

- The use of lower cost but less selective mining methods with the "over break" material being removed at the front end of the concentrator or preparation plant.
- A substantial reduction in the quantity of ore that must be finely ground for subsequent mineral liberation and separation. Since comminution is often the single most expensive step in beneficiation, it is desirable to eliminate as many essentially barren pieces of rock as possible before the grinding step.
- A decrease in overall plant capital cost per ton of concentrate since the size of the plant from the dense medium step onward will be smaller.

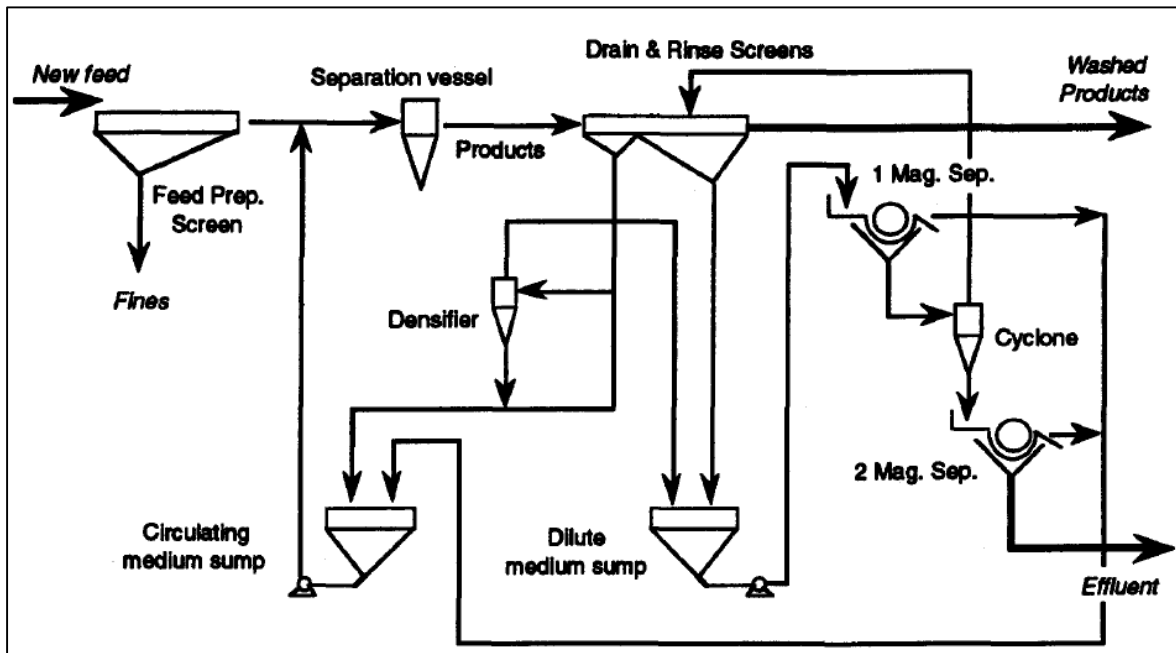


Figure 1.1 Typical DMS flowsheet [2]

Dense medium processes generally offer the following advantages over other gravity separation methods [3][1]:

- Ability to make sharp separations at any specific gravity within the range normally required even in the presence of high percentages of raw coal or mineral whose specific gravity is near the specific gravity of separation.
- Ability to maintain a separating density that can be controlled within ± 0.005 specific gravity units with closely controlled operation and sophisticated process automation.
- Ability to handle a wide range of feed sizes.
- Ability to change specific gravity of separation to meet varying market requirements.
- Ability to handle fluctuations in feed, in terms of both quantity and quality.
- Ability to remove products continuously.
- Ease of start-up and shutdown without loss of separating efficiency.
- High capacity with the use of relatively little floor space especially in relative fine particles.

Unfortunately, dense medium processes can have the following disadvantages:

- Relatively high capital costs caused primarily by the need for equipment to collect and recycle the medium.
- Relatively high operating costs caused primarily by operation of medium recycle equipment and loss of medium.

- Relatively high maintenance costs since medium is abrasive.
- Potential system startup problems if medium is allowed to settle out in pumps, sumps, and lines.

The current boom in commodities is depleting the high quality ore bodies at an unsurpassed rate. The ore bodies that will replace the existing ones will probably not be of the same quality, but the downstream processes still require high quality feedstock. Thus the gap between quality available for mining and the quality required for manufacture is widening. The only way to close this gap is to improve the ability to beneficiate inferior ore bodies.

Certainly there are many ways to beneficiate minerals, especially with the knowledge we gained in the information technology explosion. We shall see electronic beneficiation in future and it is already practiced on a small scale, but it is very much still in its infancy. What mining needs is a cost effective, efficient process that can meet the demands of diminishing quality feedstock but unrelenting demands on the quality of the products. Dense medium separation can meet these demands.

In a book on mineral processing, Wills (2006) gives a table (Table1.1) that is quite informative [4]. As we can see in some cases because of near density materials using of the dense media separation method is inevitable.

Table 1.1 Selecting separation method with respect to near gravity content [4]

Weight % within ± 0.1 of gravity of separation	Gravity process recommended	Type
0-7	Almost any process	Jigs, tables, spirals
7-10	Efficient process	Sluices, cones, HMS
10-15	Efficient process with good operation	HMS
15-25	Very efficient process with expert operation	HMS
Above 25	Limited to a few exceptionally efficient processes with expert operation	HMS with close control

In many cases, the additional costs of dense medium systems are justified by the additional recovery of salable product. Also, dense medium flowsheets generally offer more flexibility

in responding to changing market conditions than flowsheets involving all-water processes such as jigs and concentrating tables. Furthermore another gravity separation methods is very sensitive to particle size in term of capacity and their capacity decrease sharply when feed size is under 1mm. However heavy medium separation and especially heavy medium cyclones can reach high levels of capacity even in fine size fractions. It means that we can handle a large amount of feed tonnage with only a single heavy medium cyclone separator, rather than using a large number of shaking table separators in the case of fine feed. Table 1.2 shows the comparison between dense media separation and jigging for iron ore beneficiation [5].

Table 1.2. The comparison of HMS and Jigging for iron ore [5]

DMS		Jigging	
High operating cost		Low operating cost	
Efficient separation	Depends on bottom size	Less efficient separation	Narrow size classes
	Ability to handling near density materials		Recovery losses
	Optimize yield and recovery		Higher tailing grades
	Lower tailings grades		

1.2 Objective of the thesis

The objective of the thesis is to investigate the possibility of using heavy medium cyclone separation method for concentration of problematic ores, of which the enrichment is difficult with other gravity methods like jigs and shaking tables. Low grade chromite ore, iron ore, manganese ore and zinc ore samples were chosen for this investigation and heavy liquid test was used to characterize samples.

With a comprehensive literature review, appropriate models were selected and using these models and results of the experimental studies, the performance of heavy medium cyclone plants were simulated for each ore sample of concern.

In the case of iron ore a flowsheet was developed and dimensions of the main equipment were determined.

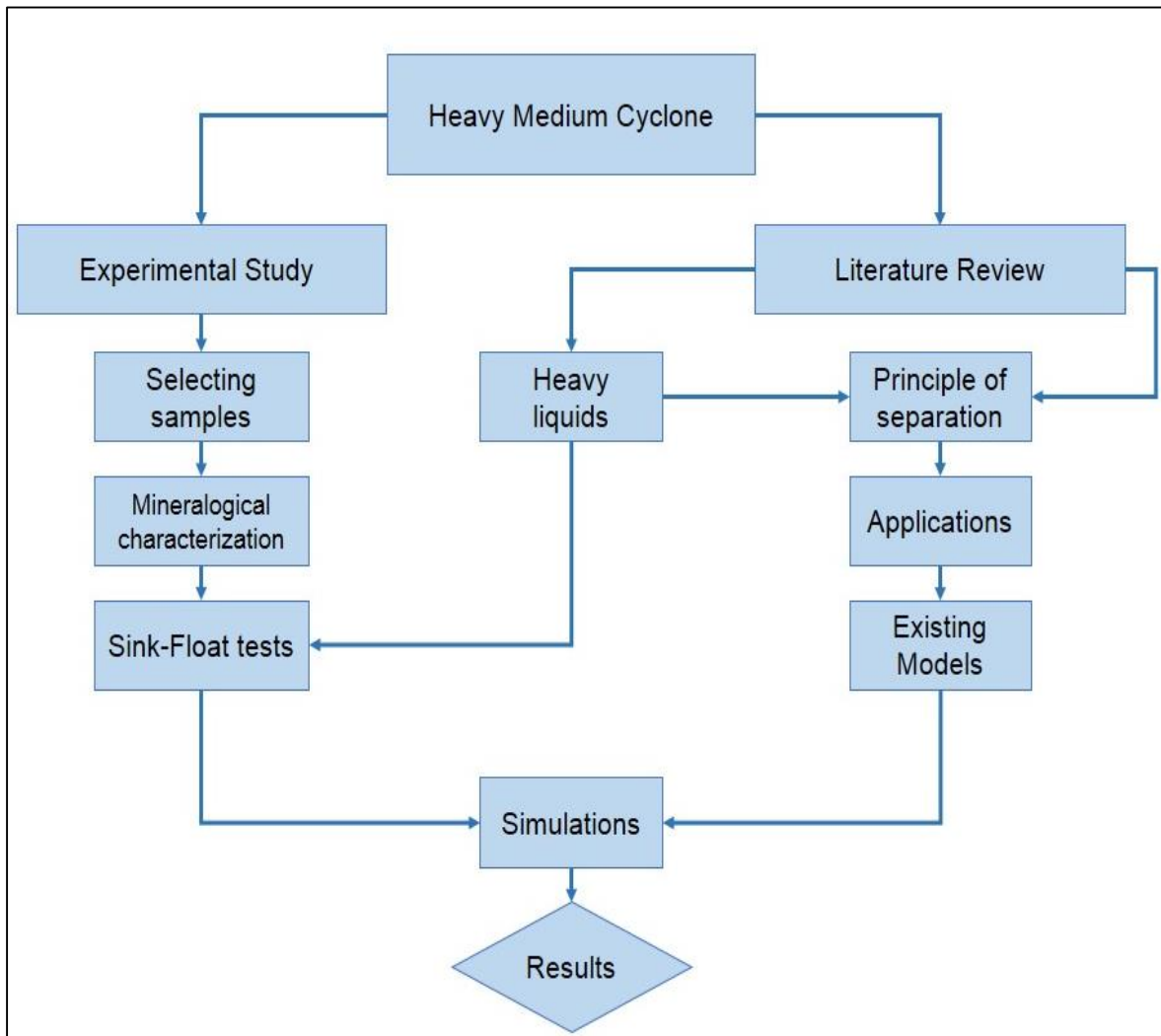


Figure 1.2. Scope of the thesis

2 Literature review

2.1 Heavy medium separation

Heavy media separation (HMS) is one of the most widely used gravity separation processes[6]. In principle, HMS is the simplest of all gravity separation processes. This process can be very closely duplicated in a laboratory. A heavy liquid of desired specific gravity is used so that minerals whose specific gravity is lower (lighter) than the heavy liquid specific gravity will float while heavier minerals sink. In mineral processing plants, the heavy liquid is a suspension of a heavy (dense) solid suspended in water. HMS is a flexible process. The separation specific gravity can be adjusted to changing ore conditions by changing the media (heavy solids) to water ratio.

In the past, various salts, clay, quartz sand, and galena have been used as the media. Current practice is to use magnetite (S.G. 5.0 - 5.2) and ferrosilicon (S.G. gr 6.7 - 6.9) for media because of the ease of recovery and recycle for these magnetic materials. Concern for pulp viscosity usually limits ground media to 35 percent by volume. Magnetite is generally used for coal cleaning and separations below specific gravity 2.5. Ground ferrosilicon or a combination of ferrosilicon and magnetite are generally used for separations for specific gravity 2.5 to 3.0. Atomized ferrosilicon is used for separations above specific gravity 3.0. Nonferrous minerals pre-concentration are generally conducted at specific gravity between 2.6 and 3.0.

2.1.1 History of dense medium separation

According to (M. Bird et al 1950)[7] Sir Henry Bessemer patented the first dense-media process, in 1858. Solutions of the chlorides of iron, manganese, barium, and calcium were proposed as separating liquids in a cone-shaped separator. One large-scale plant using calcium chloride was erected in Germany but was soon abandoned.

Du Pont (U. S. Patent 994950-1911) patented a process using carbon tetrachloride. This process was not developed past the laboratory stage, but in 1936 a process using other chlorinated hydrocarbons, patented by the du Pont Company, was installed at the Weston breaker of the Weston Coal Co., Shenandoah, Pa., for cleaning anthracite. As far as is known, this is the only commercial plant using organic liquids for the separating medium.

The Chance process, using a mixture of sand and water, was first patented in 1917 (U. S. Patent 1224138). The first plant was erected in 1921 for cleaning anthracite and in 1925 the

process was applied for cleaning bituminous coal. Those days, this was the most widely used dense media processes in the U.S.A. In 1943 there were 43 Chance plants built for cleaning anthracite and 22 for bituminous coal.

The Conklin process, using magnetite as the suspended solid, was experimented in 1922. The Belknap-Chloride washer was installed in 1935 to clean nut and egg sizes of bituminous coal. This was the second most widely used dense-media process in the U.S.A. By 1942, 25 installations had been made. Other processes were developed and installed as follows:

- Air-sand-aerated sand medium, 1923.
- Lessing-calcium chloride medium, 1928.
- Wuench-clay, gypsum, pyrite medium, 1931.
- Barvoys-barite and clay medium, 1933.
- Bertrand (Ougree-Marihaye)-calcium chloride medium, 1934.
- Tromp, magnetite or roasted pyrite medium, 1938.
- Staatsmijnen (Dutch State mines), loess medium, 1938.

Heavy medium cyclones (HMC) is one of the most important types of dense medium separators have been significantly developed during past several decades. In fact, the present modern DMC evolved from the innovations made at Dutch State Mines (DSM) during the 1940s. The DSM patented the DMC in 1942 which was introduced into the coal industry in the late 1940s. There has been a substantial increase in the size and capacity of individual DMC units from around 500 mm diameter units in 1975 to modern day units that commonly exceed 1000 mm (up to 1500 mm) in diameter [8]. Historically, there have been major developments in the understanding of DMC units, Firstly through the Dutch State Mines (DSM) in the 1950-1970 era, followed by US Bureau of Mines in the 1970-1980 era, and the Julius Kruttschnitt Minerals Research Center (JKMRC) in the 1980-1990 era. Further modern evolution has resulted in the significant increase in unit DMC capacity arising from the 1990-2000 era. In the contemporary era, large amount of studies have contributed valuable operational and separation data relating to the new style DMC units. The original DSM designs have been modified by different manufacturers, most notably by McNally, Krebs, Multotec and Minco Tech. This was mainly done in order to increase unit throughput capability and reduce wear. For instance, the McNally cycloid uses a higher medium to coal ratio than the DSM cyclone and the cycloid is mounted at 45°. Some newer DMC design features include helical (involute) feed entry, a shorter or longer body section and also a smooth transition from the cylindrical body to the cone.

Significant development of the HMC design has been undertaken through a series of very small scale tests with scale up of optimum designs to pilot and full scale for testing. However, a commercial unit has not been embraced by the industry. It is important to note that the initial designs developed by DSM were made through careful test work to provide a detailed design philosophy. Subsequent HMC designers may or may not have used such careful experimentation in their development programs. However, no public domain information could be found which validates the designs from a first principles perspective. Therefore, fundamental modelling is considered an important approach to provide a better understanding of the working mechanisms of HMCs [9].

2.1.2 Heavy Medium: Types and Features

Organic liquids, solutions of salts in water and suspensions of solids are the three main types of dense media. Autogenous media, provided by the coal itself is also rarely used as heavy media in some heavy medium separators.

In many countries heavy organic liquids are restricted for use in laboratories and are becoming less utilized because of toxic and carcinogenic nature of the organics. Table 2.1 summarizes the properties of the heavy liquids[10]. Densities of up to 12.0 can be achieved for separation of non-magnetic minerals by use of magneto hydrostatics. This density is produced in paramagnetic salt solution by the application of magnetic field gradient. This type of high density medium is applicable to separation of non-magnetic particles down to about 50 microns [11].

The medium used for separation of low density mineral may be made up of dissolved salts like calcium chloride (CaCl_2) and zinc chloride (ZnCl_2) in water where densities up to 1.35 g/cm^3 and 1.90 g/cm^3 may be produced, respectively. Due to high cost and corrosive property of ZnCl_2 dissolved salt solution is restricted to only laboratory use [12]. Combination of a heavy liquid and a grained heavy solid is an effective way to achieve up to 3 densities in laboratory environment. For example author used sodium poly tungstate and tungsten carbide combination as a suspension to reach up to 3 densities but because of high costs of materials it's limited to laboratory.

When high medium densities are required, the suspensions of finely divided high density particles in water are used. In the 1930's the Barvoys process was developed in Holland, which used a mixture of clay (specific gravity 2.3) and finely ground barites (specific gravity 4.2) in a ratio of 2:1 which gave a density up to 1.8 g/cm^3 . Froth flotation was used to

regenerate the fouled dense media by removing the fine coal. The process was abandoned owing to the high regeneration cost with flotation. Galena (specific gravity 7.5) was also used initially as medium. The high cost of cleaning of contaminated medium with flotation, oxidizing and sliming tendency of galena which impairs the flotation efficiency prevented the use of finely ground galena suspended in water. Studies have been performed to evaluate the potential of alternative materials that can be used to generate a dense medium for coal cleaning and ore concentration applications.

The most widely used medium for metalliferous ores is now ferrosilicon, whilst the magnetite is used for coal preparation. Figure 2.1 shows the achievable densities with both magnetite and ferrosilicon suspensions in water [13]. Considering the subject of this research and using greater than 2.0 S.G. in ore concentrations, only ferrosilicon was investigated in this section.

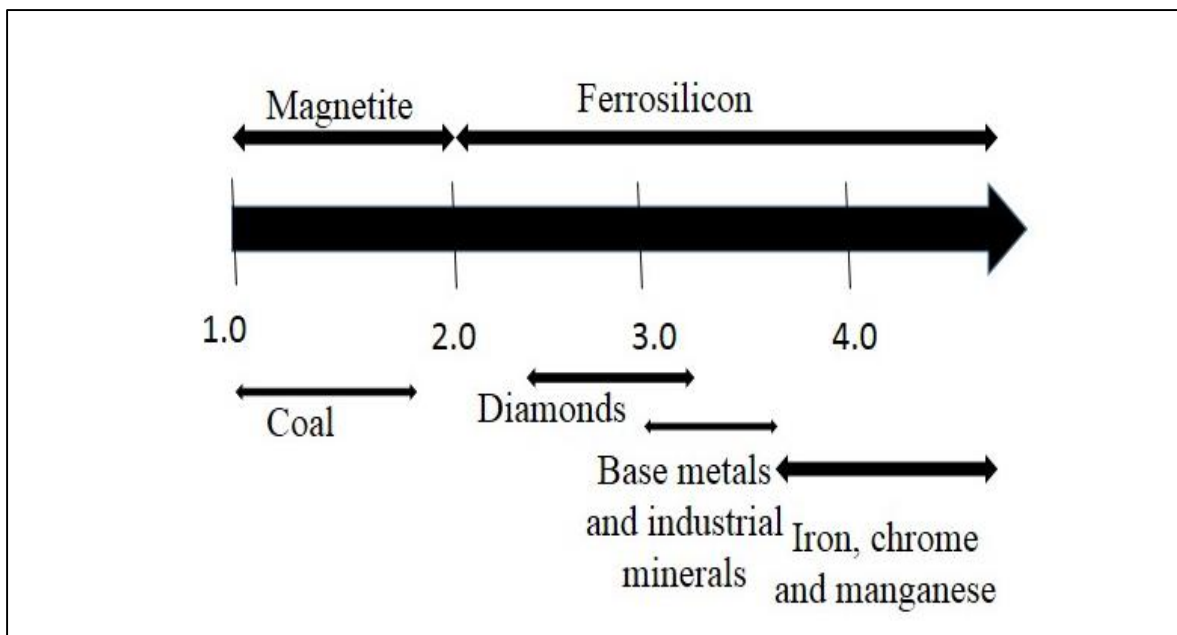


Figure 2.1 Achievable densities with both magnetite and ferrosilicon suspensions in water[13]

Table 2.1 Heavy liquids used in laboratories

Heavy Liquid	Formula	S.G.	Dilution	Health
Tri-Chloro-ethylene	CCl_2CHCl	1.46	-	Group 2A* carcinogen
Carbon-tetrachloride	CCl_4	1.50	Most organic liquids	Group 2B** carcinogen
Bromoform, Tribromomethane	CHBr_3	2.89	Alcohol, CCl_4	Liver damage, Group 3***
Tetrabromoethane (TBE)	$\text{C}_2\text{H}_2\text{Br}_4$	2.95	Alcohol, CCl_4 Chloroform	Suspected carcinogen
Di-iodo methane (Methylene iodide)	CH_2I_2	3.31	CCl_4 , Benzene	Moderate toxicity central nervous system
Clerici solution (thallium malonate/thallium formate)	$(\text{TCOOH})_2\text{C}/$ TICOOH	4.20-5.0	Water	Highly toxic, cumulative poison
Lithium heteropolytungstate (LST)	Li_mX_n $(\text{W}_{12}\text{O}_{40})$	2.95	Water	Low to moderate toxicity
Sodium polytungstate (SPT)	$\text{Na}_6(\text{H}_2\text{W}_{12}\text{O}_{40})$	3.1	Water	Low to moderate toxicity
Lithium metatungstate (LMT)	$\text{Li}_6(\text{H}_2\text{W}_{12}\text{O}_{40})$	3.5	Water	Low to moderate toxicity

* Group 2A is a probable carcinogen

** Group 2B is a probable carcinogen

*** Group 3 is unclassifiable carcinogen

2.1.2.1 General Properties and Types of Ferrosilicon

Ferrosilicon of 14 to 16 percent silicon has become widely accepted as the most suitable medium for the heavy-medium separation of ores having a specific gravity in the range of approximately 2.5 to 4.0. Ferrosilicon has many properties essential to a metal or alloy powder that is to be used as a heavy medium, some of the more important being the following:

- Resistance to abrasion,
- Resistance to corrosion,
- High specific gravity,
- Magnetism, which allows easy magnetic recovery with subsequent easy demagnetization
- Low cost

Ferrosilicon containing between 14 and 16 percent silicon is found to have the optimum combination of these properties. If the silicon content is lower than 14 per cent, the specific gravity and magnetic properties are improved, but resistance to corrosion decreases rapidly. Above 16 percent silicon, the corrosion resistance of the alloy is not significantly improved, but the magnetic properties and specific gravity deteriorate [14].

The density of the medium is controlled by the amount of medium solids present. The density where ferrosilicon is used varies from about 2.8 to 4.0 g/cm³, which is about 30% to 53% by volume, which represents 75% to 88% by mass. At the high end of the range, the viscosity of the fluids must be controlled very well to enable separation to take place efficiently. Figure 2.2 Shows the relationship between solids mass percentage against density [13].

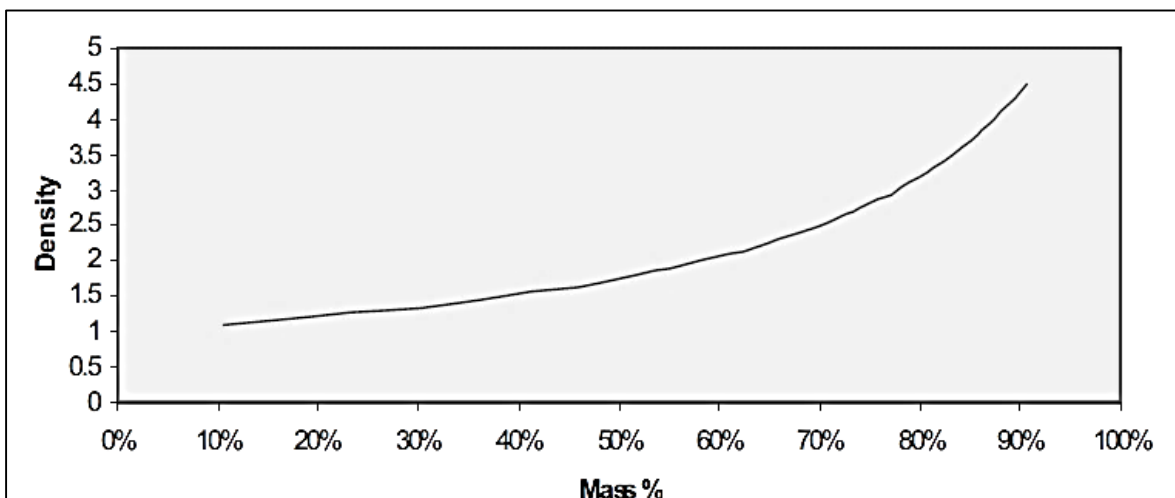


Figure 2.2. Medium Density VS. Ferrosilicon Mass Percentage[13]

The chemical composition of ferrosilicon is practically the same for all grades available on the market and is actually determined by the corrosion and magnetic properties of the material. The manufacturing method however plays a dominant role in the shape of the particles and therefore in the rheology of the medium. Therefore considering particles shape, ferrosilicon can be divided to two general types:

- Milled Ferrosilicon

Milled ferrosilicon is produced by the reduction of quartzite sand and iron ore with coke as a reductant in an electric arc furnace. The product from the furnace is cast into small ingots or granulated and milled in a ball mill to the required size. The particle shape of milled ferrosilicon is irregular. Figure 2.3 shows a scanning electron micrograph of milled ferrosilicon.

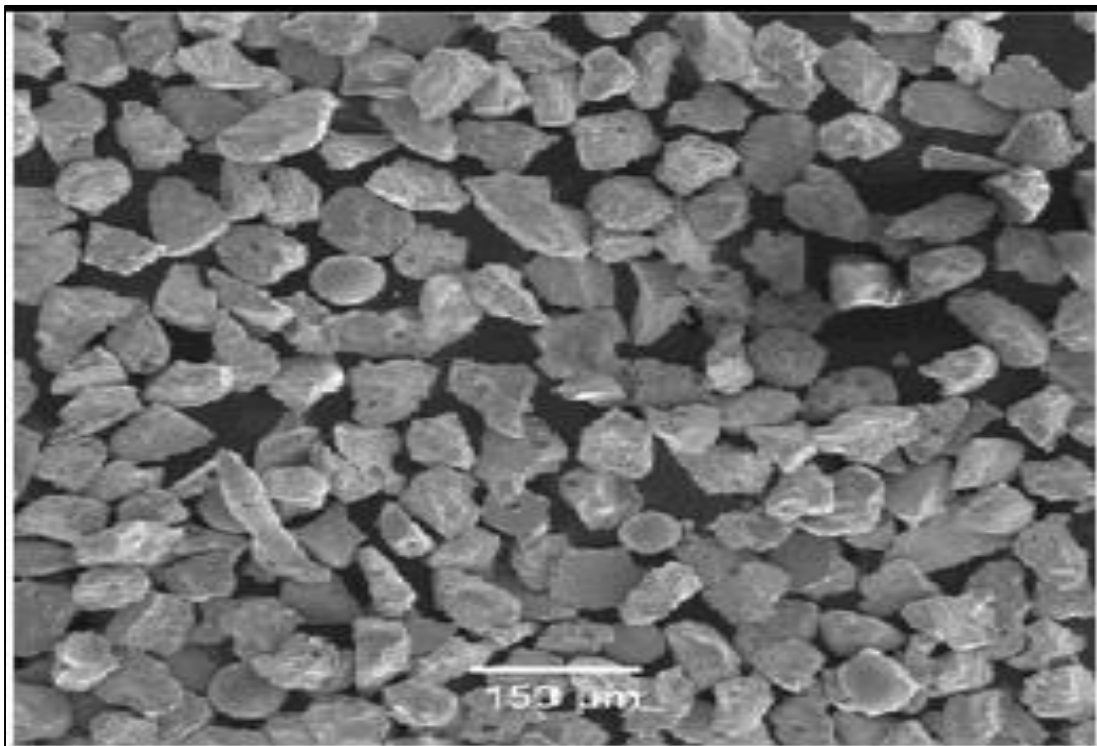


Figure 2.3 Scanning electron micrograph from milled ferrosilicon [13]

The particles are typically irregular with sharp edges and very few spherical particles are visible. The finest grades have a d50 around 25 microns and are used at the lower end of the density range, usually from as low as a density of 2.0 to about 3.0 g/cm³ at the upper end. Tables 2.2 and 2.3 show size distribution and chemical properties for different types of milled ferrosilicon [14]

Table 2.2. Specifications for milled ferrosilicon 14-16 percent silicon (size analysis)[14]

Tyler mesh	48D	65D	100D	150D	270D
+65	5	0.5	0	0	0
+100	15	3.0	0.2	0	0
+150	30	8.0	1.2	0.5	0
+200	50	20.0	5.0	2.0	0.2
+325	75	55	35	25	10
-325(Typical)	25	45	65	75	90
-325(limits)	25-30	42-49	60-70	70-80	90+

Table 2.3. Chemical and Physical Specifications of Milled Ferrosilicon[14]

Silicon	14-16%
Carbon	1% max
Sulphur	0.05% max
Phosphorus	10.0% max
Rust index	1.0% max
Non-magnetics	0.75% max
Specific gravity	6.7-6.95

- Atomized Ferrosilicon

There are two types of atomized ferrosilicon:

- Steam and Water Atomized Ferrosilicon

This process uses either steam or water at high pressure to break up a stream of molten metal in an open or closed atomizer setup. The powder is cooled down rapidly in this process and the particle shape is more spherical than that obtained with milled ferrosilicon. A scanning electron micrograph of this type of ferrosilicon is shown in Figure 2.4.

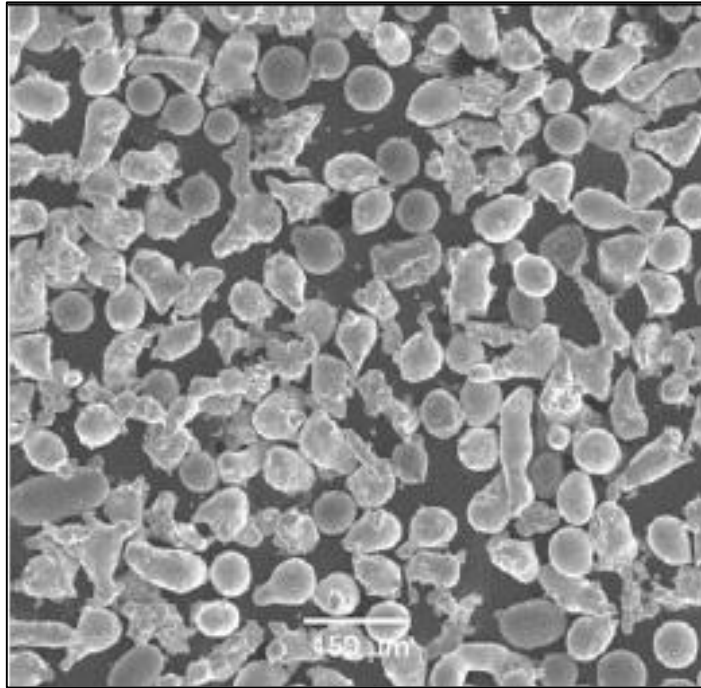


Figure 2.4 Scanning electron micrograph from steam atomized ferrosilicon [13]

When this micrograph is compared to the milled product, the presence of many more spherical particles is apparent. There is however still an amount of irregular shaped particles present. This product is typically used in the mid-range of densities from about 2.8 to 3.6 g/cm³ and in a few cases slightly higher [13].

- Gas Atomized Ferrosilicon

Gas atomized ferrosilicon is produced in a closed atomizer in very much the same way as steam atomized ferrosilicon, but instead of steam, a jet of high pressure nitrogen is used to break up the stream of molten metal. The droplets are cooled down in a chamber under gravity. The resultant particle shape is predominantly spherical as depicted in Figure 2.5. This product is used where high densities above 3.6 gr/cm³ are required.

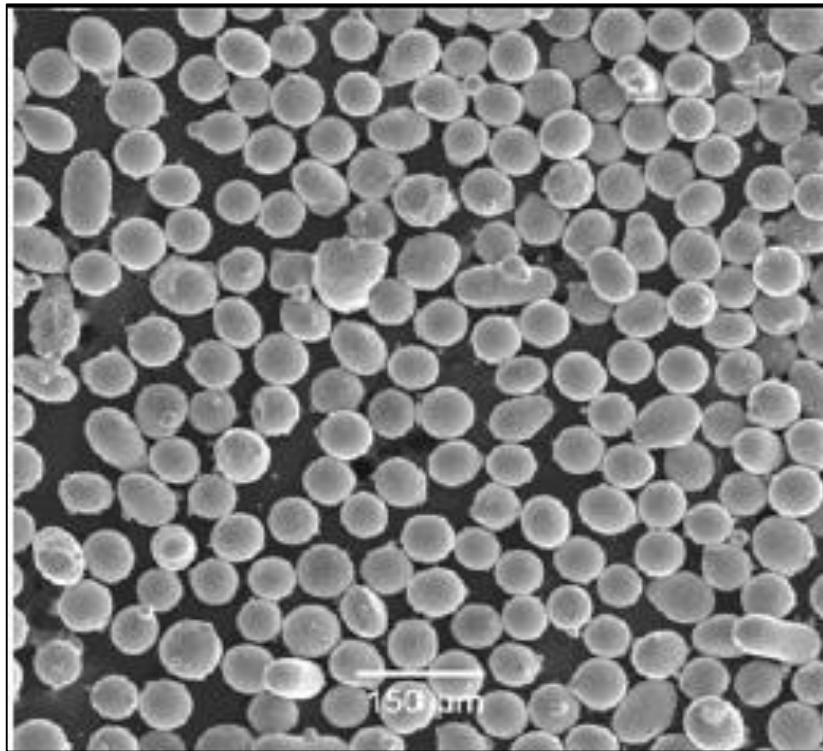


Figure 2.5 Scanning electron micrograph from gas atomized ferrosilicon [13]

These two family of atomized ferrosilicon have moderately same physicochemical specifications. Tables 2.4, 2.5 and 2.6 show the size analysis, physicochemical and chemical specifications of atomized ferrosilicon alternately [14].

Table 2.4 Specifications for atomized ferrosilicon 14-16 percent silicon (size analysis)[14]

Tyler mesh	Sishen coarse	ISCOR coarse	Coarse	Fine	Cyclone 60*	Cyclone 40
+65	3	4	3	1	0	0
+100	13	13	11	8	0	0
+150	30	31	28	18	2	0
+200	49	44	40	33	7	2
+325	74	7	62	55	27	10
-325(Typical)	26	33	38	45	73	90
-325(limits)	23-30	30.1-35	35.1-40.5	40.6-50	65-75	-
-400(Typical)	-	-	-	-	65	85

* Cyclone 60: +100 mesh 0.02% and +200mesh 12% max

Table 2.5 Physicochemical specifications of atomized ferrosilicon [14]

Content of sphere	Normal grades	±50%
	Cyclone and special grades	±90%
Magnetite content		+99%
Pycnometer density		6.6-7 g/cm ³
Bulk density		3.5-4.2 g/cm ³

Table 2.6 Chemical specifications of atomized ferrosilicon [14]

	Normal grades	Special grades	Cyclone grades
Si	14-18%	14-16%	14-16%
C	±1%	±0.5%	1.5% max
S	0.05% max	0.05% max	0.05% max
P	0.1% max	0.1% max	1% max
Al	±0.8%	0.5% max	0.5% max
Ma	0.75% max	0.75% max	0.75% max
Cu	0.8% max	0.5% max	0.5% max
Cr	0.5% max	0.5% max	0.5% max

With proper control and selection of the d50 of the products, the range of every one of the three families of products can be extended significantly. What is important is that the manufacturing process determines the shape of the particles and in doing so also the broad application of the product. The three families of products are diagrammatically displayed in Figure 2.6.

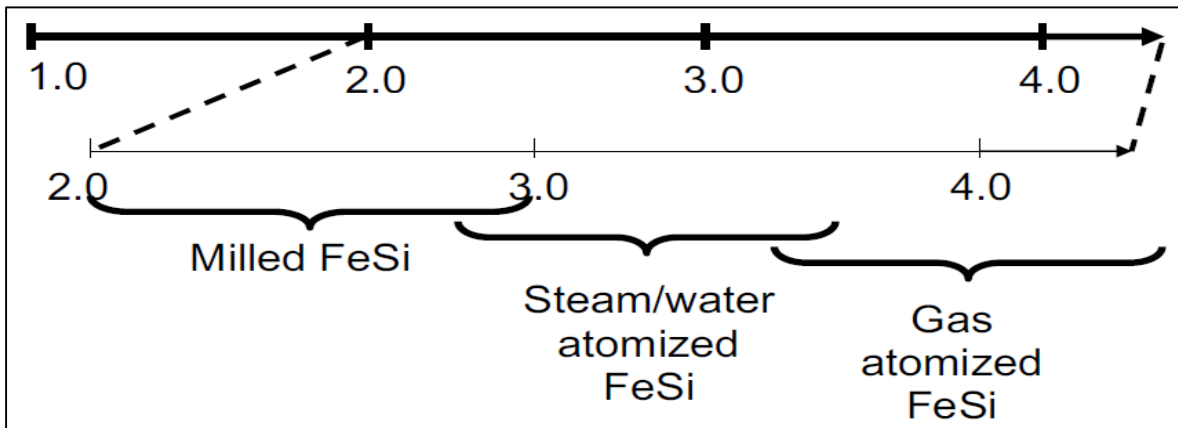


Figure 2.6 Possible density ranges for ferrosilicon types[13]

2.1.2.2 Specific Properties of Ferrosilicon

- Rheology

The rheological properties of heavy-medium suspensions play an important part both in the heavy medium separation itself and in the handling of the medium with regard to pumping and storage. The rheology of fast-settling suspensions of this kind can best be described by two properties of the suspension viscosity and stability.

- Viscosity

Viscosity is a measure of the medium resistance to fluid flow, while stability is a measure of the tendency of the medium to settle. These two properties are strongly influenced by parameters such as medium density, particle shape, particle size distribution, and the level of contamination with slimes. The viscous characteristics of the dense medium are generally non-Newtonian (which means that its viscosity is a function of the shear rate), and the term apparent viscosity (at a defined shear rate) is preferred. An ideal medium has a low viscosity to maximize separation and pump efficiency. A high viscosity is undesirable because it reduces the velocity of mineral particles being separated, increasing the chance for misplacement and reducing the separation efficiency. A low viscosity is typically obtained for a low medium density, coarse particles, smooth rounded particles, and clean uncontaminated medium [15].

Figure 2.7 presents the relationship between specific gravity of produced pulp with different kinds of ferrosilicon and pulp viscosity.[14]

- Stability

Stability is a property of a suspension considered as a non-homogeneous two-phase system; it is related to the rheology of the solid phase in an environment constituted by the liquid phase. The relative movement of the solids in the liquid phase under gravitational and surface forces determines the degree of homogeneity separation. The medium stability determines the density gradient of the medium in the separation zone and thus directly influences separation sharpness. Therefore, it is one of the most important parameters to keep under control [16].

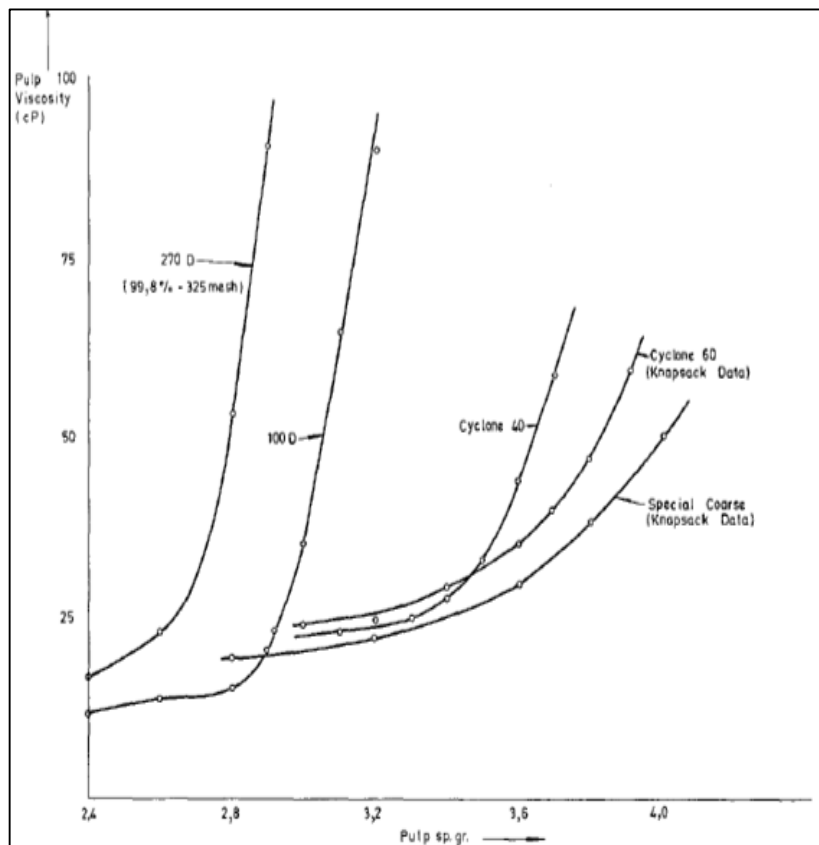


Figure 2.7 Viscosity vs. specific gravity for milled and atomized ferrosilicon [14]

An ideal medium has a high stability, which results from high medium densities, fine medium particles, irregularly shaped particles and the presence of low density contamination (ore slimes). Figure 2.8 shows medium density vs. medium stability for various slime contents (atomized ferrosilicon) [17].

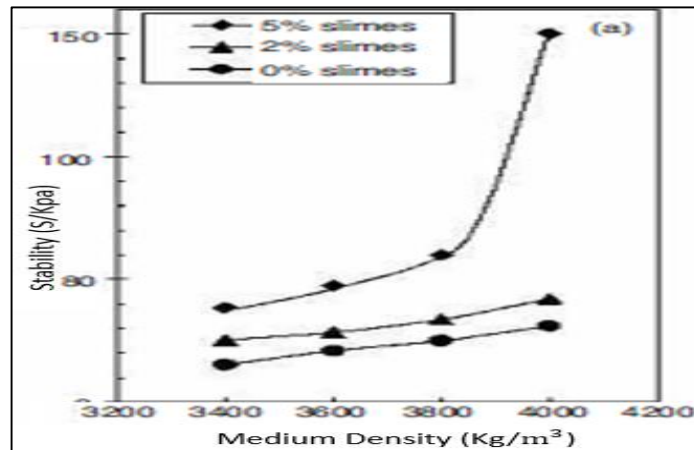


Figure 2.8 Relationship between medium density and medium stability in different slime contents [17]

The modification of the rheological properties of ferrosilicon suspensions can be achieved in three main ways:

- By the addition of polymeric compounds or other reagents
- By the addition of ore slimes or clays
- By the demagnetization of the circulating medium.

Considerable work has been carried out on the stabilization of heavy medium suspensions for static-bath separators by the addition of polymers. It is claimed that significant improvement in stability (with a corresponding increase in viscosity) can be achieved by the addition of as little as 0.1 per cent by mass of solids of certain polymers. This allows the use of coarser (and cheaper) grades of medium, easier start-up due to reduced settling, and other advantages. Reductions of viscosity by the addition of peptizing agents have also been reported. This effect is found to be highly pH-dependent. The addition of small quantities of ore slimes or clays has been found to increase significantly the viscosity and stability of ferrosilicon suspensions. In some cases, the slimes represent an undesirable constituent of the ore being treated, and a proportion of the circulating medium has to be continuously removed and cleaned through magnetic separators. In other cases, natural slimes can be used to stabilize a relatively coarse grade of medium.

The degree of magnetization of the ferrosilicon particles, induced by their passage through magnetic separators during normal recovery, has been found to influence significantly the viscosity of the medium. In order to reduce viscosity, most static-bath processes include a demagnetization coil on the pipe that returns medium from the magnetic separators to the main circuit [14].

- Corrosion resistance

The inclusion of 14 to 16 per cent silicon in the alloy results in a relatively high resistance to corrosion or rusting. This is important for three reasons:

- Corrosion leads to loss of ferrosilicon.
- The finely-divided products of corrosion tend to increase the viscosity of the medium and thus impair the separating efficiency of the process.
- Corrosion in situ can lead to the cementing of ferrosilicon particles when they stand in water, which results in difficulties in starting up a heavy medium process after a long shut down.

Corrosion is a surface phenomenon and results from the electrochemical oxidation of the ferrosilicon surface to produce non-magnetic iron oxides. Under static conditions, a passive layer is rapidly built up on the surface, which effectively prevents the progress of further corrosion. Under plant conditions, however, this passive layer is continually being removed by abrasion, which tends to accelerate the corrosion process.

The irregular-shaped particles of milled ferrosilicon have a greater surface area than the rounded atomized particles, and are therefore more susceptible to rusting. In addition, the sharp points and crevices of the milled particles make ideal nucleation points for the corrosion process. The resistance to rusting of the atomized material is extremely high owing to a passivity imparted to it during the quenching process [18].

- Adhesion Losses

One of the major sources of loss of ferrosilicon from a production plant is by adhesion to the processed ore due to inadequate washing. The extent of adhesion is partly a function of the surface characteristics of both the ore and the ferrosilicon, and it has been shown that adhesion loss is less with atomized ferrosilicon than with the milled material. Adhesion loss can be significantly increased by the presence of magnetic constituents in the ore [14].

- Magnetic Properties

Being an iron alloy, ferrosilicon is inherently magnetic. This property of the medium permits easy recovery and cleaning of the medium in circuit. A certain residual magnetism is induced in the medium by passage through a magnetic separator during normal operation. Excessive residual magnetism can have a deleterious effect on the viscosity of the medium. In addition,

if a magnetic ore is being treated, this residual magnetism in the medium will lead to excessive losses of the medium by adhesion [19].

2.1.3 Heavy Medium Separators

Heavy medium separators generally produce two products. A float product of lower density and a sink product of higher density than the medium. In some separators a third, middling product is also produced. According to (Wills, 2006) heavy medium separators are classified into gravitational (Static bath) and centrifugal (Dynamic) vessels. Drum separators and dense medium cyclones are the most important types of these two major groups respectively. Because of importance of DMC in this investigation the features of HMCs are given in details in section 2.2.

2.1.4 Dense Medium Separation Circuits

A typical dense medium circuit usually contains the following four elements (Figure2.9) [20].

2.1.4.1 Sizing and Pre-wetting

Screening of the feed material is required so that the separator can perform at the desired efficiency. It is particularly important that excessive proportions of fines do not enter the dense medium separator. The fine heavy particles will become misplaced and tend to report to the float fraction thereby reducing the overall separating efficiency. In addition, an excessive build-up of fines in the medium will increase its viscosity, which will also impair separating efficiency. Pre-wetting of the feed is required to ensure that the particles do not stick together and raft across the surface of the medium. Pre-wetting also provides a consistent and predictable flow of water into the separator.

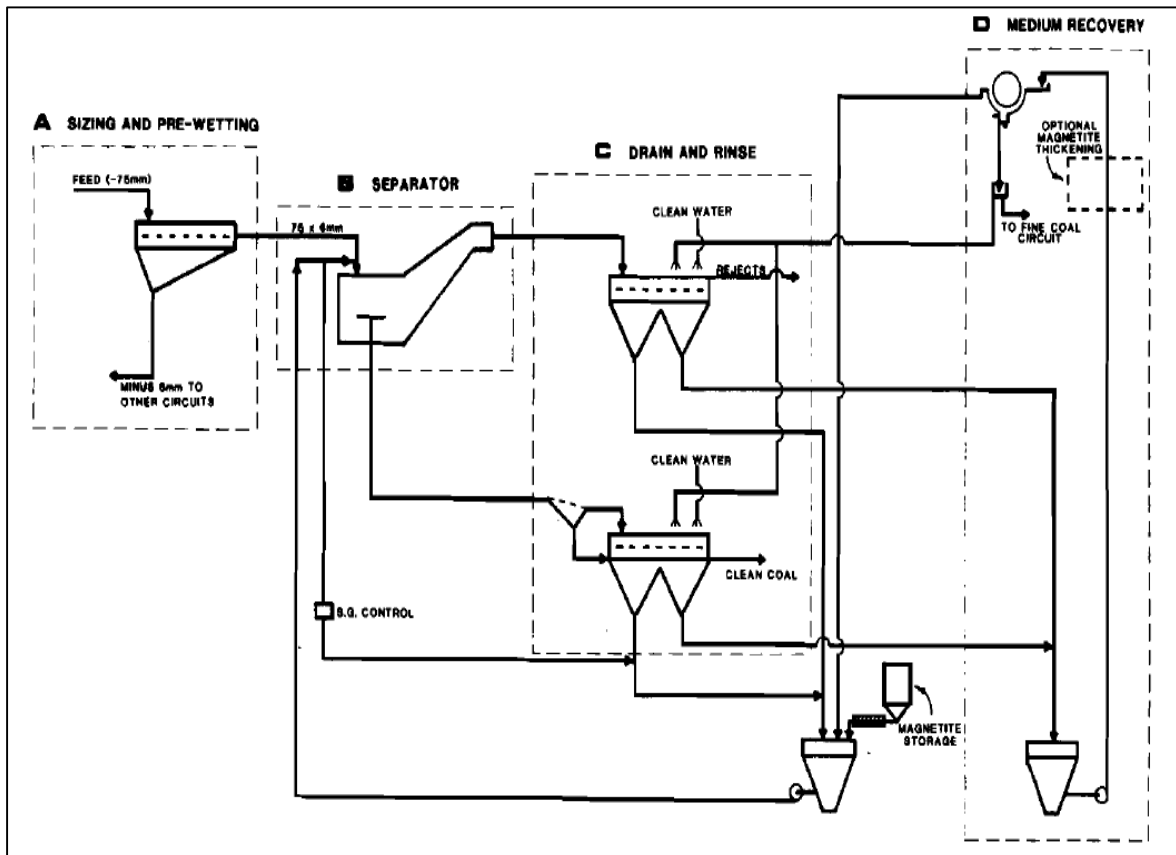


Figure 2.9. Typical dense medium vessel circuit [20]

The sizing of the cyclone feed is normally carried out at 0.5 mm, using sieve bends. The sieve bends are then immediately followed up with horizontal linear motion dewatering screens for moisture control. The capacity of sieve bends is a function of open area, which depends upon the wedge wire profile width and the aperture. The sieve aperture required to deslime at 0.5mm is 0.75mm. For sizing raw material with a top size greater than 15 mm, the profile of the wedge wire is usually 2.2mm wide x 4.5mm deep. For smaller feed sizes, the wedge wire profile is reduced to 1.5mm wide x 4.0 mm deep. Typically for desliming at 0.5mm the capacity of a sieve bend is between 87 .5 to 112.5 t/h/m.

As stated above, the sieve bends discharge onto a dewatering screen so that the moisture content of the feed to the heavy media circuit can be predicted. Since the main function of this type of screen is not classifying but rather to dewater, the screen open area is not a factor. Water, in the form of sprays, can be used on the screen to maximize undesirable fines passing to the cyclone circuit. The width of the screen, which is usually 4.88 m (16 ') long and fitted with 0.5mm aperture wedge wire profile screen decks, is calculated using the following formula:

$$\text{Screen Capacity} = 19((dm)^2 \times (sp. gr)^2)^{0.33}$$

Where d_m is the mean particle size and sp.gr. is the specific gravity of the feed [20].

2.1.4.2 Separation

The two major types of dense medium separators are vessels and cyclones, which examined in previous section. In heavy medium cyclones the top size of the feed to a heavy media cyclone is generally determined by the diameter of the cyclone inlet opening. Typical ranges of maximum feed particle sizes are a function of the cyclone feed opening, i.e., approximately 1/3 of the cyclone inlet diameter. The maximum feed particle size and cyclone diameters are as follows in Table 2.7.

The bottom size is dictated mainly by the lowest size at which efficient screening and draining and rinsing can take place using conventional sieve bends and screens. Practical experience has shown that this size is approximately 0.50 mm for cyclones up to 0.66 m diameter. Some cyclones are treating sized coal down below this particle size with efficient separations. However, specialized circuits have to be designed for these particular instances.

The configuration of the cyclone, i.e., inlet, overflow and underflow openings can greatly affect the efficiency of the cyclone separation. Standard diameter ratios of the inlet, overflow and underflow orifices to the cyclone diameter are approximately 0.2, 0.4 and 0.3 respectively (a comprehensive information about cyclone geometry and its effects in cyclone performance will come in separate section). The cyclone pulp capacity, (media and coal) of a cyclone is primarily a function of the pressure at which it operates. The more normal operating range is between 150 and 250 kPa. For efficient separations, the media to coal ratio of the feed to a cyclone should not be less than 3.5: 1 but more ideally 4: 1. Table 2.8 shows typical dry tonnes throughput capacities[20]:

The feeding mechanism into a separation vessel especially HMCs is very important. There are two major method of feeding in DM cyclone circuits: one is gravity feeding method and another is pumping method. In recent years because of developments in manufacturing pump there is a tendency for using pumps in cyclone feeding. Advantage of the gravity-fed plant is that the pressure drop across the cyclone is kept constant by the constant head (on the assumption that the density of the medium is constant) and is not dependent upon pump efficiency, which may change as a result of wear or other factors. A disadvantage is the additional height required, resulting in increased capital costs [21].

Table 2.7. Heavy media cyclone diameter and maximum particle size [20]

Cyclone Diameter		Maximum Particle	
mm	in	mm	in
550	20	35	1.25
600	24	40	1.5
750	30	50	2.0
840	33	75	3.0
1020	40	100	4.0

Table 2.8. Heavy media cyclone diameter and capacity [20]

Cyclone Diameter		Capacity	
mm	in	Dry t/h	Pulp m ³ /h
550	20	45-68	235-300
600	24	95-127	390-420
750	30	175-200	590
840	33	250-300	865
1020	40	350-400	1180

2.1.4.3 Draining and Rinsing

When the float and sink products leave the separator, they also carry the medium with them. In order that this medium may be recovered, the products are allowed to drain on the first one to two meters of a vibrating screen, or a screen and sieve bend combination. This drained medium, which is at the correct specific gravity is collected and immediately pumped back to the separator. It is called the correct medium.

The drained products will continue to pass along the vibrating screen. In order that the remaining adhering medium may be removed from the products and eventually be recirculated back to the correct medium circuit, it is necessary to rinse the products. This is usually achieved by spraying the products initially with water from the magnetite recovery circuit followed by clean water. The medium which has now been removed from the products has become "diluted" by the spray water. As a result the medium collector beneath

the screen is divided into two compartments to collect the correct medium and the dilute medium.

2.1.4.4 Medium Recovery

In simple medium recovery circuits, the dilute medium is pumped directly to a magnetic separator which usually consists of a large permanent magnet located inside a rotating drum. The dilute medium flows past the drum surface. The magnetic particles are attracted to the drum, removed from the liquid and eventually recirculated back to the correct medium circuit. The non-magnetics continue to flow through the separator. The water and non-magnetic solids pass to the fine product treatment circuit in the plant.

2.2 Heavy medium cyclone

Heavy medium cyclones are used extensively in mineral processing to beneficiate various materials including coal, lead-zinc, chrome, manganese, tin, tungsten, fluor spar, magnesite, sylvite, garnet, diamonds, gravel, etc. According to (Reeves, 2002), the cyclone had been installed in over one-quarter of the coal preparation plants worldwide [22]. Further de Korte (2000) reported that about 93% of 58 coal preparation plants in South Africa employed dense medium cyclones [23]. The structure of dense medium cyclone is illustrated in Figure 2.10. This equipment separates minerals according to their differences in densities, whereby the heavier particles are sent to the sinks and the light particles to the floats. Feed enters tangentially through the inlet with high pressure so that a vortex is created within the cyclone. Consequently, an air core that extends from the floats through the sinks along the axis of the cyclone is developed. The inward vortex carries the float particles to the float stream and the outward vortex carries the sink particles to the sink stream. A slurry mixture of ore particles and heavy medium constitutes the feed slurry. Cyclone feed is normally de-slimed beforehand to remove fines, typically smaller than 0.5 mm, which would have an adverse effect on the medium quality and cyclone performance.

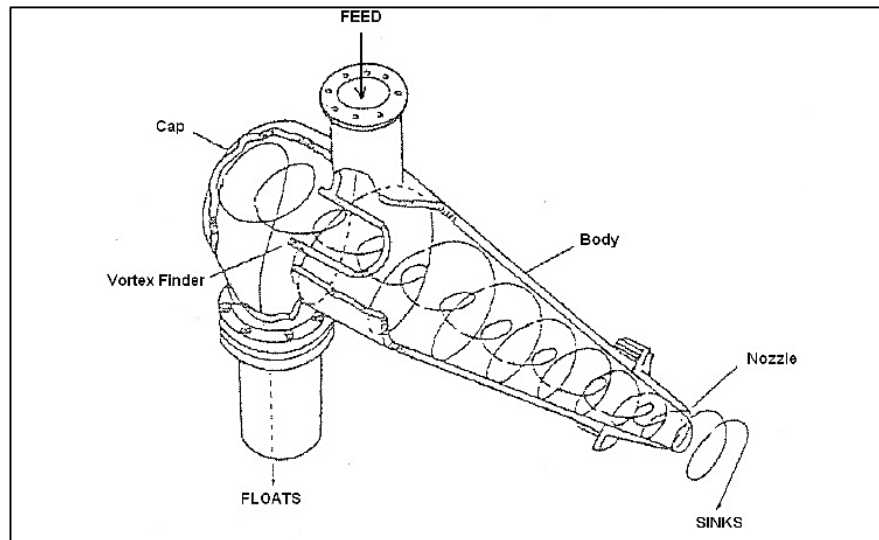


Figure 2.10. Cyclone geometry [24]

2.2.1 Operating Principle of HMCs

Heavy medium cyclone (HMC) is an important equipment to separate dispersed solid particles from a fluid suspension by centrifugal and vortex action. Its working principle has been well documented [25],[26],[4]. The feed, which is a mixture of dense medium slurry and ore, enters tangentially near the top of the cylindrical section under pressure, thus promoting a strong swirling flow. Heavy particles move towards the wall where the axial velocity vector points downward and are discharged through the spigot. The lighter particles moves towards the longitudinal axis of the cyclone, where there is usually an axial air core present and the axial velocity vector points upward; and passes through the vortex finder. The ore to be treated is suspended in a very fine medium, normally finely ground magnetite or ferrosilicon, and this pulp is tangentially fed into the cyclone through the inlet to a short cylindrical section, which also carries what is termed as the vortex finder. The discard portion of the ore (sinks) leaves the cyclone at the spigot, and the (floats) via the vortex finder. The cylindrical section of the cyclone can be extended by the introduction of a barrel section which effectively increases the residence time within the cyclone and also can improve the sharpness of separation.

2.2.2 Theory of Separation in Dense Medium Cyclones

The clear likeness between hydrocyclones and dense medium cyclones make it valuable to examine the theoretical basis of certain models persisting hydrocyclone behavior. According to [27] comprehensive review of theoretical and empirical models predicting the cut-size in hydrocyclone was undertaken by Bradley [28].

The equilibrium orbits concept helped formulate many of the theoretical models and was based on the knowledge of the velocity distributions within a cyclone.

2.2.2.1 The Equilibrium Orbit theory

Flow within a cyclone is generally accepted to consist of two spiral motions each having the same spin. One spiral moves axially upward towards the overflow and the other, moves downward towards the apex. A locus of zero vertical velocity is implicit in this flow regime. By resolving the outward centrifugal force and inward fluid drag force on a particle, equilibrium orbits were theorized for particles of various sizes and densities. Those particles with orbits outside of the locus of zero vertical velocity would report to the underflow and those inside, to the overflow. Hence the cut-size was considered to be that size of particle in equilibrium that an orbit coincident with the locus of zero vertical velocity [27].

Stoke law was invariably invoked for calculation of the fluid drag force. Three conditions were therefore necessary, these being that streamline flow prevailed, free settling was possible and terminal velocities were actually attained. Despite confirming these conditions for applicability of the equilibrium orbit theory in hydrocyclones, (Bradley, 1965) [28] remarked that its use would not give exact correlation in all cases.

According to (Scott, 1985) [27], (Bradley,1965) [28] showed that for hydrocyclones most of the theoretical predictions for the cut-size reduced to a common form.

$$d_{50} = \left[\frac{D_c^3 \cdot \mu}{Q \cdot (\rho_s - \rho_l)} \right]^{0.5} \quad (2.1)$$

Where D_c is cyclone diameter, μ is viscosity, Q the feed flow rate and ρ the density of particle (s) and liquid (l). The form of this relationship, with respect to viscosity and the solid/liquid density difference is a direct consequence of applying stokes law.

2.2.2.2 The Influence of Turbulence

Turbulence within the body of fluid in a cyclone is likely to influence the separation process. However, calculation of the fluid Reynolds number is complicated. Given that the general equation is,

$$Re = \frac{V \cdot D \cdot \rho}{\mu} \quad (2.2)$$

the selection of appropriate velocity, V , or diameter, D , are problematic. The variables ρ and μ refer to the density and viscosity of the liquid. Also when dealing with particulate medium

these parameters become less well defined because sedimentation of the medium solids generate density and viscosity gradients within the cyclone [27].

Undoubtedly, turbulent conditions prevail at the inlet and quite possibly in the body of the cyclone.

According to (Scott,1985) [27], work by (Schubert and Neese, 1973) [29] led to the development of a hydrocyclone classifier model which postulate an equilibrium between centrifugally induced settling and turbulent transportation (eddy diffusion) of particles. The particle number flow rate, N , is represented by,

$$N = - D_t \frac{dn}{dy} \quad (2.3)$$

Where D_t is the eddy diffusion coefficient and dn/dy the particle concentration gradient with respect to the y coordinate. Superimposing a sedimentation flux caused by a force field the combination of eddy diffusion and induced settling made the particle flow,

$$N = - D_t \frac{dn}{dy} - V_t . n \quad (2.4)$$

where n is the particle concentration and V_t the terminal settling velocity of the particles. The force field acts against the direction of the y coordinate. The value of N becomes zero on reaching equilibrium and equation (2.4) was thus solved to give the concentration distribution of the particles.

$$\frac{n}{n_0} = Exp \left[\frac{V_t}{D_t} . y \right] \quad (2.5)$$

Where n_0 is the concentration at the bottom of the vessel ($y = 0$) used in the conceptual model. Eventually, this equation was incorporated into a model for predicting the cut-size of a hydrocyclone. The terminal velocity of the particles was, again, considered in terms of Stokes law because fluid flow relative to the particles that is within an eddy, was assumed to be laminar.

Whether considers a laminar fluid flow regime within a hydrocyclone or a turbulent one, particular terminal velocities are evidently an integral part of the cut size model. Generally speaking, these velocities are calculated using Stokes law and as such velocity becomes a process variable.

2.2.3 The Practical Medium Flow Regime

According to (Scott,1985) [27], in 1980 Napier-Munn [30] suggested that, by a simple rearrangement of equation (2.1), the separation density in dense medium cyclone might be expressed by,

$$\rho_{50} = \rho_1 + K \left[\frac{\mu}{d^2} \right] \quad (2.6)$$

Laminar flow is implicit in the form of this function by virtue of the fact that the exponent of particle size is 2 and viscosity is represented as a process variable. Similar relationships, which are equally characteristic of turbulent flow, also exist.

2.2.3.1 The Drag Coefficient

Dimensional analysis show the drag force on a particle to be [31]:

$$R = K \cdot d^2 \cdot V^2 \cdot \rho_s \left[\frac{\mu}{d \cdot V \cdot \rho_s} \right]^t \quad (2.7)$$

where K is the proportionality constant. The drag force or resistance, R, per unit area can be described by,

$$\frac{R}{A} = C_d \cdot v^2 \cdot \rho_s \quad (2.8)$$

where,

$$C_d = \frac{K \cdot d^2}{A} \left[\frac{\mu}{d \cdot V \cdot \rho_s} \right]^t \quad (2.9)$$

The terminal velocity, which is the same for all size/density species in the equilibrium orbit can be calculated by executing a force balance such that,

$$\frac{\pi \cdot d^2}{4} C_d \cdot \rho \cdot V^2 = \frac{\pi \cdot d^3}{6} (\rho_s - \rho_l) \cdot a \quad (2.10)$$

(Drag force) (Centrifugal or gravitational force)

and the terminal velocity is,

$$V_t = \left[\frac{3}{3C_d} \right]^{0.5} \left[\frac{d \cdot (\rho_s - \rho_l) \cdot a}{\rho_l} \right]^{0.5} \quad (2.11)$$

where a is the acceleration and (2×C_d) is referred to as the drag coefficient, ψ. This is a general relationship which spans laminar, intermediate and turbulent flow regimes. What needs to be known to solve for V_t, the terminal velocity, is the value of the drag coefficient

over the full spectrum of possible Reynolds numbers. This is well known for both the laminar and turbulent regions where,

$$\psi = \frac{24}{Re} \quad \text{and} \quad \psi = 0.44 \quad (2.12)$$

(Laminar)

(Turbulent)

By substituting these values into equation (2.10) the terminal velocity can be calculated.

Presenting with the equilibrium orbit it can then be shown that,

$$\frac{\rho_{50} - \rho_l}{\rho_l} \propto \frac{\mu}{\rho_l d^2} \quad \text{and} \quad \frac{\rho_{50} - \rho_l}{\rho_l} \propto \frac{1}{d} \quad (2.13)$$

(Laminar)

(Turbulent)

The laminar solution naturally agrees with that of equation (2.6). The difference between the two regimes is that viscosity disappears as a process variable when conditions are turbulent and separation density becomes less sensitive to particle size [27].

2.2.3.2 Calculation of the Particle Reynolds Number

Table 2.9 shows the approximate amounts for velocities and accelerations within a 400 mm DSM dense medium cyclone [27].

The cyclone constants α and β are given by,

$$\alpha = 3.7 \frac{D_i}{D_c} \quad (2.14)$$

and,

$$\beta = \frac{\alpha}{\left(1 - \frac{D_i}{D_c}\right)^n} \quad (2.15)$$

Where D_i is the feed inlet diameter and D_c is the cyclone diameter. The exponent n has a value of 0.8 for water. To account for the increased viscosity of a particular medium, α was reduced on the basis of,

$$\alpha = K \left(\frac{\rho}{\mu}\right)^{0.14} \quad (2.16)$$

where K is the proportionality constant. The small exponent means that densities and viscosities in the general region of 3000 kg.m^{-3} and $3 \times 10^{-3} \text{ N.s.m}^{-2}$ respectively, all cause a reduction in α by a factor of approximately 0.7. Although the following relationship is empirical,

$$VR^n = \text{constant} \quad (2.17)$$

There is a reasonable physical basis for reducing the exponent n by the same factor [28]. Using this equation the centrifugal acceleration,

$$a = \frac{v^2}{R} \tag{2.18}$$

could be calculated for various radii within the cyclone (as shown in Table 2.10).

Table 2.10. presents the particle Reynolds numbers for two medium conditions and the range of sizes. Accepting the transition zone between laminar and turbulent flow to span the Reynolds numbers 0.2 to 500, it is apparent that this region is representative of the flow condition, for most of the selected particles [27].

In Figure 2.11, the terminal velocity of near gravity particles in the separation zone of a cyclone are shown to decrease with size. To preserve the terminal velocity associated with the equilibrium orbit, the particle/liquid differential, and therefore the separation density, must increase.

Increasing the feed medium density, and therefore viscosity, results in a shift of all particle sizes to lower Reynolds numbers and laminar flow. Presumably if the rapid increase in separation density was associated with a region of low Reynolds numbers, the phenomenon of rapidly increasing separation density would appear at a coarser size for higher medium densities [27].

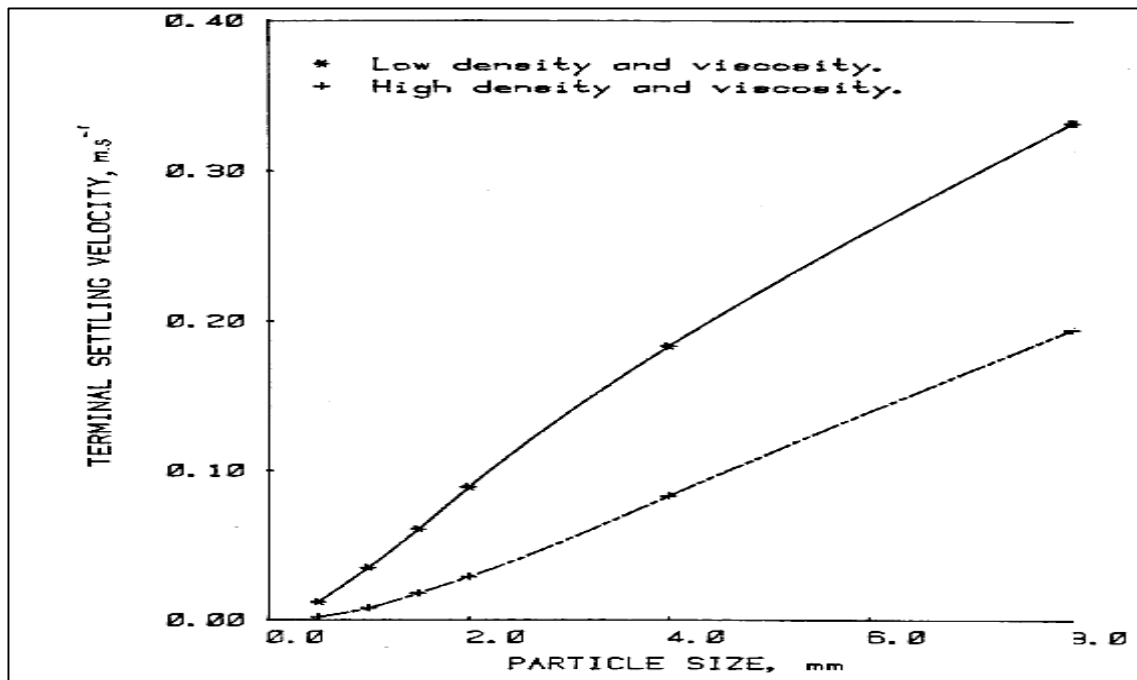


Figure 2.11. The effects of particle size and medium viscosity on the terminal settling velocity of particles within a 400mm dense medium cyclone [27]

Table 2.9. Approximate velocities and accelerations within a 400mm dense medium cyclone [27]

Cyclone Data			Water	Medium
Cyclone Diameter		D_c , m	0.4	
Inlet Diameter		D_i , m	0.08	
Radius at center of feed inlet		R_i , m	0.16	
Radius of maximum tangential velocity. $R_o=R_c/8$		R_o , m	0.025	
Mid-point radius		R_m , m	0.0925	
Flow rate		Q , m ³ /s	0.033	
Inlet pipe velocity		V_i , m/s	6.63	
Cyclone constants		α	0.74	0.52
		β	0.88	0.59
		n	0.8	0.56
Tangential velocity at	R_i	V_e , m/s	5.83	3.91
	R_o	V_o , m/s	25.74	11.06
	R_m	V_m , m/s	9.04	5.31
Centrifugal acceleration at	R_i	a_i , m ³ /s	212.4	95.6
	R_o	a_o , m ³ /s	26501.9	4892.9
	R_m	a_m , m ³ /s	883.5	304.8

Table 2.10. Particle Reynolds number [27]

Particle size	Reynold's Number	
	Medium density 2500g/cm ³	Medium density 2900g/cm ³
8.0 mm	414.9	50.1
4.0 mm	114.9	10.7
2.0 mm	27.4	1.9
1.5 mm	14.3	0.9
1.0 mm	5.4	0.3
0.5 mm	0.9	<0.1
Viscosity N.S/m²	16×10^{-3}	90×10^{-3}
($\rho_s - \rho_l$)	50.0	50.0
Acceleration m/s²	300.0	300.0

2.2.4 Heavy Medium Cyclone Geometry

In essence the cyclone is a very simple device, being an assembly of sub-components that results in a piece of equipment with a single inlet and two outlets. There are no, or at least there should not be any, moving parts. In practice it is a hugely complicated device due to the interdependency of the factors that affect its performance. No one specification, it seems, can be altered in isolation of the others.

The basic geometry we see today was derived by Dutch State Mines (DSM) approximately fifty years ago and much of the work they undertook and most of the conclusions they drew from the excellent fundamental test-work remain valid today. Strangely they never developed much in the way of mathematical models and their guidelines are thus essentially based on that fundamental work and much observation. The primary interest of DSM was of course the beneficiation of coal, however DSM cyclone technology has subsequently been applied in many other industries such as diamonds, chrome, iron-ore etc.

The heavy medium cyclone is a device that is separating ore particles on both a size/shape and density basis and at the same time separating the particles that make up the medium. As could be seen in Figure 2.12 there are numerous interactions that take place, and these are influenced by the cyclone geometry [32].

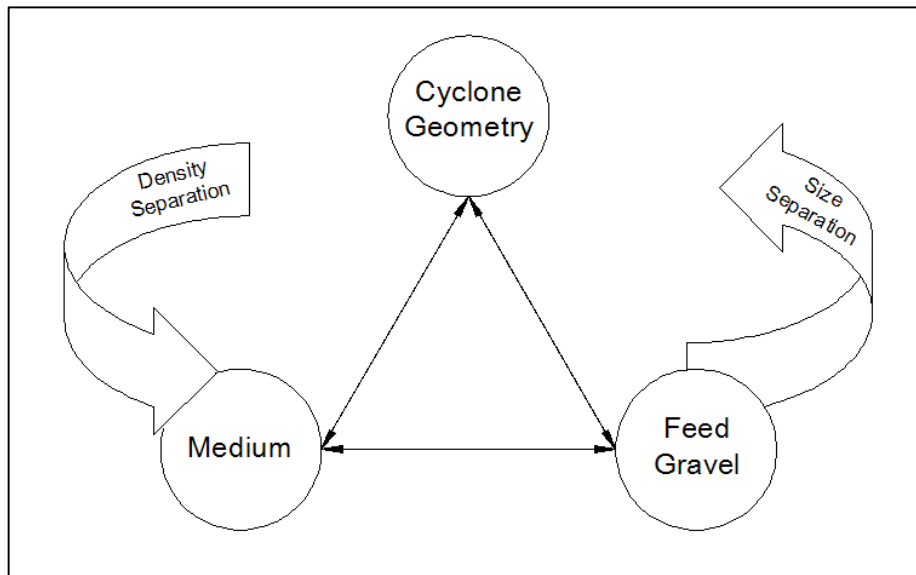


Figure 2.12. The complex inter-relationship between the variables [32]

In a dense media cyclone circuit, the ore particle feed stream is mixed with a medium consisting of a recoverable fine powder in a carrier fluid, usually water. That mixture is fed to the cyclone under pressure generated by either a pump or steady head device. Upon entry into the cyclone the straight path of the material is converted into a circular motion and centrifugal, drag, and other forces are generated. It is these forces that start the process of particle separation. How these forces are generated and how they act is predominantly the result of the geometry of the cyclone. The heavier and/or coarser material is directed to the outside wall and then to the spigot. Regardless of cyclone orientation this is normally referred to as the underflow or sinks. The lighter / finer material is forced to the center of the cyclone where it is directed to the opposite end of the cyclone and exits via the overflow.

Here is different parts of heavy medium cyclone and their influence in cyclone performance. Figure 2.13 shows Dutch State Mines cyclone layout.

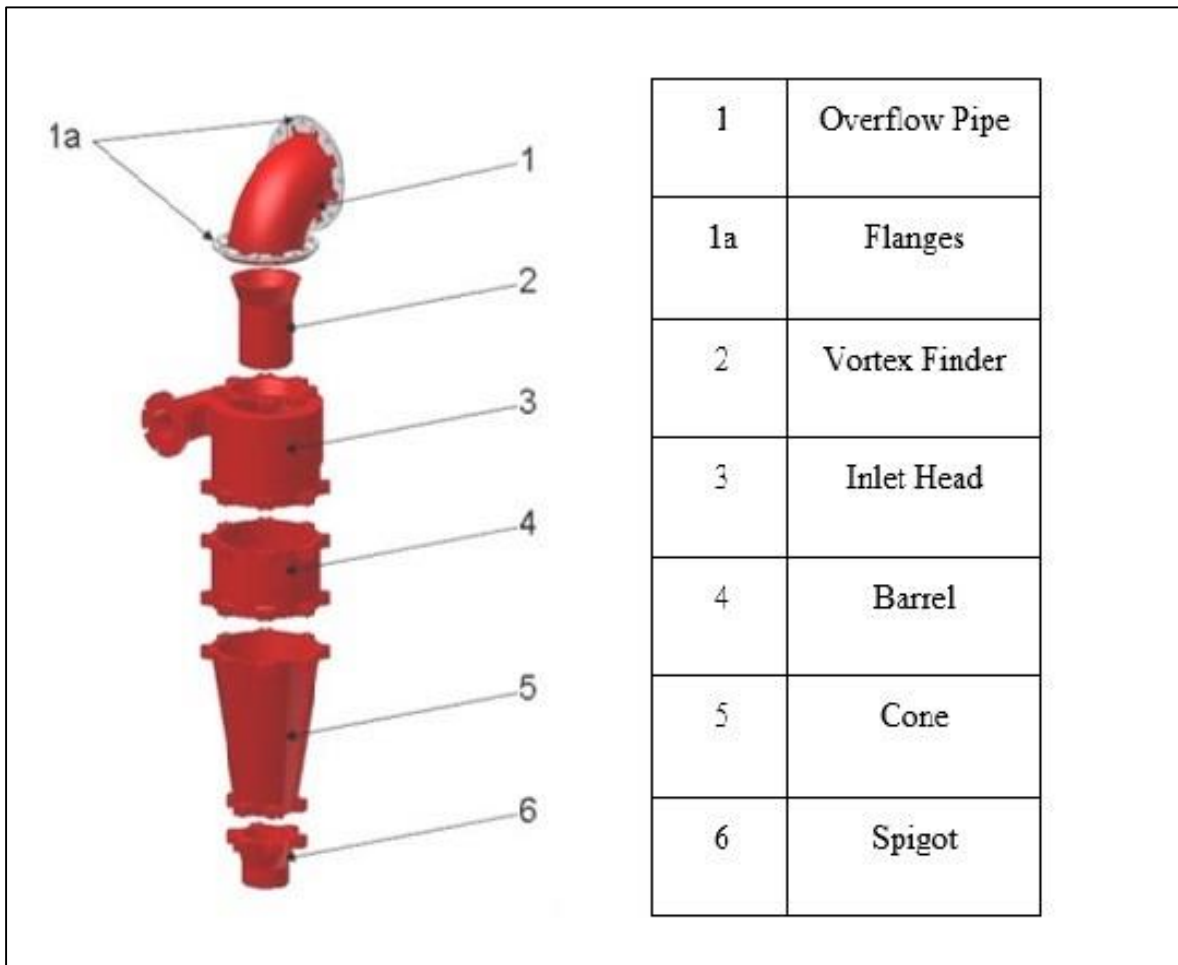


Figure 2.13. Cyclone layout [32]

2.2.4.1 Inlet Head or Cyclone Body

Three aspects are considered;

- Flow stability preceding feed entry into the cyclone

Work conducted by Köen at Cullinan Mine indicate that a square inlet run-in section of certain straight length improved efficiency. The hypothesis was that the medium / gravel mixture achieved stability, or perhaps more correctly a somewhat less turbulent condition and this enhanced the separation that subsequently took place in the cyclone [33].

Figure 2.14 shows the relationship between cyclone straight section length and it's effective diameter [32]

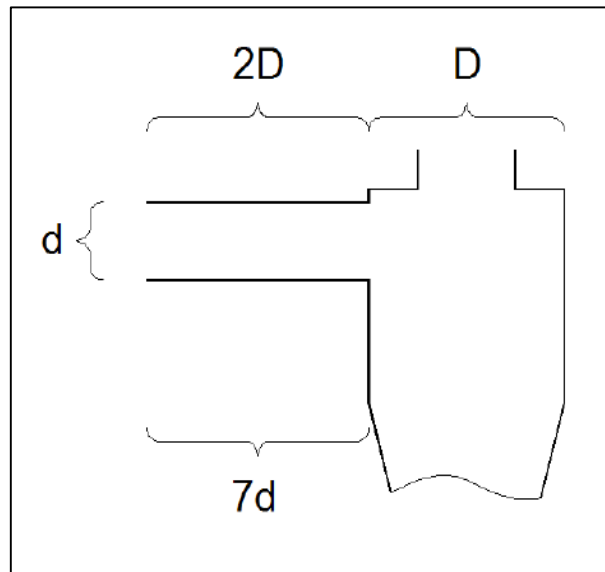


Figure 2.14. Cyclone straight section “run-in”

- Inlet Nozzle

The inlet nozzle is the interface between the cyclone and the feed pipe. The first DSM inlets were circular and the shape has evolved over the years. The openings are now almost exclusively circular, square, or rectangular and the shape of the inlet nozzle has been reported as affecting efficiency [33]. The maximum particle size that can be treated by the cyclone is in part related to the dimensions of the inlet nozzle. The norm is that the maximum particle size that can be treated without blockage is 0.33 times width or height of a round or square nozzle section and 0.25 times the width (rather than the length) of a rectangular opening.

The effective diameter of the inlet nozzle is generally between $0.2D$ and $0.27D$ (D =cyclone body diameter), though early workers reported cyclone performance was acceptable if the inlet equivalent diameter was between $1/7D$ and $2/7D$ ($0.14D$ and $0.28D$) [34].

Figure 2.15 shows different types of meeting between inlet nozzle and cyclone body [32].

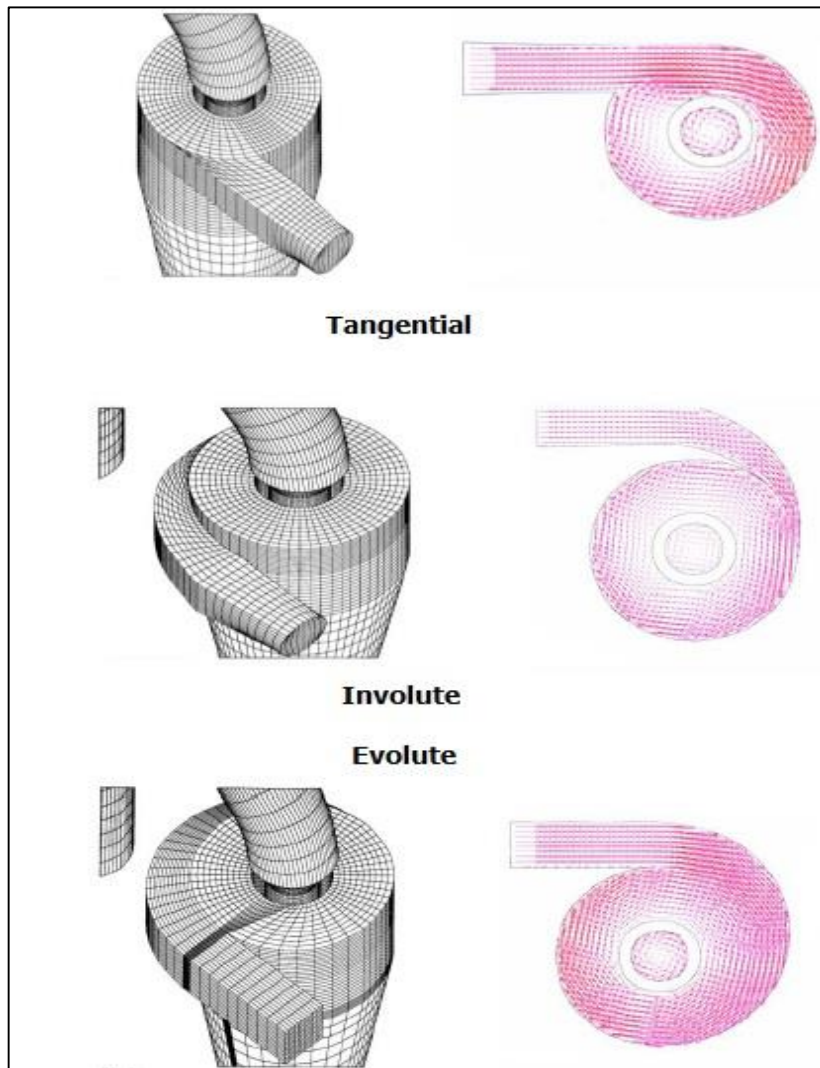


Figure 2.15. Different types of meeting between inlet nozzle and cyclone body [32]

- Inlet or Cyclone Body

The body consists of a cylindrical section of fixed depth to which the inlet is attached. The internal diameter of this cylinder is referred to as “D” and it is usual to express other cyclone dimensions as a fraction or multiple of this number. The original DSM cyclone had a tangential entry of the feed into the cyclone. The impact of the new feed impinging on the circulating stream gave rise to considerable turbulence. Notwithstanding the fact that at its best the cyclone is an intrinsically turbulent device, this increase in disruptive flow has the effect of limiting both capacity and separation efficiency. By avoiding disruptions to the cyclone surfaces and changing the shape of the cyclone gradually, in order to introduce the feed as smoothly as possible, there are increases to both efficiency and capacity. Development by suppliers has led to the scrolled evolute entry where the incoming feed meets the circulating material slightly below the roof of the inlet head thus causing reduced

turbulence. Sources indicate that a 40% reduction in turbulence could be achieved [35]. A scrolled evolute entry increases the density differential and raising the cut density by some 0.1 to 0.2 units when compared to an equivalent tangential entry cyclone, and allowing a lower medium feed density to achieve the same result. This in turn could reduce unit operating costs.

Entry of the material using a scrolled evolute inlet increases the capacity of the cyclone by some 15 to 30% over a tangential entry as could be seen in table 2.11 [32].

Table 2.11. Capacity comparasion in various inlet types

	Inlet Design				
	Tangential	Involute	Scrolled / tangential	Evolute	Scrolled Evolute
Relative capacity at one unit Pressure drop.	1	0.6	1.1	1.3	1.3

As the particles and medium change from straight line to curved flow there is a rapid increase in g forces. A large diameter cyclone may show 10g whilst a very small diameter cyclone in a fine coal (0.1mm) recovery application could exhibit 1000g. Mainly because of this fact it is generally accepted that a smaller diameter cyclone will, all other factors remaining constant, exhibit a better separation performance. Of course it is possible to increase diameter and keep similar velocities by increasing the head. For instance a 1000mm diameter cyclone running at 10.5 D head shows similar particle velocities to a 700 mm unit operating at 9D. Figure 2.16 shows the relationship between cyclone diameter and its centrifugal acceleration [36].

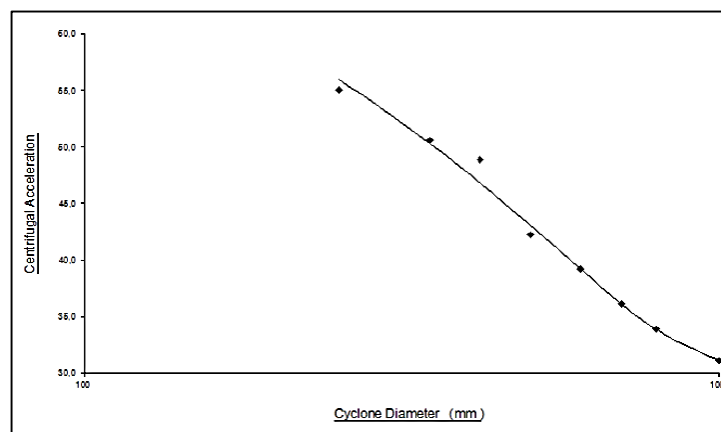


Figure 2.16. Cyclone diameter vs. centrifugal acceleration [36]

The negative aspects of opting for a smaller diameter cyclone are firstly that gravel and medium streams travel faster and therefore wear is significantly increased and secondly there comes a point where smaller cyclones simply cannot mechanically handle the larger particle sizes due to their smaller inlet nozzles.

The smaller the diameter of the inlet section then, for a fixed volume, the greater the tangential velocities and thus the greater the efficiency of the cyclone. Of course feed capacity and the maximum particle size that can be handled are reduced at the same time. As the amount of near cut density material increases so one sees smaller cyclone inlet sections being utilized to help effect the more difficult separation. There comes a point where the “breakaway” phenomenon must be taken into consideration. The smallest size of particle that can be efficiently separated increases in relation to the g forces present and it thus follows that this breakaway particle size is related to the cyclone diameter.

$$d_{50} = 6 \times \phi^{1.64} \times 10^{-5} \text{ [32]}$$

where d_{50} = Breakaway Size (mm), ϕ = Cyclone Diameter (mm) Figure 2.17 shows this relationship [32].

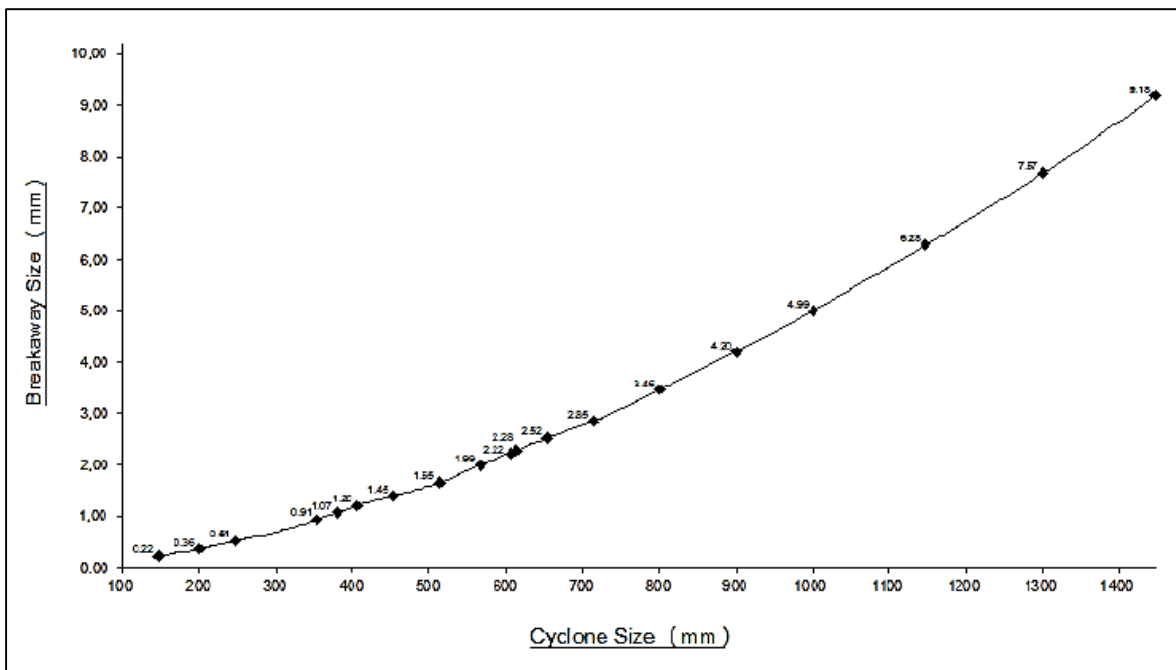


Figure 2.17. Breakaway size vs. Cyclone diameter [32]

2.2.4.2 Vortex Finder

The role of the vortex finder is, as the name suggests, finding and directing the vortex stream consisting of the finer medium and light / fine particles in the gravel stream.

There are two aspects to consider. The first is the protrusion depth, and the second the diameter of the opening.

If the vortex finder does not protrude deep enough into the inlet body section and along the axis of the cyclone, there is an increased likelihood of coarse / dense material short circuiting with a negative impact upon efficiencies. If the vortex finder protrudes too far into the inlet section, then the capacity of the cyclone is reduced but with no increase in efficiency [32].

2.2.4.3 Cone

In general it can be said that the narrower the included angle of the cone, the greater the efficiency and it is believed that this is less of a geometry issue than the fact that a greater cyclone volume is obtained by a smaller angle. The greater volume leading to increased residence time. The increased cone height means an increase in residence time and free vortex height.

As the denser / coarser material flows towards the spigot, it increases in velocity due to conservation of momentum, in much the same way as a figure skater increases spinning rate by drawing in outstretched arms.

The standard for the diamond industry appears to be an included angle of twenty degrees for primary concentration and sometimes forty degrees in a re-concentration mode [37].

2.2.4.4 Spigot

DSM arrived at a standard geometry that dictated that the standard or normal spigot was 0.7 times the vortex finder. This remains the “norm” for standard configuration cyclones and in practice it is confirmed that it can wear up to the point it is 0.85 times the vortex finder diameter before a rapid fall-off in performance. Decreasing the spigot size leads to an increase in density differentials. To avoid blockages, the spigot should be at least four times the maximum particle size to be encountered [32].

Magwai and Bosman [38] have been listed a number of parameters that influence the spigot capacity of a heavy medium cyclone; and these are (in decreasing order of importance) D_u , D , D_i , H , and D_o :

- D_u (spigot diameter) and D (cyclone diameter) have the strongest influence on the spigot capacity. There is, however, a limitation on how much D_u can be increased; when D_u/D_o (vortex diameter) ratio is more than 85% the separation efficiency deteriorates according to [39] (Figure 2.18)

- D_i (inlet diameter) also presents a viable option to increase the capacity of a cyclone that is spigot constrained, however, at the expense of increased medium flow-rate.
- Spigot capacity can also be increased through H (barrel height), although its influence is relatively weak.
- Increasing the spigot capacity through D_o does not seem to be a reasonable option because this would be at the expense of the floats capacity and D_o 's influence on the spigot capacity is small. In cases where only a small portion of the ore in the feed exits through the floats stream, the use of D_o to increase the spigot capacity becomes an option because overloading at the floats would not be a concern any longer.

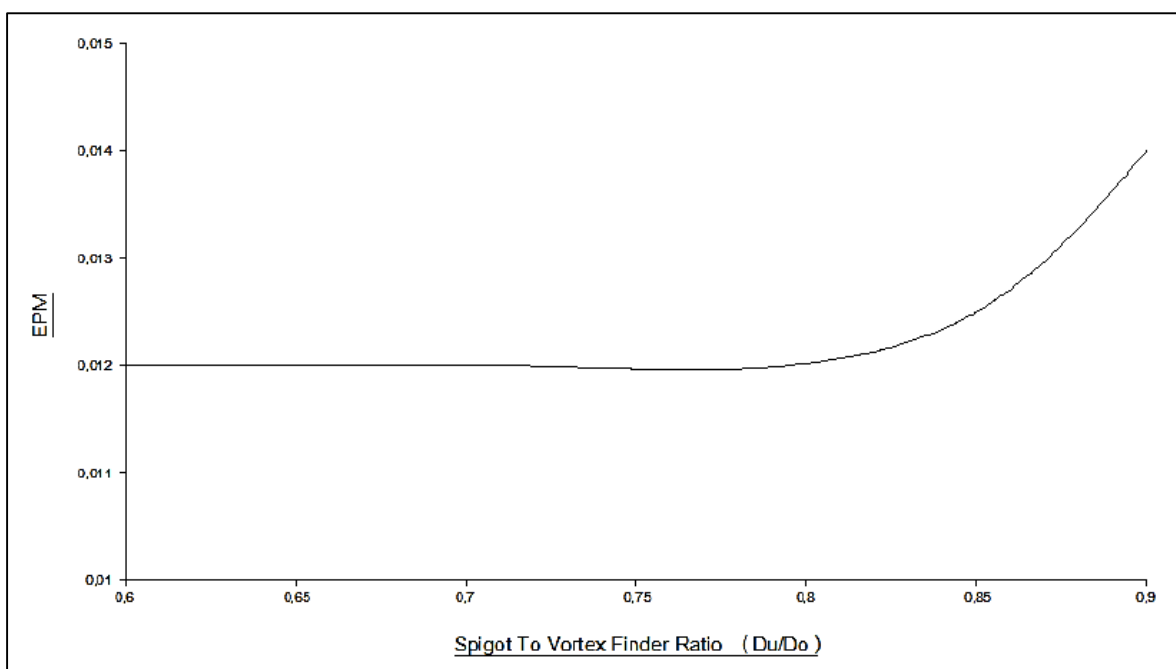


Figure 2.18. Spigot / vortex finder relationship [32]

2.2.4.5 Barrel Extension

The primary outcome of using a barrel section to extend the body of the cyclone is an increase in the residence time and thus an improvement to separation efficiency [33]. An alternate suggestion was that a finer cut was obtained improved because the barrel extension moved the “separation zone” further away from the tip of the vortex finder [37]. The same argument could of course be applied to the use of a narrower cone angle.

On a test rig with a 100mm cyclone, Hyland added one barrel extension, and doubling of the effective cylindrical length from 0.75D to 1.5D was achieved. This led to a 10% increase in throughput without reduction in performance. The standard commercially quoted increase gain by adding a barrel extension is between five and ten percent for design purposes [32].

The optimum length of a barrel extension is arguable and must depend upon the degree of process change that the installer wishes to implement. Various lengths between 0.3D and 2.5D have been proposed however the industry standard appears to be 0.67D and as used by DSM. Figure 2.19 shows the effects of barrel extension in heavy medium cyclone performance.

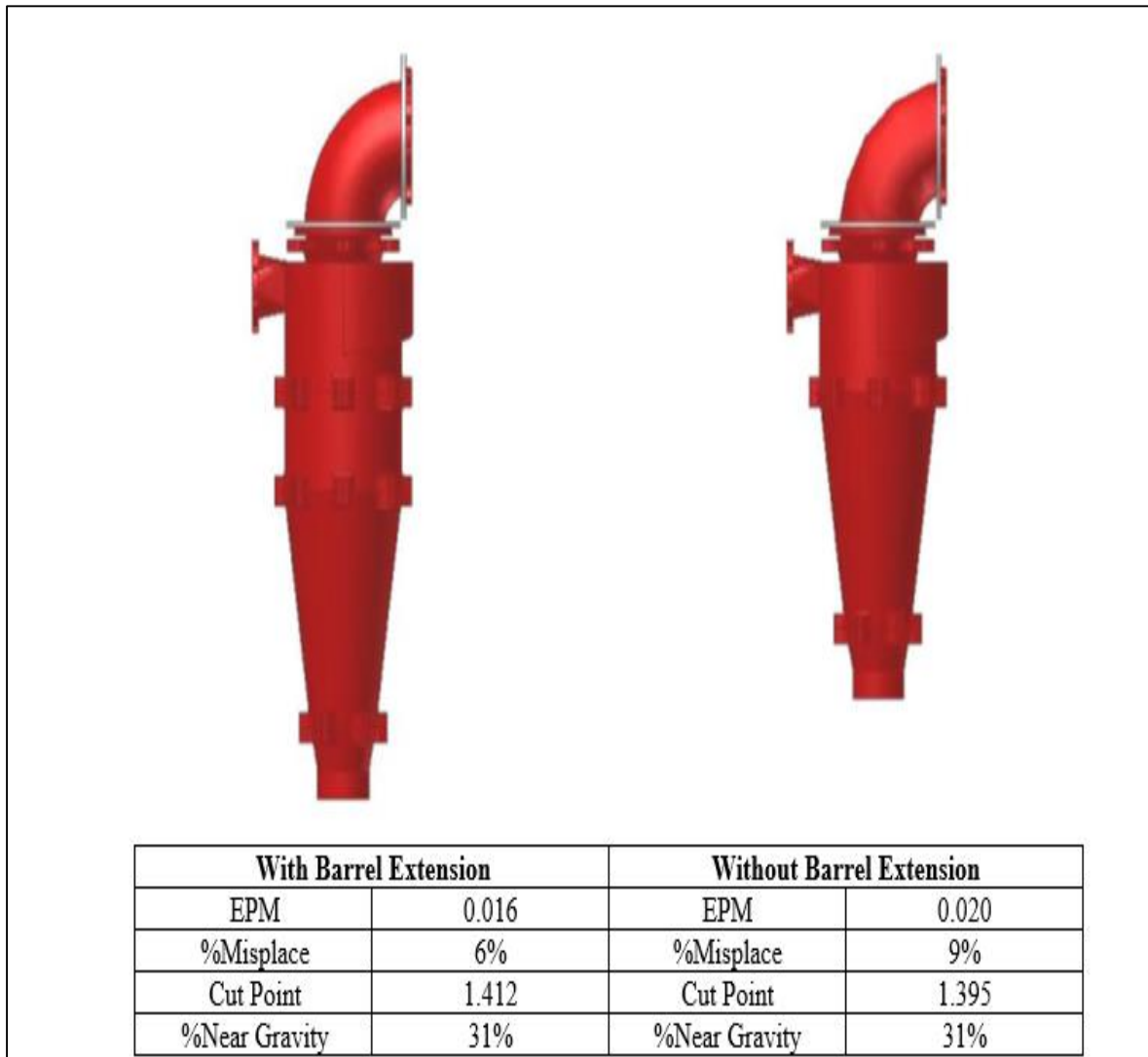


Figure 2.19. The effects of adding a barrel extension on efficiency [32]

2.2.5 DM Cyclone Efficiency, Models and Simulation Method

2.2.5.1 Partition Curve

Any sink and float process can be described by a partition curve. Partition curve reports the amount (weight fraction) reported to the sinks versus solid density. If α is the partition coefficient, $(1 - \alpha)$ is the amount of material reported to the floats.

The partition curve depends on:

- feed properties (particle size distribution and density weight distribution)
- employed device and settings
- dense medium stability and viscosity

In Figure 2.20 a typical partition curve is reported. The main important parameters describing the partition curve are [40] :

- efficiency of separation (E_p): gives a measure of the curve slope
- cut density (ρ_{50}): is the density of the solids reported 50 % to the sinks and 50 % to the floats
- offset: is the density difference between cut density and medium density ($\rho_{50} - \rho_m$)

Better separation occurs in low E_p values. Ideal separation (reported in figure 2.30 as a vertical line) has $E_p = 0$ and offset = 0.

E_p and offset values depend on both feed and operational conditions like cyclone geometry, head pressure, separation density, medium stability and viscosity and flow rate. Coarser particles have smaller E_p and offset values than fine particles. Effect of cyclone geometry and medium properties on separation performance were discussed in previous section.

Figure 2.21 shows the partition phenomenon in ideal and real conditions [40].

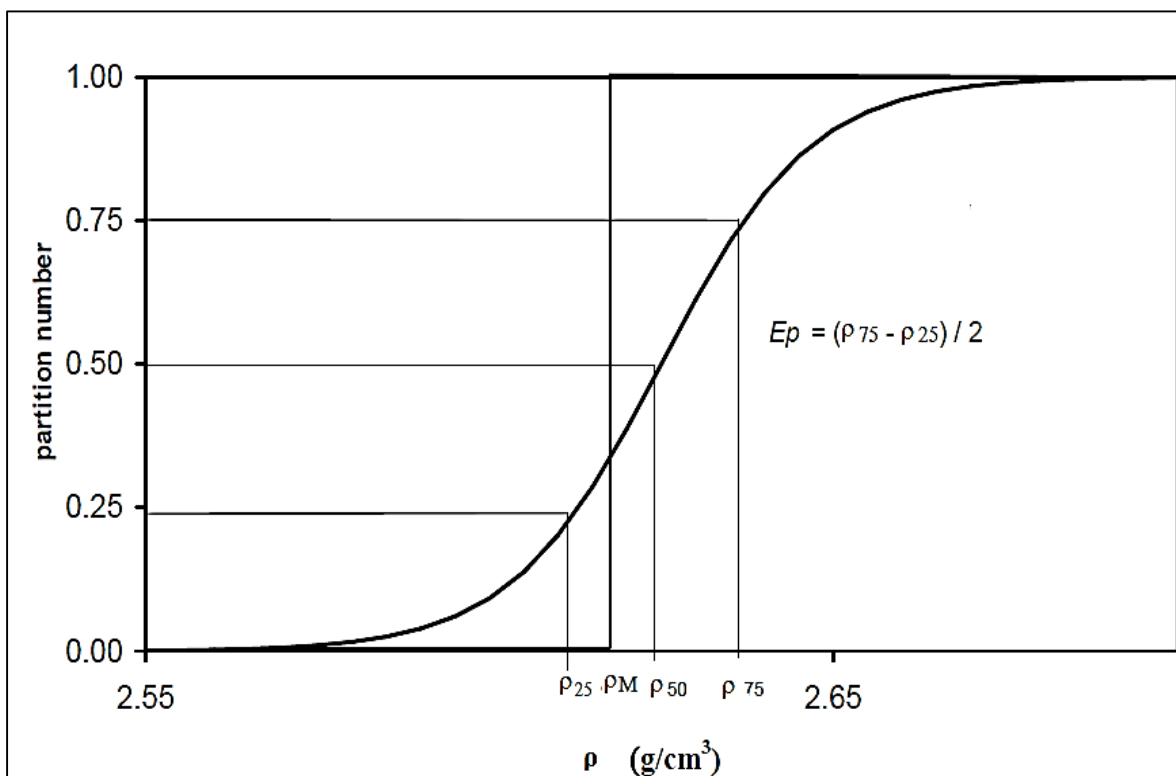


Figure 2.20. Partition curve and main parameters [40]

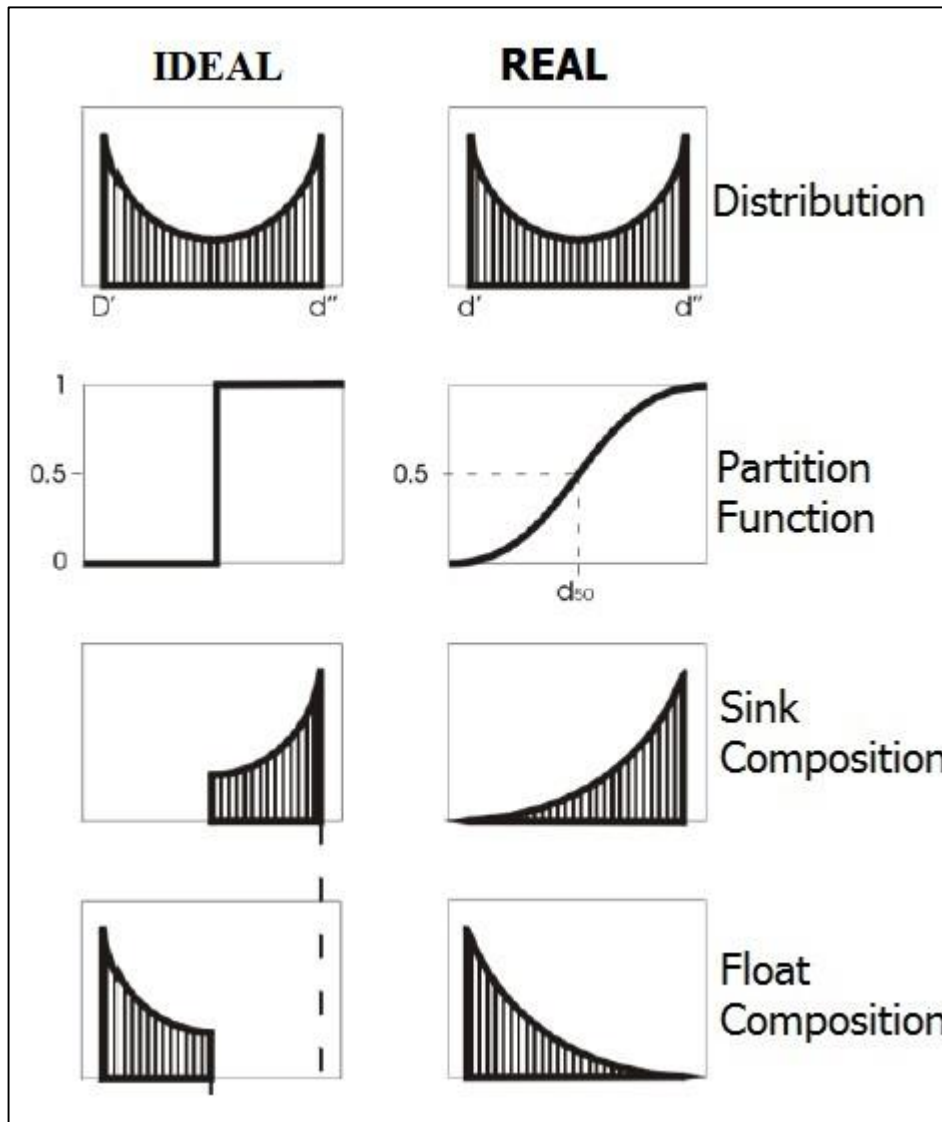


Figure 2.21. the partition phenomenon in ideal and real conditions [40]

2.2.5.2 Heavy Medium Cyclone Models

2.2.5.2.1 DMC Empirical Models

Since the development of HMCs has been almost exclusively based on empirical methods, researches in the 1980s and 90s were aimed at producing a dense medium cyclone model that included all the variables of practical interest to the plant operator such as cyclone geometry, medium properties, mineral characteristics and operational conditions. Such a model enables predictions of the effects of alternative operating procedures without the need for a mass of planned test work.

2.2.5.2.1.1 The Dutch State Mines Model

It is well known that the first dense medium cyclone was developed by the Dutch State Mines (DSM) in 1940s [41]. One of the authors has presented that the separation density or cut-point (D_{50}) was “practically independent of particle size”. In the following decade the DSM designed and commissioned a large amount of dense medium cyclone plants, and used the following relationship between E_p and cut point for coals of the approximate size range 0.5-10mm: $E_p=0.027\rho_{50}-0.010$. DSM published a number of papers on the design and operation of dense medium cyclone plants around 1960 (Krigsman, 1959, 1960; Krigsman and Leeman, 1962; Leeman, 1964). The development of sieve bends, and their importance in de-sliming, and especially in medium drainage was noted.

The information published by the Dutch State Mines is predominantly in the form of a guide to good operating practice; however, it is imperfect in scores of key areas. For example, the effects of apex diameter on cut-point and efficiency are ignored [41].

2.2.5.2.1.2 U.S. Bureau Model

As early as 1946, Geer and Yancey (1946) illustrated the results of an outstanding series of tests using a dense medium cyclone of their own design. They investigated the effects of coal washability and the sizes of cyclone orifices and feed pressure for each of a number of particle sizes. The findings sustained DSM claims relating to the efficiency of dense medium cyclones and while they provided clear qualitative demonstrations of the effects of variations in several operating variables, they are not directly relevant to current coal washing practice.

The U S Bureau of Mines model identified that different size fractions separate at different densities, but it just simply provides a mathematical description of the relationship between the partition curves for separate size fractions. It suffers from being based on an overall cut-point which will depend upon the size distribution of feed. It provides no guide to the selection of operating conditions, and important measurements appear to have been unnoticed in the development of the database from which it is derived [41].

2.2.5.2.1.3 Davis Model

Davis (1987) had concluded that the partitioning behavior of coarse particles was influenced only by the densities of feed, overflow and underflow medium. He conducted 122 tests making use of a 200mm dense medium cyclone of DSM design, plus replicates, to illustrate the effects of apex diameter, inlet pressure, feed medium density, magnetite size/type and feed medium viscosity. Based on these data, he developed regression equations to show the

correlations of tracer separation density and E_p with the densities of feed, overflow and underflow medium. In addition, Davis established that concept as an explanation of the correlations which he observed between E_p and the differential between underflow and overflow medium densities. He also presented empirical equations for overflow and underflow medium densities as functions of feed medium density, magnetite type and inlet pressure. The parameters were re-estimated for four sub-sets of data, relating to the four apex diameters which he used [41].

2.2.5.2.1.4 Wood Model

Davis (1987), Clarkson (1989) and Wood (1990) have developed currently available dense medium cyclone models. The models may be corrected by taking into consideration coal particles at high loading, following the procedure described by Wood. The logic flow of the Wood model is shown in Figure 2.22 [41].

Where D_c is the diameter of DMC body part, Q is the flow-rate, and $Head$ is the inlet pressure quoted in terms of "cyclone diameters of medium head", D_o is the inside diameter of the vortex finder, D_u is the inside diameter of the spigot, ρ is the density, PRR is the intercept (63.2% passing size) of a Rosin-Rammler magnetite size distribution, ρ_{50} is the separation density (density of a particle which has 50% probability of reporting to sinks), ρ_{50A} is the separation density for coarse particle to overflow, R_{max} is the upper density limit of a range of particle retention, d is the particle size, E_p is the Ecart Probable, PN is the partition number (% to underflow). For subscripts, d is for a particle of size d , uz is of underflow with zero non-medium solids, fz is of feed with zero non-medium solids, oz is of overflow with zero non-medium solids, om is of overflow medium, fm is of feed medium, um is of underflow medium [41].

Sub-Models 1 to 4 describe the medium behavior, as following:

Sub-Model 1 – Volumetric capacity:

- Estimate the feed slurry flow rate if there were no coal.

$$Q_f = 76 D_c^{1.93} Head^{0.45} \left(\frac{D_u}{D_o} \right)^{0.15} \quad (2.19)$$

Sub-Model 2 – Medium split:

- Estimate underflow and overflow rates with no coal.

$$\frac{Q_{uz}}{Q_{fz}} = 0.79 Head^{-0.37} \left(\frac{D_u}{D_o} \right)^{4.2} \quad (2.20)$$

$$Q_{uz} = Q_f \times \frac{Q_{uz}}{Q_{fz}} \quad (2.21)$$

$$Q_{oz} = Q_f - Q_{uz} \quad (2.22)$$

- Estimate medium flow to underflow.

$$Q_{um} = 0.97Q_{us} + \frac{Q_{uz}^2}{Q_{us}+Q_{uz}} \quad (2.23)$$

- Estimate the medium split

$$\frac{Q_{um}}{Q_{fm}} = \frac{Q_{um}}{Q_{om}+Q_{um}} \quad (2.24)$$

Sub-Model 3 – Underflow density:

$$\rho_{um} = 0.459 \rho_{fm} \left(\frac{Q_{um}}{Q_{fm}} \right)^{(0.194(\rho_{fm}-2.04))} P_{RR}^{0.17} Head^{0.082} D_c^{0.10} \quad (2.25)$$

Sub-Model 4 – Overflow density:

$$\rho_{om} = \rho_{fm} \left(\frac{1 - \frac{Q_{um}\rho_{um}}{Q_{fm}\rho_{fm}}}{1 - \frac{Q_{um}}{Q_{fm}}} \right) \quad (2.26)$$

Sub-Model 5 – Separation density for coarse particles.

$$\rho_{50}^A = -0.196 + 0.36 \rho_{fm} + 0.532\rho_{om} + 0.274\rho_{um} \quad (2.27)$$

Sub-Model 6 – Upper density limit of particle retention.

$$R_{max} = -0.374 - 0.260\rho_{fm} + 0.959\rho_{om} + 0.958\rho_{um} \quad (2.28)$$

Sub-Model 7 – Separation densities for particles of any size.

$$\rho_{50d} = \rho_{50}^A + 0.088 \left(\frac{1}{d} - \frac{1}{10} \right) \quad (2.29)$$

Sub-Model 8 – Ecart probables for particles of any size.

$$Ep_d = \frac{0.037}{d} \quad (2.30)$$

Sub-Model 9 – Partition number for any size/density class (Whiten Equation).

$$PN = \frac{100}{1+e^{1.099 \left(\frac{\rho_{50}^A - \rho_d}{Ep_d} \right)}} \quad (2.31)$$

2.2.5.2.1.5 Scott & Napier-Munn Model

Scott and Napier-munn have developed a DMC model that based on their tests-works on Mount Isa pre-concentration plant. Two realizations of the model were presented in their article in 1990 [42]. One based on a pilot study with a 200 mm cyclone, and another based on a field study of 200 mm and 400 mm cyclones at Mount Isa Lead-Zinc concentrator. Aspects considered include the effect of cyclone diameter, crowding due to high throughputs and the prediction of product medium densities using a classification model. The summary of latter model is shown below.

$$z = 19.6 + 0.16 \Delta\rho - 6.3 V_{mo} \quad (2.32)$$

$$\ln(k) = 6.87 + 0.59 \ln(\mu) + 0.30 \ln(D_c) \quad (2.33)$$

$$E p_i = z + k \cdot d_i^n \quad (n=-1.0) \quad (2.34)$$

$$Y_p = 0.61 R_m \quad (2.35)$$

$$\ln\left(\frac{V_p}{V_f} - 1\right) = -1.59 + 0.73 \ln(V_f) - 1.52 \left(\frac{\mu}{Q}\right) \quad (2.36)$$

$$Y_{ij} = \frac{1}{1 + \exp[\ln(Y_p^{-1} - 1) + 1.099(\rho_p - \rho_{ij})/E p_i]} \quad (2.37)$$

where ρ_p is pivot density, ρ_{50} is separation density, Q is cyclone volumetric flow rate, R_m is pulp split to underflow, V is velocity, V_f is volume fraction of solids in feed medium, V_{mo} is volumetric medium pulp to ore ratio, V_p is medium solids volume fraction equivalent to pivot density, Y_p is pivot partition number, z is $E p$ crowding parameter, μ is equivalent apparent Newtonian viscosity and $\Delta\rho$ is density differential [42].

2.2.5.2.2 DMC Mathematical Models

Even though some empirical models of DMC have been developed, in fact, restricted by the research techniques, previous work has to be limited to phenomenological description that infrequently touches the fundamentals (e.g. the particle-particle, particle-fluid and particle-wall interactions), and the so called DMC modelling is just empirical formulation.

Furthermore, some deficiencies in design which may be difficult to identify through an empirical approach, can be readily identified and corrected using a first principles approach. Moreover, a fundamental approach is able to provide a better understanding of the working mechanisms of DMCs [9].

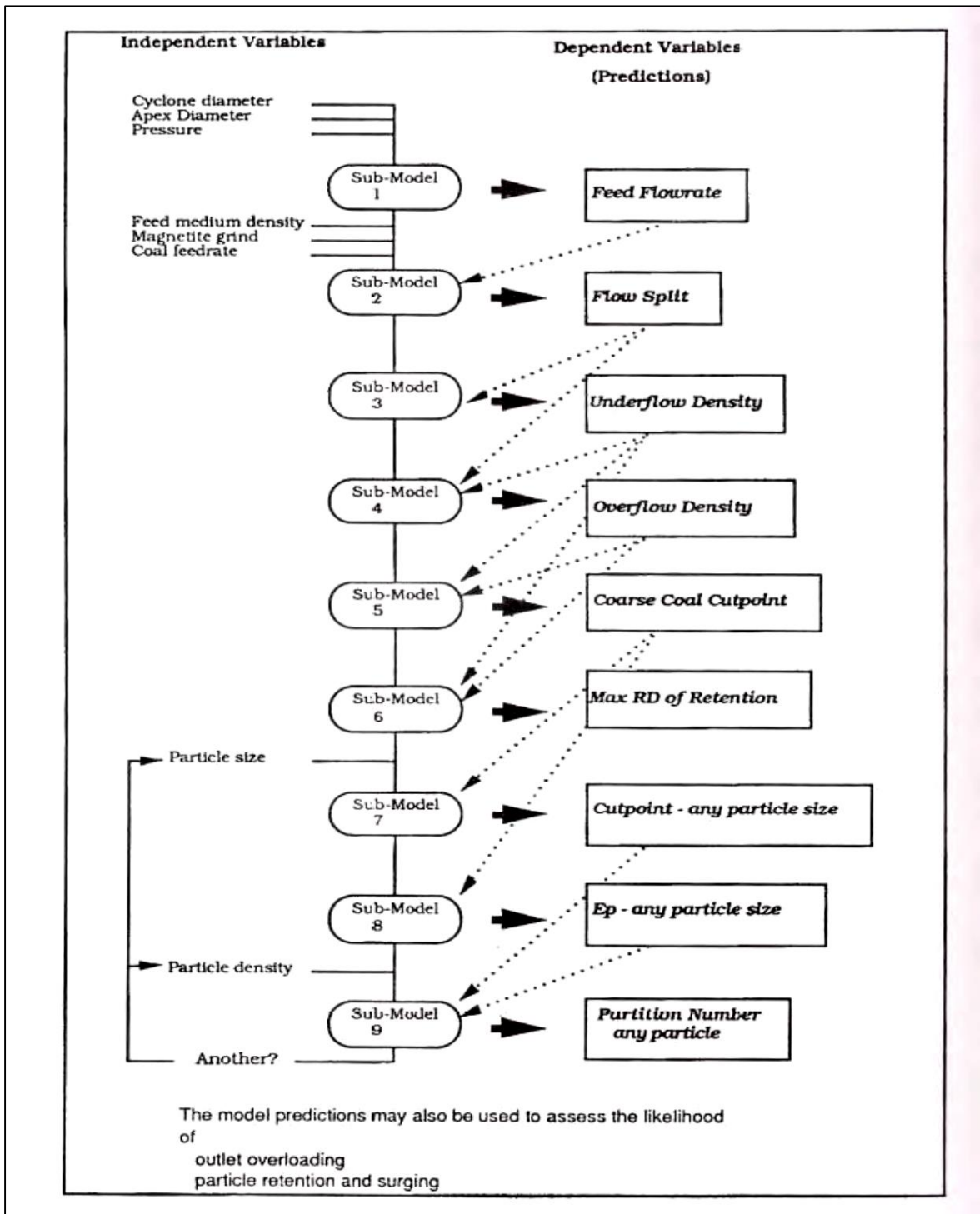


Figure 2.22. Logic flow in the Wood dense medium cyclone model [41]

The mathematical formulations required to model DMCs divided into two main aspects: modelling of medium flow and raw coal particle flow, allowing for their mutual interaction [43]. Computational Fluid Dynamics (CFD) is an important technique in this area. In recent years, the combined approach of CFD and Discrete Element Method (CFD-DEM) has been and is able to demonstrate particle-particle and particle-fluid interactions [9].

2.2.6 Applications

According to (Burt, 1984) heavy medium separation has many applications, and it can be used for the separation of almost any material which has two or more constituents of different specific gravity. Whilst the tonnage of coal treated by HMS probably exceed all other applications put together, heavy medium separation is applied to a wide variety of metalliferous and industrial minerals[44]. Some important non-coal applications of Heavy medium separation and especially HMCs are listed in this section.

2.2.6.1 Iron ore

(Burt, 1984) reported that according to (Anon, 1963) the treatment of iron ore is a major application, and at one time accounted for half of the non-coal applications, particularly in the USA. Both static and dynamic Heavy medium separation is in use. Typical performance of HMS as applied to iron ore is given in Table 2.12 [45].

Table 2.12. Typical Heavy medium separation of Iron ores

Separator	Ore Type	Ore Size (mm)	SG	Feed Fe%	Conc. %Wt	%Fe	Recovery (%)
Drum	Siderite	100-10	2.95	28	87	31.08	97.7
Cyclone	Oolite	8-3	2.64	26	72	32.7	84.0
Cyclone	Hematite	60-6	3.08	35	64	49	94
Cyclone	Goethite	3-0.5	2.71	47	73	57	91

ISCOR's Sishen Mine's iron ore beneficiation plant is one of the best examples of using dense media separation in case of iron ore. This mine was established in 1953 and is situated in the Northern Cape approximately 280km north-west of Kimberley. It is one of the seven largest open cast mines in the world. The Sishen iron-ore-mine produces 3 products with size gradings of 25 to 8 mm, 11 to 5 mm and 5 to 0, 2 mm and has a product capacity of 20 Mtpa. Concentrate is produced at an average Fe content of 66.2 %Fe for the two coarser products and an average of 65.3 %Fe for the fine product. Three stage crushing is practiced to reduce the size of run-of-mine ore to -90 mm after which it is screened into five different size fractions of which four are heavy media beneficiated in static baths and cyclones and the fifth fraction discarded to slimes dams[46]. Figure2.23 shows this plant's schematic flowsheet.

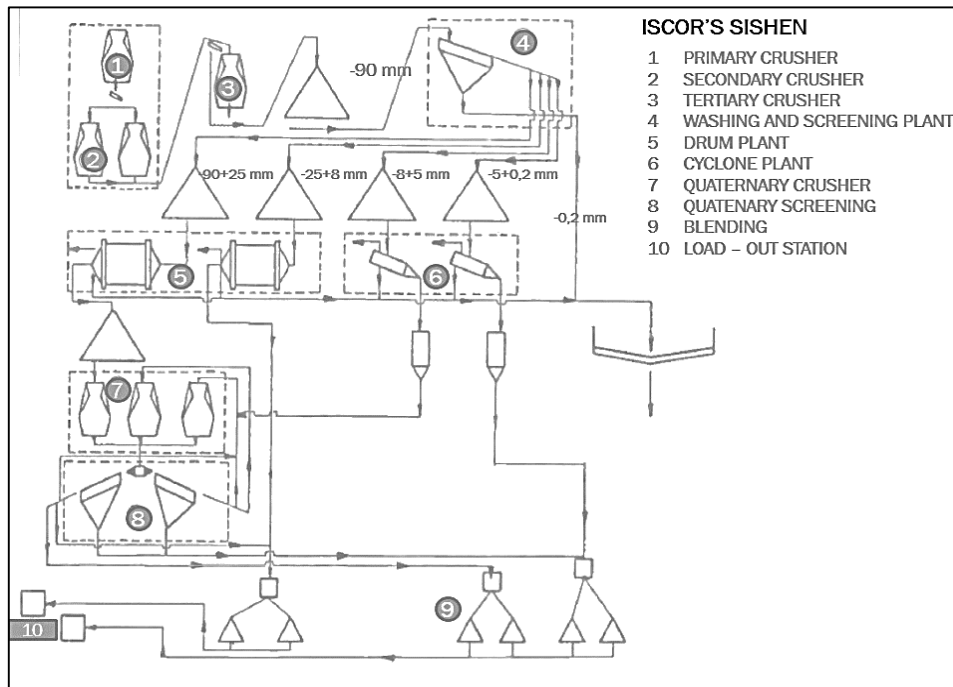


Figure 2.23. Schematic flowsheet of heavy media plant in ISCOR's Sishen iron mine[46]

Atomized ferrosilicon is used in this plant and separation density is near $3 - 3.1 \text{ g/cm}^3$.

2.2.6.2 Diamond

According to Chaston et al [21] a heavy medium technique was first used in diamond processing at Premier Mine in 1946 in the form of heavy medium cones, which were introduced to treat the coarser, +3 mm feed material. The success of these cone installations led to experiments in heavy medium cyclone operation for the recovery of the smaller diamonds down to the lowest size at which diamond recovery is usually attempted 0.5 to 1 mm. Heavy medium cyclone plants were installed at the Williamson Diamond mines in Tanzania in 1955 and now heavy medium cyclones represent the major primary concentration process used in diamond recovery plants. Table 2.13 shows the historical and technical properties of some famous African diamond plants. One of the best examples of using DMS in diamond industry is Argyle diamond plant. The Argyle Diamond Mine is located in the East Kimberley Region in the north of Western Australia, approximately 100km south of Kununurra. The Argyle lamproite pipe is a large diamond deposit of world significance. Proven ore reserves in the pipe's southern section, which has a higher grade than its northern end, are 61 million tones at a grade of 6.8 carats/ton, sufficient to provide for 20 years of operation at the design treatment rate of three million tons of ore a year[47]. Figure 2.24 shows the block flowsheet of this plant. According to the flowsheet this plant has two stages of DMC processes that second cyclone cleans first cyclone's underflow.

Heavy medium cyclone efficiency is extremely good (Table 2.14) and partition curves are very sharp with low of E_p [47].

2.2.6.3 Lead- Zinc

The viability of a dense medium process is based initially on the difference in density of the mineral species to be separated. Silicious gangue (2650 g/cm^3) and galena (7580 g/cm^3) are obvious examples of minerals which could be separated in a dense medium of intermediate density.

Where any inherent density differential will only become apparent upon crushing to achieve a degree of liberation and there is no near gravity materials, dense medium separation could be used as pre-concentration purpose. For example, in 1980s dense medium pre-concentration was considered in Mount-Isa lead-zinc and silver beneficiation plant because studies showed that 30% of run-of-mine ore could be rejected at approximately 96% metal recoveries and it was possible to increase plant lead output from 50000 to 180000 tons per annum without changing existing grinding circuit capacity.

Figure 2.25 and Table 2.15 show the schematic flowsheet and metallurgical features of Mount-Isa pre-concentrator plant respectively. Feed density distribution and partition curve parameters of this plant in different pulp densities is shown in Table 2.16 [27].

Table 2.13. Historical and technical information about African Diamond plants[21]

Mine	Year installed	Feed to cyclone t/h	Feed size range (mm)	S.G of medium (Feed)	Type of medium	Medium use (g/t)	Conc ratio	Diamond recovery
Williamsons	1955	155	-6+1	2.05	80%Man 20% FeSi	1600	1:475	97
Premier mine	1964	160-200	-6+3	2.30	65DFeSi	300	1:250	97
Dreyars pan	1966	21	-20+2	2.30	100DFeSi	600	1:50	99
CDM No1	1968	80	-25+2	2.76	100DFeSi	450	1:65	99
CDM No4	1969	360	-25+2	2.72	100DFeSi	400	1:50	99
Premier mine (RP)	1970	340	-8+1.8	2.62	65DFeSi	350	1:125	98
Orapa	1971	350	-25+1.6	2.55	100DFeSi	350	1:100	98
Koffiefontein	1971	560	-30+0.5	2.71	100DFeSi	700	1:300	98

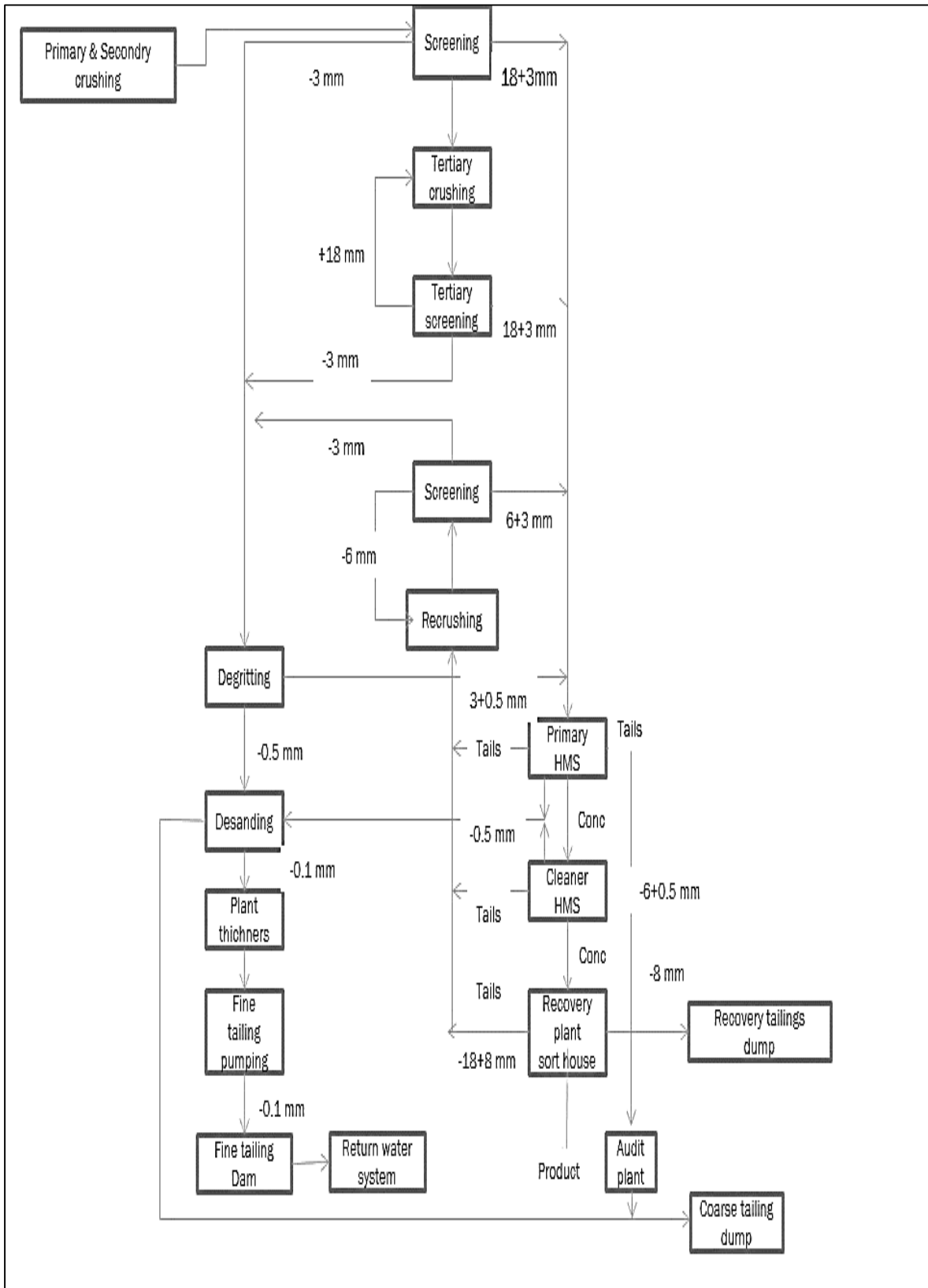


Figure 2.24. Argyle process plant - block flowsheet[47]

Table 2.14 Efficiency features of Argyle diamond DMC plant[47]

Observation	1	2	3	4	5	6	
Module Feed (S.G)	2.62	2.63	2.65	2.51	2.62	2.64	
S.G ₅₀	2mm	3.22	-	3.18	3.02	3.01	3.03
	6mm	3.18	3.09	3.15	3.04	3.00	3.03
	10mm	3.10	3.03	3.05	3.10	2.98	3.02
Ep	2mm	0.08	-	0.08	0.02	0.3	0.03
	6mm	0.05	0.02	0.02	0.01	0.01	0.3
	10mm	0.01	0.01	0.01	0.03	0.02	0.01

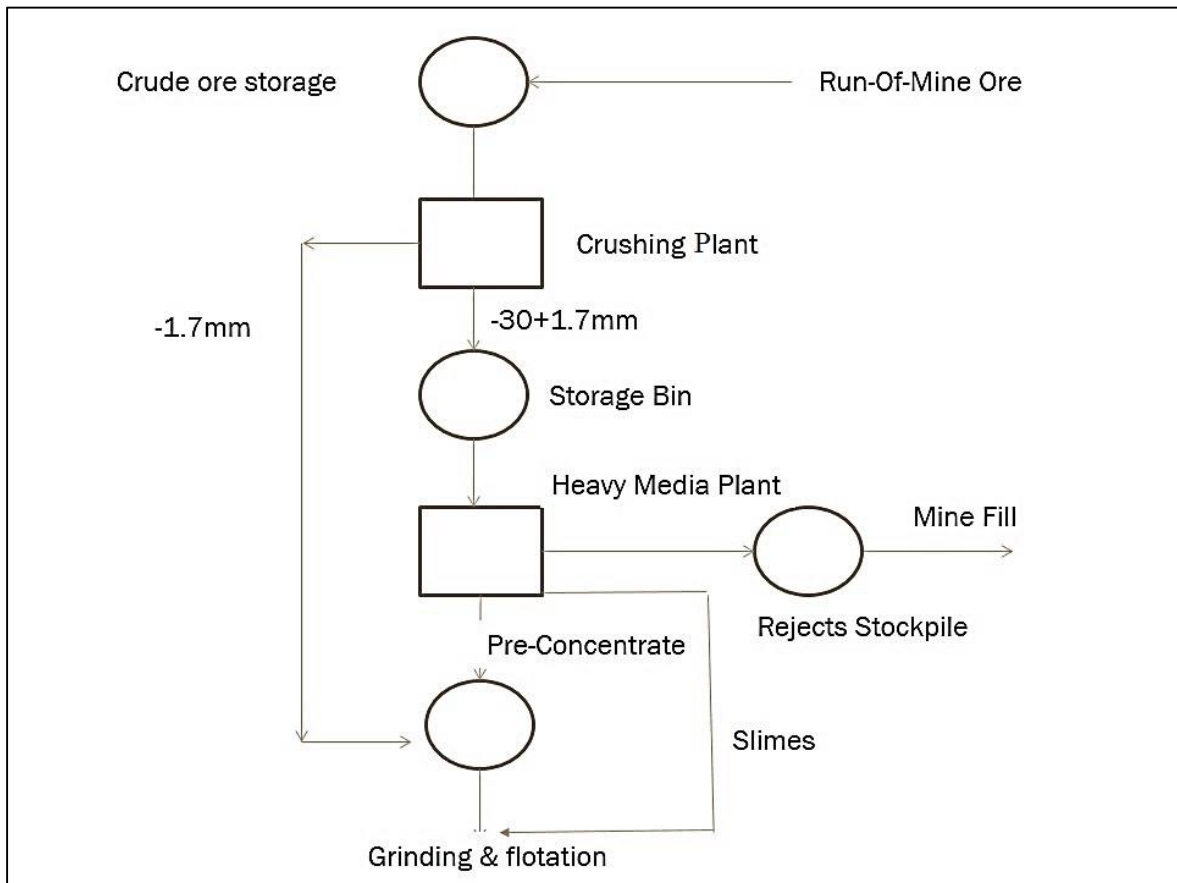


Figure 2.25. Schematic flowsheet of Mount-Isa pre-concentration plant[27]

Table 2.15. Metallurgical features of pre-concentration plant in Mount-Isa [27]

Stream	tph	% of Feed	Assay			%Metal Distribution		
			% Pb	% Zn	% Ag (g/t)	Pb	Zn	Ag
Feed	800	100	6.70	6.70	160	100.0	100.0	100.0
Pre-concentrate	534	66.75	9.63	9.65	230			
Slimes	6	0.75	11.8	7.20	250	97.3	97.0	97.3
Rejects	260	32.5	0.56	0.63	13	2.7	3.0	2.7

2.2.6.4 Chromite

According to (Burt, 1984) chromium is one of the most widely used and versatile of all the elements. It is used in metallurgical, chemical and refractory industries. In the metallurgical industry chromium is an essential component of stainless steels. Tool and alloy steels, heating elements and for plating metals. In its mineral form it is used as a refractory for lining high temperature furnaces, and in cement and glassmaking industries[48].

Chromite has the general formula: $(Cr, Fe, Al)_2 O_3 (Fe, Mg) O$. Aluminum and iron can substitute for chromium, whilst Manganese can substitute for iron in the Lattice. Gravity concentration is ideally suited to the upgrading of the chromite. Many chromite recovery plants are relatively simple. Many include heavy medium separation, either as a pre-concentrator, or to produce a finished product[44].

For example the Troodos mine, which was in operation in Cyprus until suspension in mid-1982, produced much of its concentrate as -65 +20mm lump. The plant utilized a range of gravity concentration equipment, from heavy medium separation to a Bartles Crossbelt concentrator.[44]

Table 2.16. Feed density distribution and partition curve parameters of Mount-Isa HMS plant in different pulp densities[27]

Ore size mm	Feed Parameters			Efficiency Parameters		
	μ	σ	SG _{min} g/cm ³	SG ₅₀ g/cm ³	E _p g/cm ³	Rejects %
Medium Density 2460 g/cm³						
-4.0+3.3	-2.04	2.64	2780	2910	64	35.1
-3.3+2.3	-2.15	2.91	2790	2920	56	37.9
-2.3+2.0	-2.11	2.89	2790	2930	72	37.4
-2.0+1.7	-	-	-	2940	61	46.2
-1.7+1.0	-	-	-	2980	111	57.5
Medium Density 2680 g/cm³						
-13.0+8.0	-1.86	2.15	2770	3030	38	45.9
-8.0+5.6	-1.79	2.67	2880	3030	37	45.5
-5.6+4.0	-1.96	2.69	2780	3000	50	45.6
-4.0+2.0	-2.05	2.70	2780	3010	55	47.1
-2.0+1.7	-2.27	3.04	2790	3060	73	63
-1.7+1.0	-	-	-	3180	107	64.6

The schematic flowsheet given by Burt [44] (Figure 2.26) is based on the Mousoulos and papadopoulos's paper[49]. Ore, grading approximately 30% Cr₂O₃ was crushed to 65mm (1), and then sized into three fractions: -65+20mm, -20+4mm and -4mm (2). The two coarse fractions are fed to Wemco heavy medium separators (3, 7). The separator (3) handling the coarsest fraction operated at an effective density of 3550 g/cm³ using atomized ferrosilicon.

Table 2.14 (continued)

Ore size	Feed Parameters			Efficiency Parameters		
mm	μ	σ	SG _{min}	SG ₅₀	E _p	Rejects
			g/cm ³	g/cm ³	g/cm ³	%
Medium Density 2860 g/cm³						
-13.0+8.0	-2.18	2.81	2790	3060	28	53.1
-8.0+5.6	-1.89	3.01	2780	3060	34	49.6
-5.6+4.0	-2.18	2.70	2780	3060	43	53.2
-4.0+3.3	-2.24	2.74	2780	3100	45	56.2
-3.3+2.3	-2.06	2.68	2770	3100	55	53.7
-2.3+2.0	-2.03	2.69	2770	3120	68	54.2
-1.7+1.0	-	-	-	3270	152	64.5
-1.0+0.7	-	-	-	3450	215	70.2
-0.7+0.5	-	-	-	3610	301	71.7
-0.5+0.25	-	-	-	4020	506	71.9

Sinks then upgraded by hand picking and floats passed, with the mid-size fraction the second drum (6) separating at 2800 g/cm³ which rejected the flow fraction. Intermediate sinks were screened (9) at 20mm and 1mm, the +20 fraction being crushed in two stages (10, 11) to 12mm, the -20+1mm fraction from the screen passing to heavy medium cyclone (13) with effective separating density of over 3550 g/cm³, a finished grade intermediate product. Cyclone reject along with screen crushed oversize were ground in rod mill (16) and, with screen (9) undersize at 2mm (18), screen oversize being circulated to the mills and undersize being further processed on a bank of tables (19). The finer fractions of the table tailing were later scavenged on a Bartles crossbelt concentrator (22). Recoveries in excess of 90%, to a grade of 48% Cr₂O₃ and a chromite iron ratio of 2.75 were claimed for this portion[49].

2.2.6.5 Fluorspar (Fluorite)

Whilst flotation is the major method of fluorspar concentration, pre-concentration using heavy medium separation is used in some operations. Burt [44] reported that according to Ryan [50] and Anon [51] one significant producer using heavy medium separation is the Buffalo Fluorspar Mine, Transvaal, South Africa. The flowsheet of the ore preparation and pre-concentration circuits are shown in Figure 2.27.

Ore with an average fluorspar content of 18% is crushed in 3 stages to 12 mm (1-6) with crushed ore passing to 2, 1000 t bins (7). Ore from the bins passes to preparation screens (8) sizing at 1.9mm. Oversize which approximately 280 t h^{-1} is subjected to heavy medium separation using Dyna Whirlpool separators (9) using ferrosilicon as the medium. Underflow pass to medium recovery wash screens (10) and thence to the main mill ore bins (15), whilst overflow, after medium removal (11) rejected to wastes. Fines from preparation screen (8) are sized at 0.04mm by cyclone (12) and dewatering screens (13) in series, and +0.04 mm fraction pass direct to the mill ore bins (15). The -0.04 mm fraction is thickened (14) and pumped direct to the flotation plant. The pre-concentration plant rejects approximately 60% of plant feed, prior to grinding and flotation stages [50].

2.2.6.6 Manganese Ores

According to Burt [44] manganese is one of the “steel industry” metals. The most important manganese ore is pyrolusite (MnO_2) and over 90% of manganese ore produced is used in the iron and steel industries, where it is an essential additive in the steel making process. The remaining 10% of that produced is used in a variety of industries including chemicals, fertilizers, batteries and ceramics[52].

The Groote Eylandt Mining plant in northern Australia which produced approximately 10% of total non-Soviet production. Here concentration was by heavy medium separation, as shown in Figure 2.28 [53].

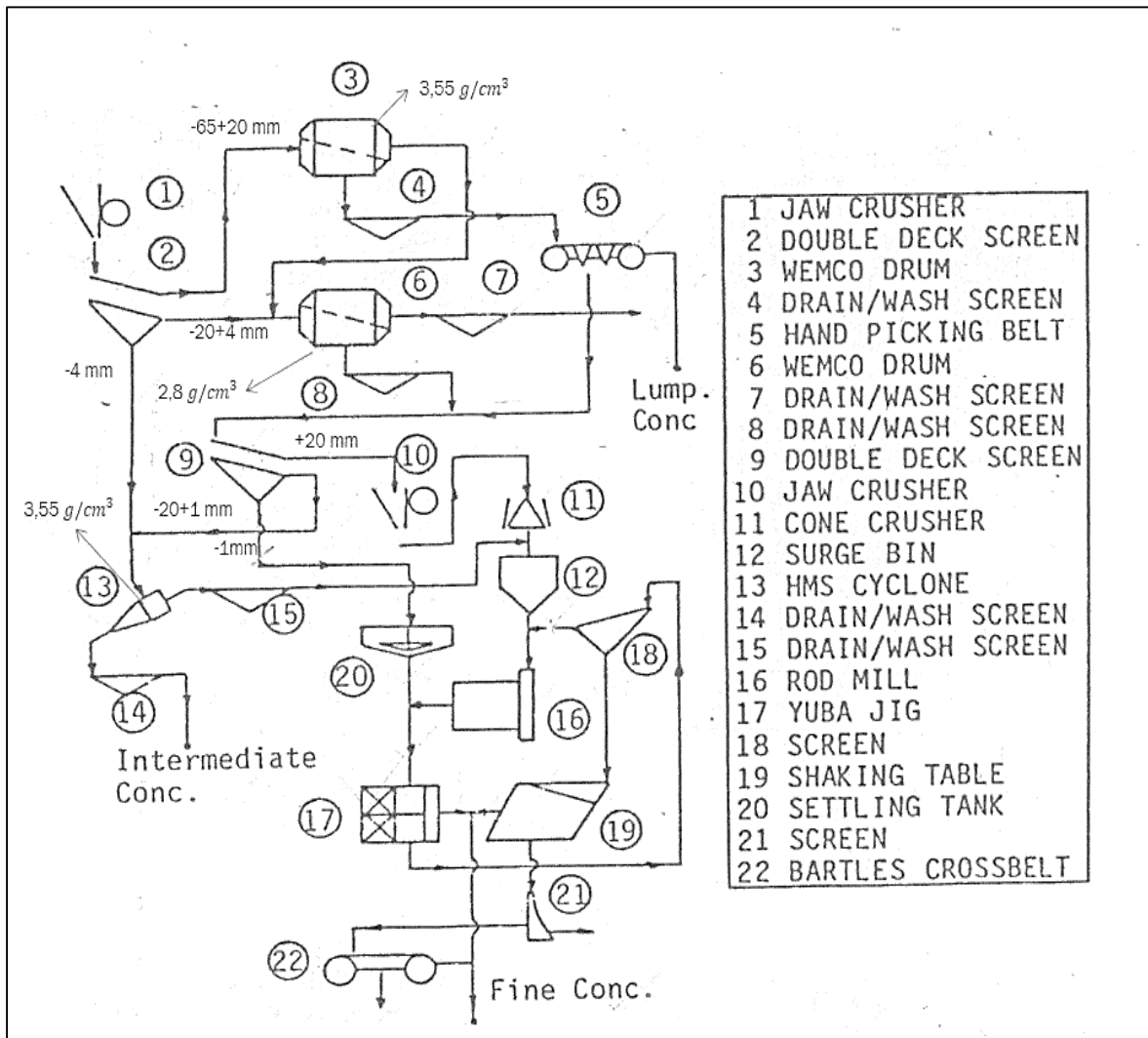


Figure 2.26. Schematic flowsheet of Troodos chromite mine, Cyprus[49]

As Burt [44] reported mine ore is crushed in two stages to 75 mm by gyratory crushers, the secondary unit being in closed circuit (2). Crushed ore is sized, on double deck screen at 6mm (3) oversize passing to a surge bin (4). Undersize is classified at 0.5mm (5) the -6.0 +0.5mm, fines, fractions passing to a second surge bin, whilst the -0.5mm fraction is sized, by cyclone and classifier for rejection either as backfill or to tailing ponds. The +6mm lump ore and -6 +0.5mm fines are treated in two heavy medium separation circuits. From the surge bins material is conveyed rotary drum scrubbers (6, 7), the product from which is screened on double deck screen (8, 9). Screen oversize passes to surge bins (10) and thence to a heavy medium drum separator (11) separation with densities up to 3.6 kg L⁻¹, using spherical ferrosilicon, underflows are drained and washed (13) and stored in product bins.

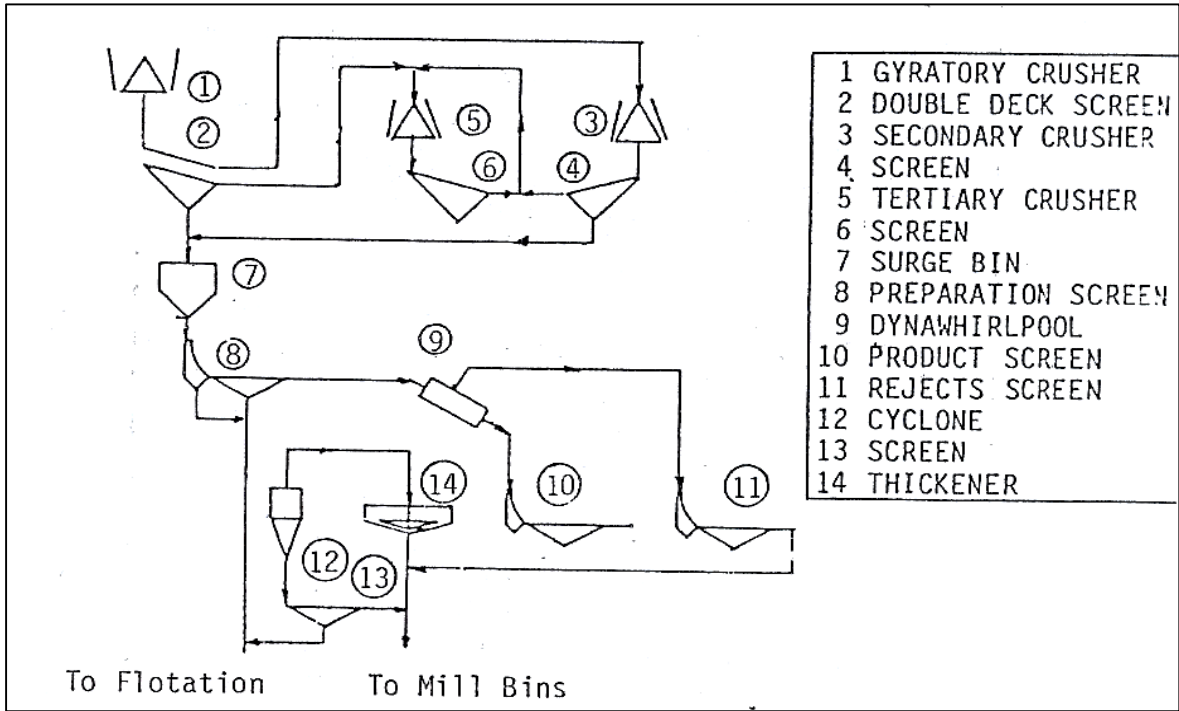


Figure 2.27. Crushing and pre-concentration at Buffalo Fluorspar Mine, South Africa[50]

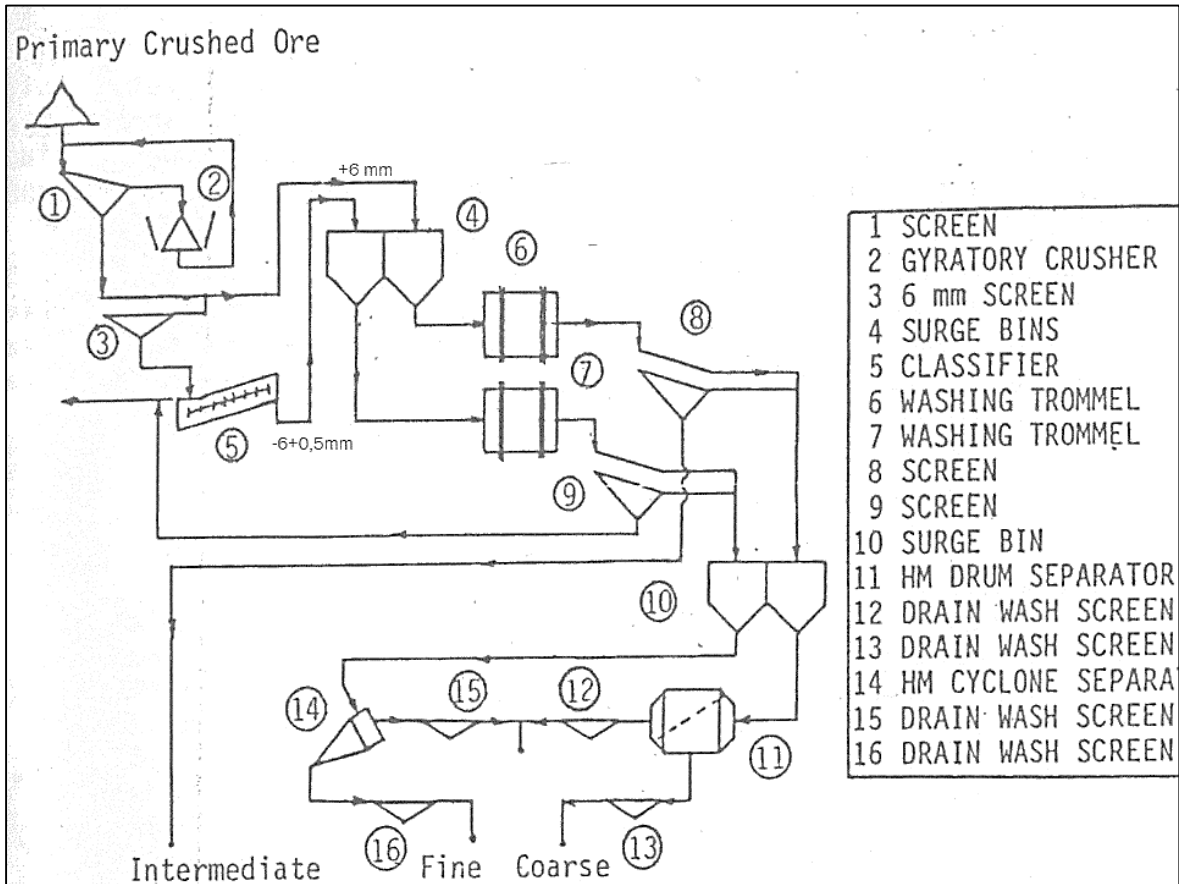


Figure 2.28. Schematic flowsheet at Groote Eylandt Mining Co. Australia[53]

2.2.6.7 Tungsten Ores

Wolframite is the main mineral of tungsten. The largest wolframite mine in Europe is Panasqueira of Beralt Tin & Wolfram, in the ancient mining district of Serra Estrela, Portugal. Mining commenced in 1912 and has continued thereafter. The largest expansion commenced in 1977 with a new inclined shaft to open up lower ore horizons and development of the Barroca Grande pre-concentration plant, with pre-concentrates being upgraded, at the rate of 160 t/d, at the older Cabeça do Plato plant. According to Burt [44] a schematic flowsheet of the Barroca Grande pre-concentrator is shown in Figure 2.29 [54]. Ore from underground is crushed in a two stage closed circuit, crushed product being sized on the heavy medium preparation screens (6), oversize passing to a suitable surge bin (11). Screen undersize is classified in two cyclone banks, in series (7, 9) prior to further screening on an aero vibe screen (10); oversize passing to the heavy medium surge bin. The heavy medium vessel Stamicarbon 500mm dia. cyclone (12) using up to 0.5 kg of ferrosilicon per ton as medium. Sinks and floats are each drained (13, 14) and the concentrate sent to the Cabeça do Palo plant for upgrading by grinding, tabling and magnetic separation [44]

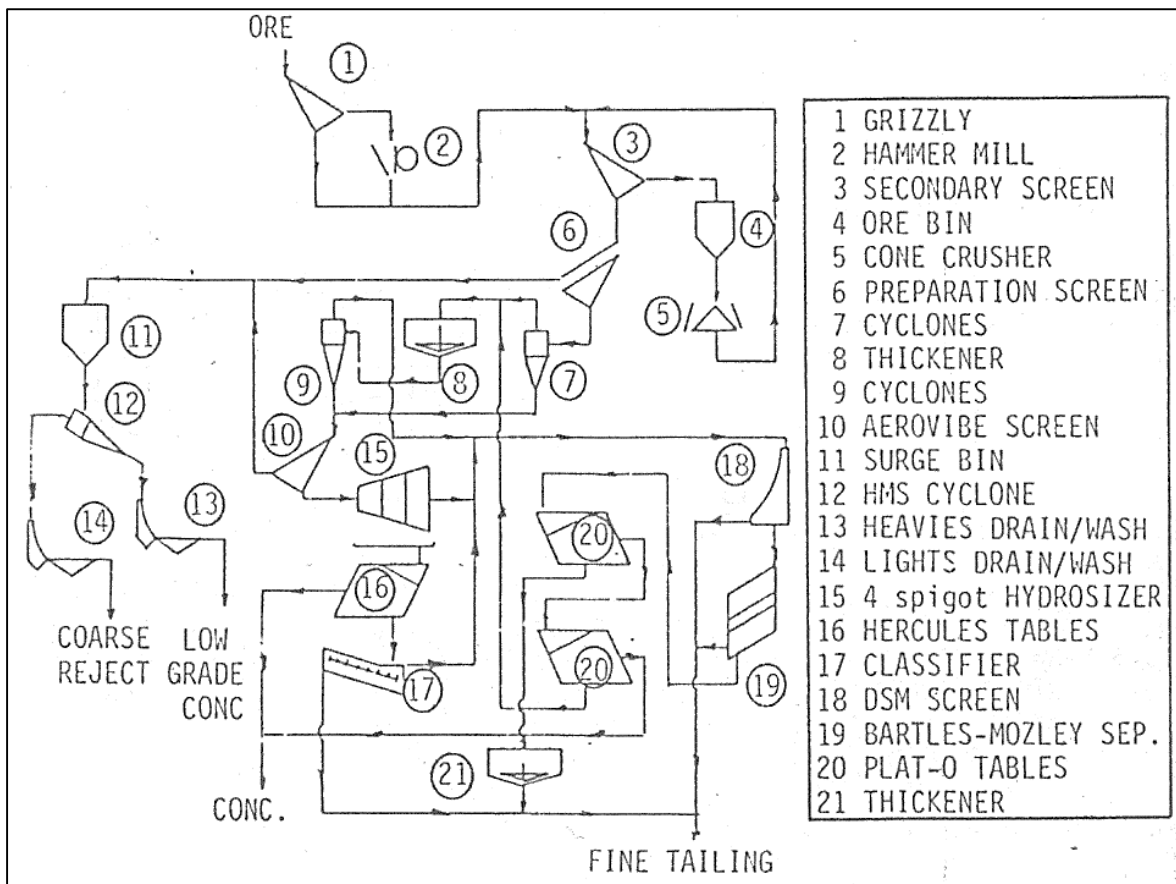


Figure 2.29. The Barroca Grande pre-concentrator of Beralt Tin & Wolfram, Portugal[44]

2.2.6.8 Andalusite

Andalusite (Al_2SiO_5) is one of the more desirable high alumina content aluminosilicates used for the manufacture of refractories. Andalusite refractories are favored over other high alumina minerals in abrasive conditions and where resistance to high temperatures and thermal shock are required[55].

According to Burt [44], Carroll and Matthews [56] reported a typical flowsheet for the treatment of a primary South African andalusite ore (Figure 2.30). Ore is crushed in a roll crusher (1) and fed, via wet screens (2) to a washing, desliming circuit consisting of washing trommels (3) and cyclones (16). The washing trommels reject the +25mm to waste, whilst the cyclones deslime the fines at 0.6mm. The -25 +0.6mm fractions is attrition milled (4) and again wet screened (5) to remove slimes and to upgrade the material to approximately 50% andalusite. This material passes to the primary heavy medium cyclone separator (6), the andalusite concentrate (sinks), after medium removal by screens (7) being dried (8) and subjected to high intensity magnetic separation (9) grading over 57% andalusite and less than 1% iron. Primary reject is treated in a secondary heavy medium cyclone separation circuit (11-5) to produce second grade product grading 54% andalusite with less than 1.8% iron.

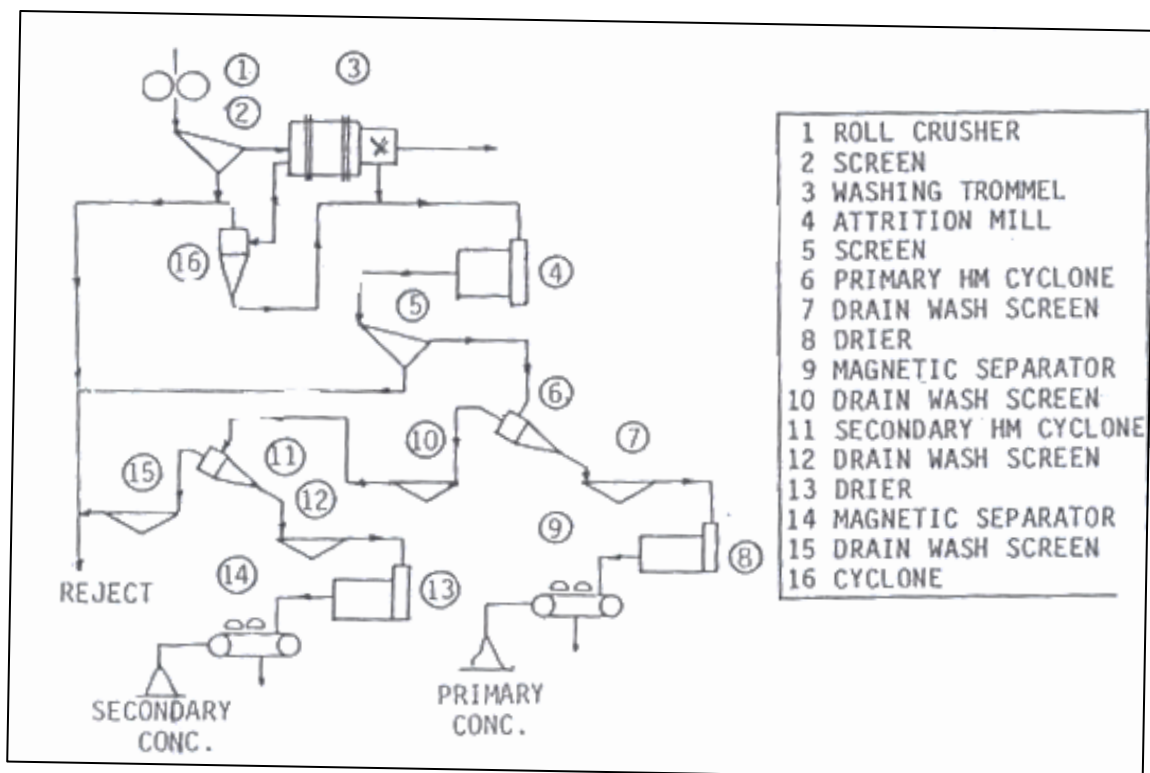


Figure 2.30. Andalusite treatment at a South African plant[56]

3 Experimental Studies and Results

During this study, different kinds of minerals were studied to investigate their behavior at different densities. In this section, first feed characteristics in terms of type, size, mineralogy and etc. will be discussed separately then used method will be described and finally the results will be shown for every mineral.

3.1 Feed Characteristics

3.1.1 Iron Ore

-9.5mm iron ore, which was the tailing of laboratory scale low intensity magnetic separation process, was blended and a sample was taken. Then, size distribution of sample determined. According to the magnetic separation method, it was assumed that the tailing of the process does not have any magnetite mineral. Figure 3.1 shows the schematic illustration of laboratory scale magnetic separation and Figure 3.2 shows distribution of the given sample.

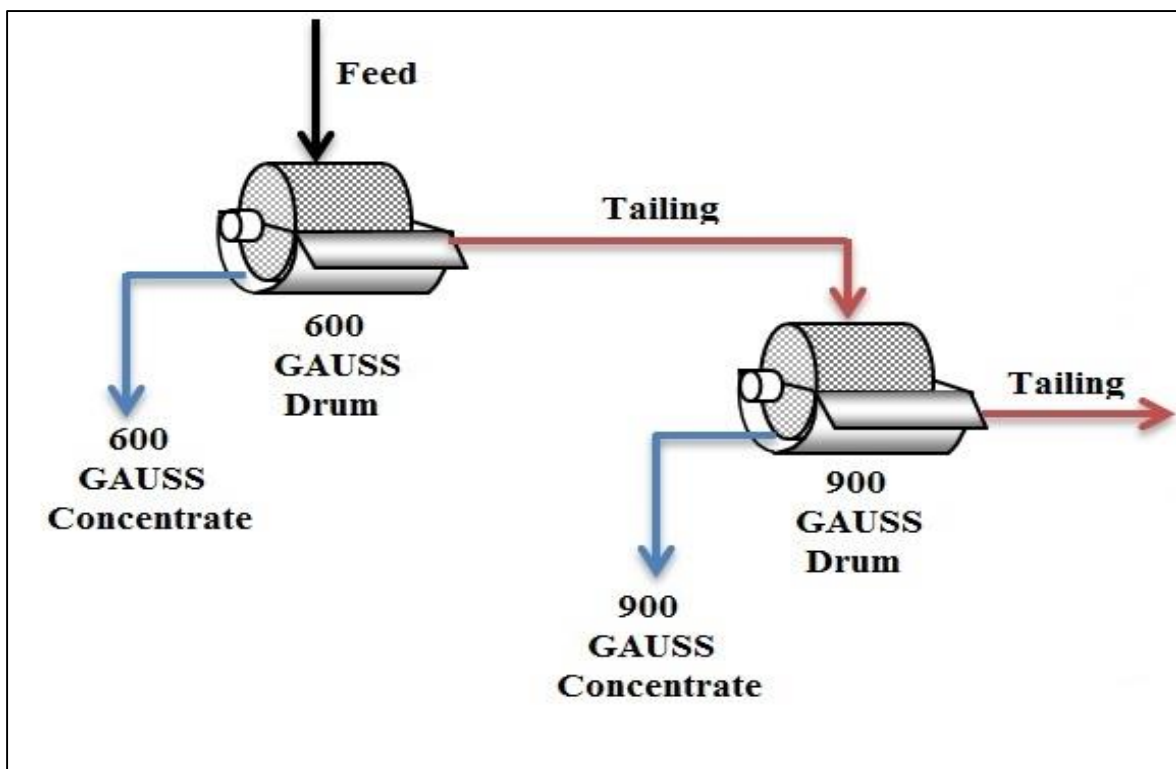


Figure 3.1. Schematic illustration of magnetic separation process

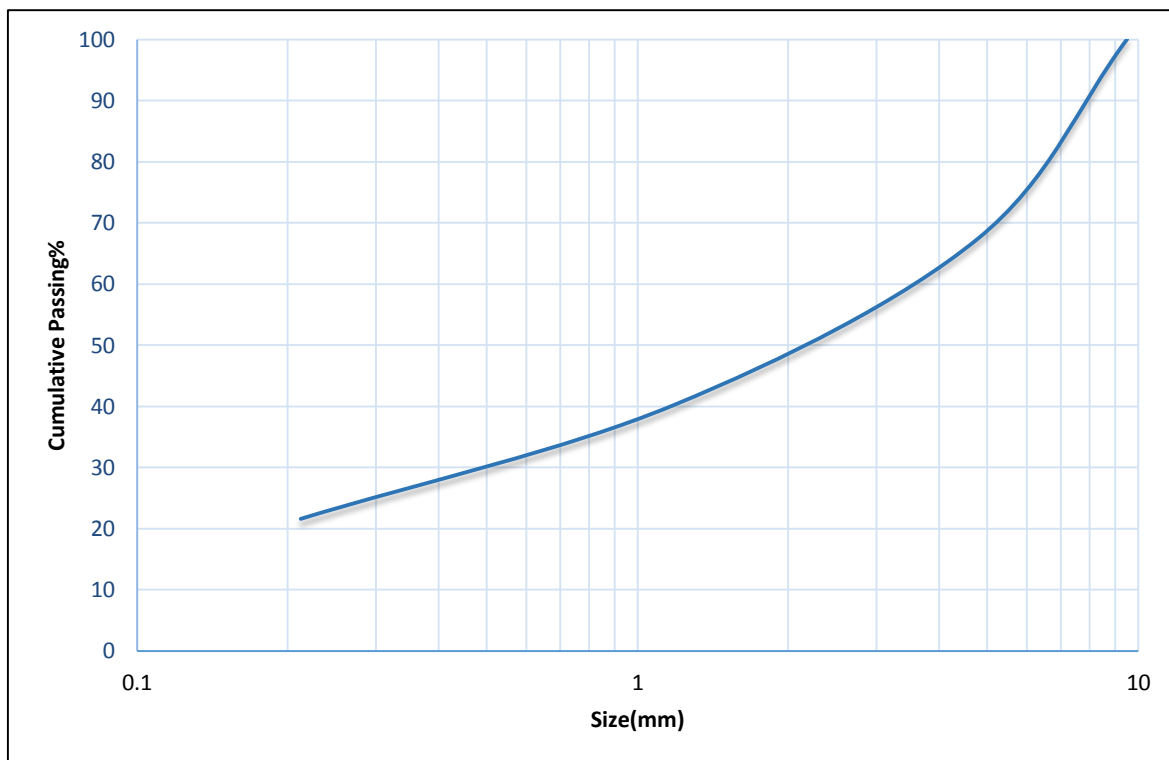


Figure 3.2. Size distribution analysis of iron ore sample

Chemical analysis showed that Fe content of the sample is 31.9% and according to the XRD analysis results Fe element mostly related to hematite (Fe_2O_3) with specific gravity of 5.26 and goethite ($\text{FeO}(\text{OH})$) with specific gravity of 3.3-4.3. Also specific gravity of the sample was measured as 3.18. After size distribution analysis of the sample, new samples were taken at -9.5+4.75 mm, 4.75+1.18mm, -1.18+0.212mm and -0.212mm size fractions and these samples were prepared for sink-float tests.

3.1.2 Manganese Ore

All of the 65kg manganese ore sample was crushed by a jaw crusher in the laboratory to -16mm and then new sample was taken with coning-quartering method. The results of the size distribution analysis is given in Figure 3.3.

The specific gravity of the feed sample was calculated to 3.07 and the Mn content of the sample was 25.47%. According to the XRD analysis, the main manganese mineral in the sample was pyrolusite (MnO_2) with specific gravity of 4.4-5.06 and the main gangue mineral was quartz with specific gravity of 2.59-2.63. Taken sample was divided into four size fractions (-16+5mm, -5+1mm, -1+0.2mm and -2mm) for sink-float tests.

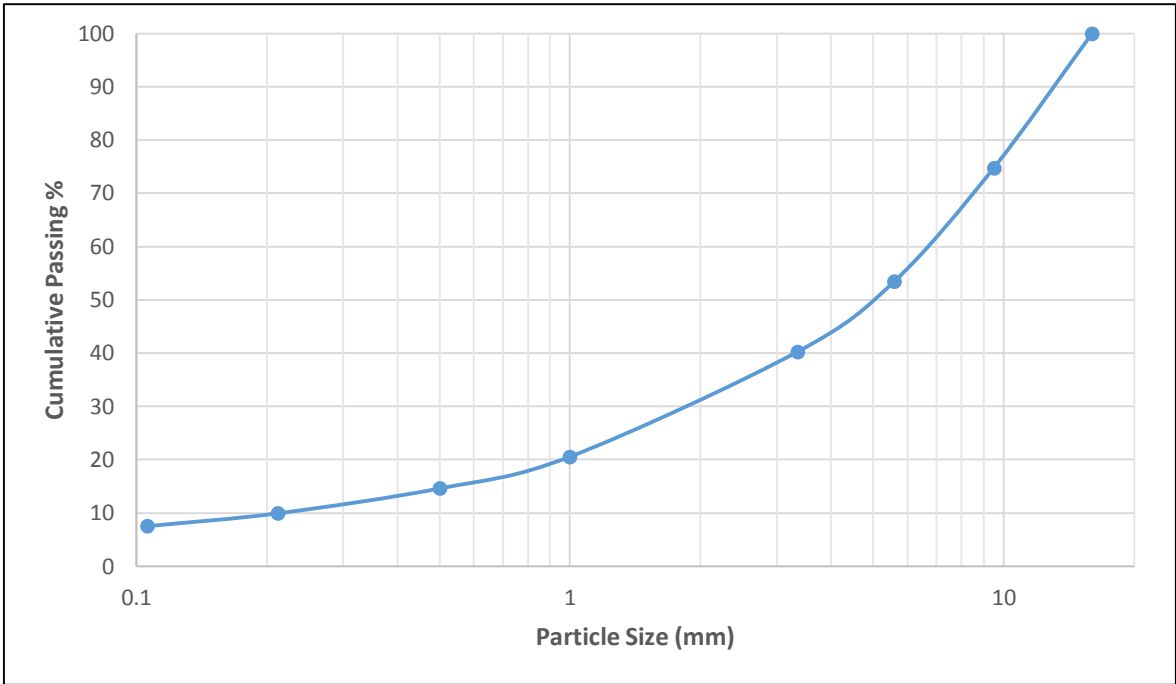


Figure 3.3. Particle size distribution of crushed manganese ore sample

3.1.3 Chromite ore

Chromite ore sample was taken from rod mill discharge of Sivişli mine plant in Adana region of Turkey and Size distribution, chemical and mineralogical analysis and fractional liberation degree of the sample was determined. Figure 3.4 shows the particle size distribution of the sample.

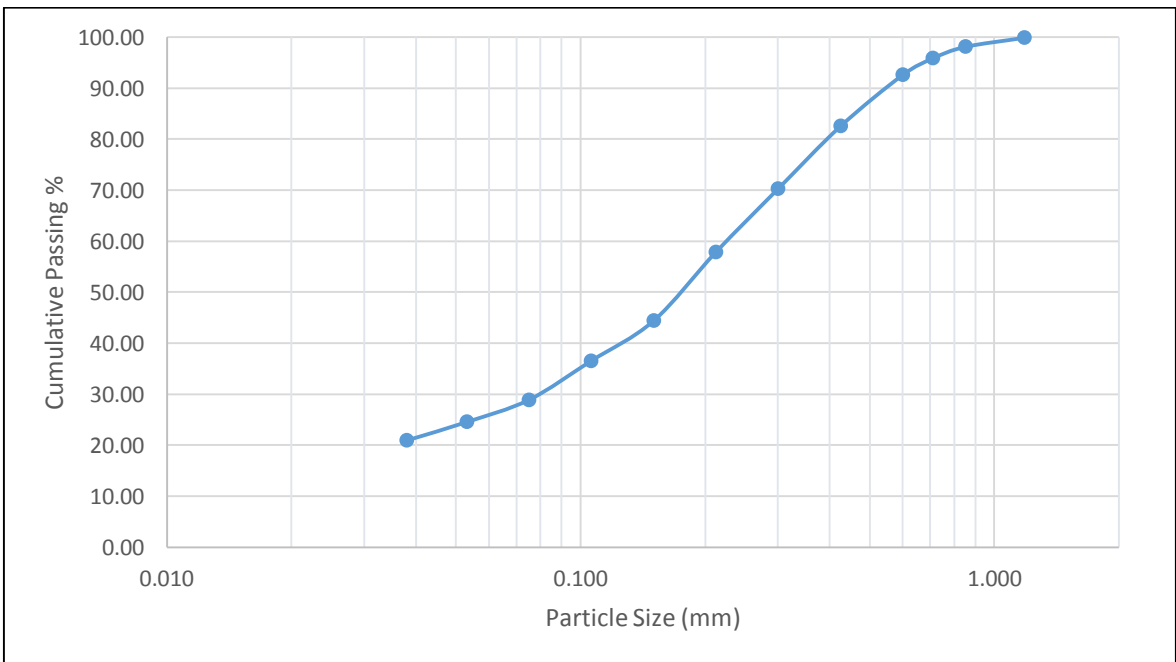


Figure 3.4. Particle size distribution of chromite ore sample

In order to get a quantitative measure about liberated and locked particles and their effects on separation method, degree of liberation determined for different size fractions of the sample. This test was done by counting liberated and locked particles using stereo microscope. Table 3.1 shows degree of liberation of different size fractions of the target ore and Figure 3.5 shows pictures of different size fractions.

For determination of Cr₂O₃ content of the feed and different size fractions of it, chemical analysis were done in the laboratory using titration method. Table 3.2 shows the results.

According to XRD analysis ore consists of magnesiochromite ((Mg,Fe)(Cr,Al)₂O₄) with specific gravity of 4.2, magnesite (MgCO₃) with specific gravity of 3-3.2, chromite (FeCr₂O₄) with specific gravity of 4.5-4.8, lizardite (Mg₃(Si₂O₅)(OH)₄) with specific gravity of 2.38 and Chrysotile Mg₃(Si₂O₅)(OH)₄ with specific gravity of 2.53. Figure 3.6 shows the XRD pattern of the sample.

Mean specific gravity of the feed sample was measured as 2.58.

Table 3.1. Degree of liberation for different size fractions of Sivişli chromite ore

Size Fraction (µm)	Degree of Liberation (%)
-850+600	3.89
-600+425	26.77
-425+300	35.21
-300+212	53.39
-212+150	71.97

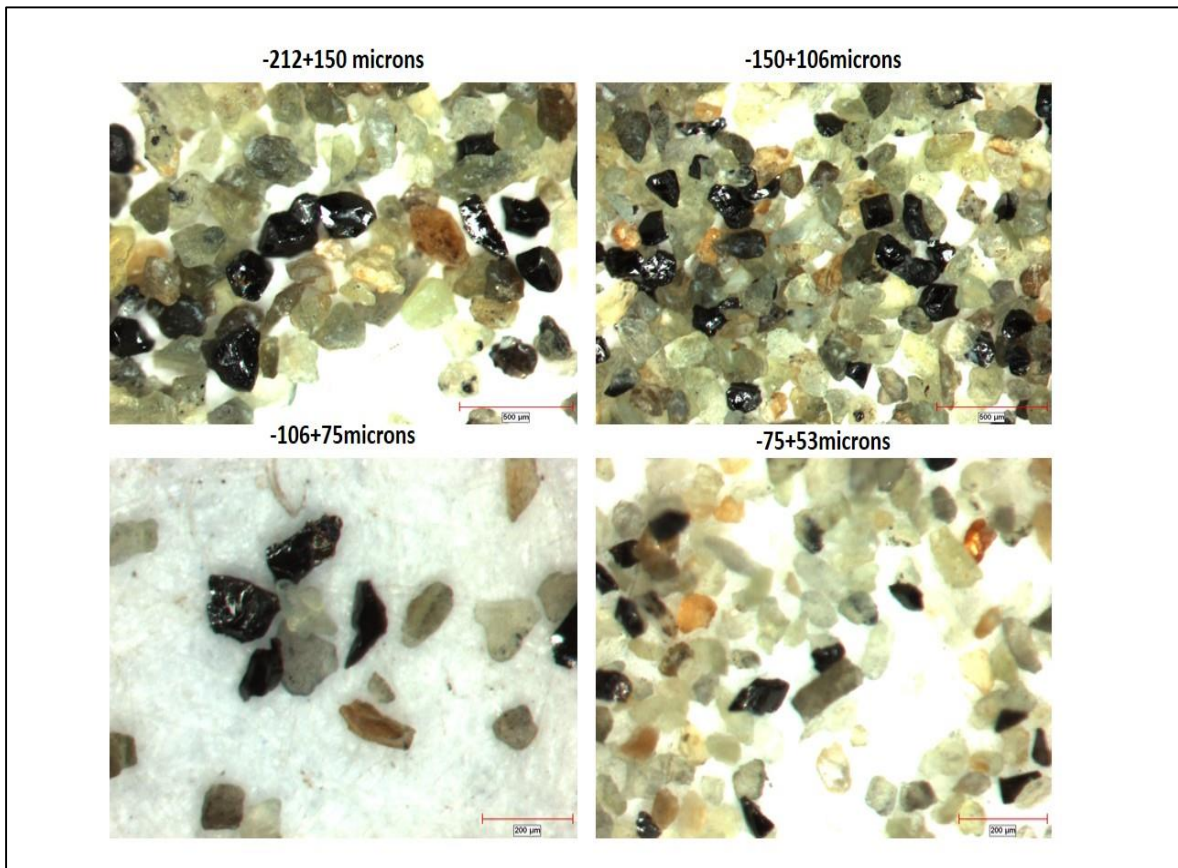


Figure 3.5. Photomicrographs of four different size fractions of chromium sample

Table 3.2. Cr₂O₃ content of different size fractions of chromite ore sample

Size Fraction (μm)	Weight (%)	Cr ₂ O ₃ (%)	Cr ₂ O ₃ Distribution (%)
-1180+425	18.29	3.53	11.49
-425+212	24.75	5.84	25.73
-212+150	13.44	7.50	17.93
-150+106	7.83	9.19	12.80
-106+75	7.64	9.00	12.23
-75+53	4.36	7.42	5.75
-53+38	3.60	6.10	3.90
-38	20.10	2.85	10.18
Total	100.00	5.62	100.00

3.1.4 Zinc Ore

There were two samples of zinc ore that were taken from two different parts of a zinc processing plant. These two samples were named sample1 and sample 2 then were reduced to about 1kg from every sample with coning and quartering method. Size distribution analysis were done on both samples and produced size fractions were combined in three size intervals: $-8+1.7\text{mm}$, $-1.7 +0.212\text{mm}$ and -0.212mm . Figure 3.7 shows particle size distribution for sample1 and sample2.

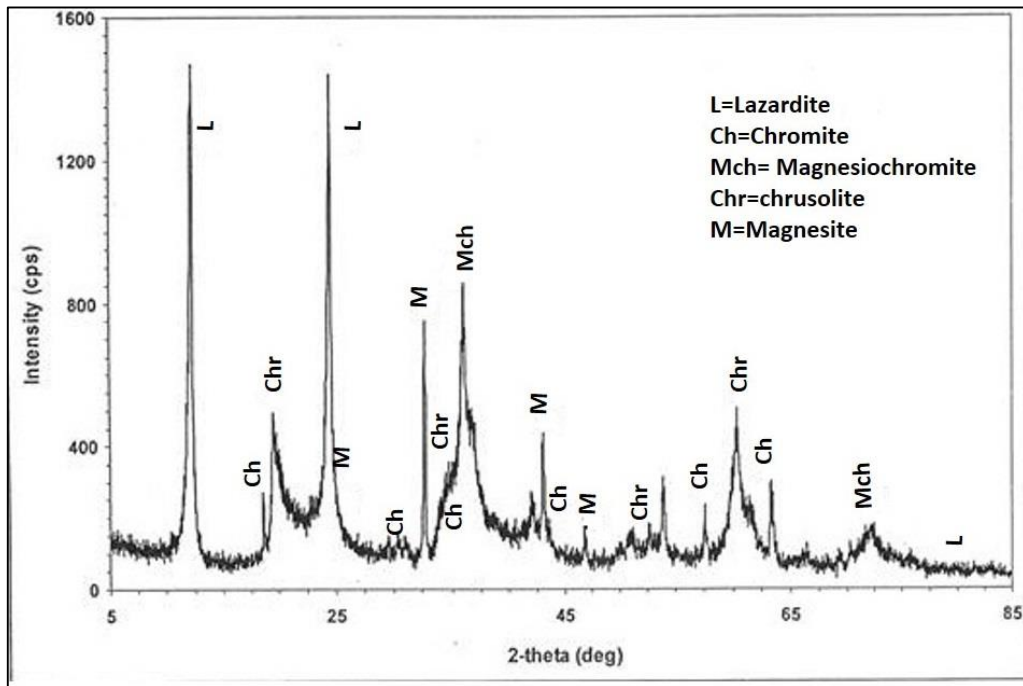


Figure 3.6. XRD pattern for chromite ore

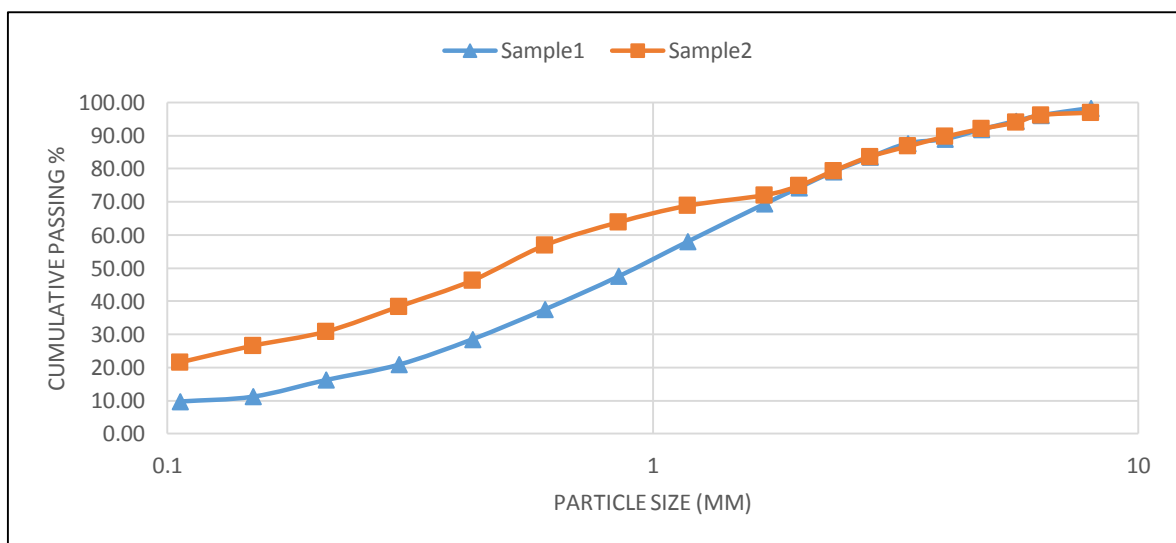


Figure 3.7. Particle size distribution for two Zinc samples

3.2 Methodology

After characterizing and preparing ore samples in narrow size fractions, sink-float tests were done. Doing sink-float tests for high density materials has been a challenging issue. In this section used sink-float method will be described.

3.2.1 Background

Heavy liquids have wide use in the laboratory for the appraisal of gravity-separation techniques on ores. The aim is to separate the ore samples into a series of fractions according to density, establishing the association between the high and low specific gravity minerals. The mineral grains either ‘sink’ or ‘float’ in the heavy liquid selected and are recovered for further analysis. As described in section 2 there are variety of heavy liquids and suspensions that have been used for different minerals but unfortunately most of them are highly toxic and highly viscous.

3.2.2 Organic Heavy Liquids

Unfortunately, there are only a limited number of high density (‘heavy’) liquids and these tend to be more toxic as their density increases. The most commonly used heavy liquids in these analyses are volatile halogenated organic solvents (e.g. diiodomethane, relative density 3.31). Tetrabromoethane (TBE), having a relative density (RD) of 2.96, was commonly used and may be diluted with white spirit or carbon tetrachloride to give a range of densities below 2.96. Using such heavy liquids, acetone can be used as a diluent and for washing the organic from the separated products. Considerable effort must be expected in handling volatile, flammable and toxic organic liquids in sample washing and recovery (recovery of TBE is often only 90%). Bromoform (relative density 2.89) may be mixed with carbon tetrachloride (relative density 1.58) to give densities in the range 1.58–2.89. For densities of up to 3.3, diiodomethane (methylene iodide) is useful, diluted as required with triethyl orthophosphane. However, this presents significant health and safety hazards.[57]

In this research densities under 2.9 were provided using tetrabromoethane (TBE) and acetone combination.

3.2.3 Inorganic heavy liquids

Aqueous solutions of sodium polytungstate (SPT) have certain advantages over organic liquids, such as being virtually non-volatile and non-toxic, and densities of up to 3.1 can be achieved. But it is relatively expensive and needs some extra cares like:

- Working only in dust free environment
- Using only pure glass, plastics or 100% stainless steel equipment
- Using only warm distilled or demineralized/deionized water (very sensitive to calcium ions)

3.2.4 Heavy suspensions

In order to achieve separation densities above 3.0, heavy suspensions can be used for float-sink separations. ‘Cargille’ liquids, heavy metal particles dispersed in organic liquids, have been produced with relative densities ranging up to 7.5. The use of these liquids was limited to separation of coarser particle sizes, usually larger than 0.6 mm, due to the suspension physical properties. The heavy metal particles in Cargille liquids settle slowly and form a soft mass at the bottom of the suspension. Before use, the suspension must be stirred to disperse the metal particles uniformly throughout the liquid. An alternative is the use of mercury-bromoform emulsions, which have a maximum relative density of 7.0, and can be used successfully on particles as small as 0.1 mm[57].

According to Koroznicova (2007) [57], Rhodes et al (1993) have developed a technique using finely divided ferrosilicon in solutions of sodium polytungstate (SPT) for high-density separations. The use of heavy suspensions, comprised of lithium heteropolytungstates (LST) with ferrosilicon, for sink-float analysis has been demonstrated by Eroglu and Stallknecht (2000).

In this research suspension of sodium polytungstate (SPT) and tungsten carbide powder (TC) were used and suspensions with specific gravities of 3.2 and 3.5 were prepared.

Preparing heavy suspension of SPT and TC consists of four stages:

- Preparing SPT solution with 2.5 g/ml density, this way the viscosity will not be high to separate fine particles
- Transmission approximately 20-30% of SPT solution into a separate container and taking this container on the magnetic stirrer
- Starting to stir the SPT and adding the TC powder slowly to make a slurry. Having homogenous suspension this process has to be done very slowly.
- Adding the TC-SPT suspension to the SPT solution and stirring them very slowly and adjusting desired density by adjusting the amount of TC-SPT.

Figure 3.8 shows the preparation process of TC-SPT suspension.



Figure 3.8. Illustration of preparing TC-SPT suspension in laboratory

After preparing heavy liquids (both TBE and TC-SPT) at desired densities, sink-float tests were done for all of the samples. In the case of coarse samples (+1mm) normal beaker was used but for fine size fraction (-1mm) special funnel (Figure 3.9) was used.

After getting about 500 g of every size fraction of samples, all of this amount was filled in the lowest density container and following the complete sinking of heavy particles of the sample, these particles were separated and were filled in the heavier liquid. This process extended until separating float and sink particles from the heaviest liquid. Figure 3.10 demonstrate schematic model of this process.



Figure 3.9. Modified separation funnel

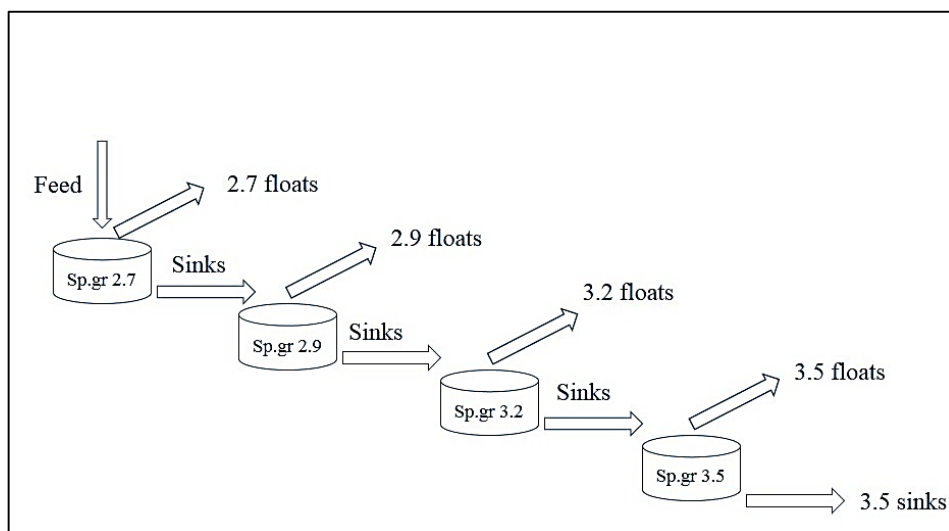


Figure 3.10. Schematic illustration of sink-float test

3.3 Results

Following sink-float tests, float and sink products were dried and weighed. Then assays were determined for each product. Below the results of sink-float tests are presented separately for every ore.

3.3.1 Iron Ore

As mentioned before, the iron ore sample which was the tailing of magnetic separation, was divided into four size fractions (-9.5mm+4.75mm, -4.75mm+1.18mm, -1.18+0.212mm and -0.212mm). Then sink-float tests were done for three coarse fractions. Tetrabromoethane and acetone combination were used for preparing liquids with 2.7 and 2.9 specific gravities and suspensions of sodium polytungstate (SPT) and tungstun carbide powder (TC) were used for preparing heavy suspensions with 3.2 and 3.5 specific gravities.

Table 3.3 shows the results of sink-float tests for iron ore sample. Also the relationship between heavy liquid density, weight of sink products, recovery and grade for size fractions of 9.5mm+4.75mm, -4.75mm+1.18mm and -1.18mm+0.212mm are presented in Figures 3.11, 3.12 and 3.13 respectively.

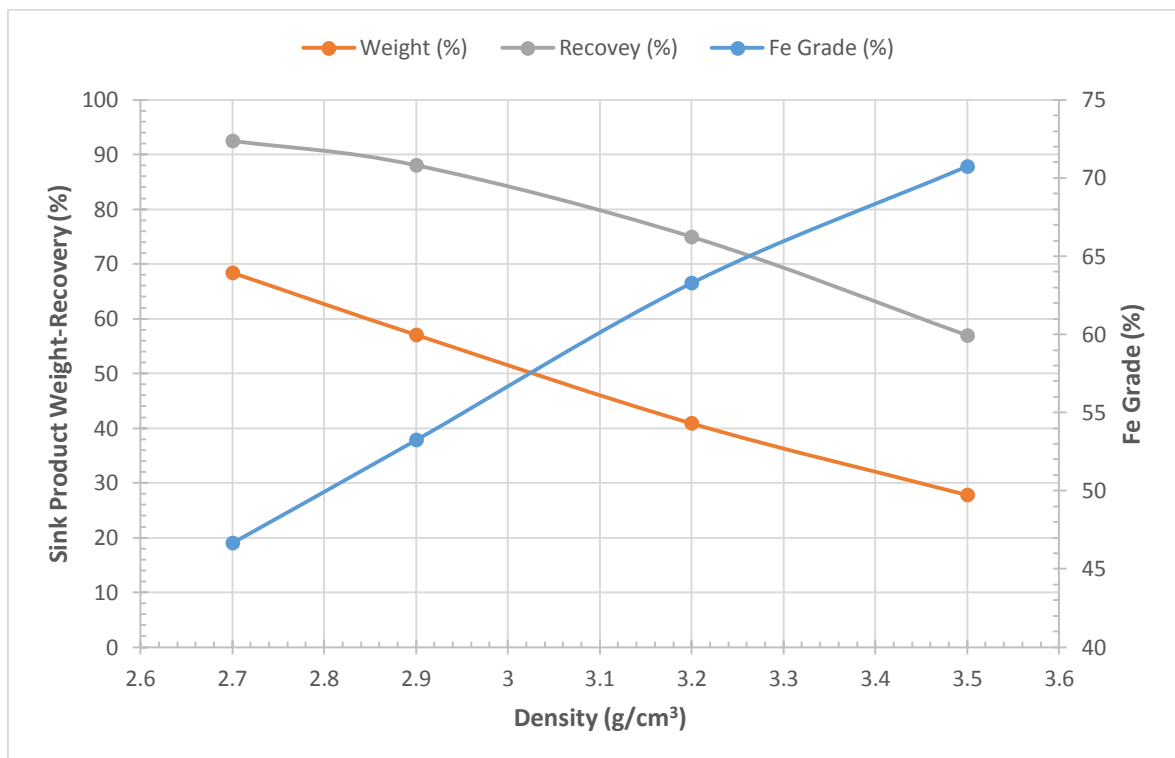


Figure 3.11. Heavy liquid density vs Fe grade (%), Fe recovery (%) and weight of the sink products (%) for -9.5mm+4.75mm size fraction

Table 3.3. Sink-float results for three coarse size fractions of iron ore sample

Size Fraction	Product	Weight (%)	Fe (%)	Recovery (%)	Cumulative to Sinks			
					Density (g/cm ³)	Weight (%)	Fe (%)	Recovery (%)
-9.5+4.75mm	Sinks 3.5	27.78	70.74	56.97	3.5	27.78	70.74	56.97
	-3.5+3.2	13.09	47.43	17.99	3.2	40.87	63.28	74.96
	-3.2+2.9	16.18	27.87	13.08	2.9	57.05	53.23	88.04
	-2.9+2.7	11.35	13.55	4.46	2.7	68.41	46.65	92.50
	Floats2.7	31.59	8.19	7.50		100	34.50	100
	Total	100	34.50	100				
-4.75+1.18mm	Sinks 3.5	32.82	67.71	63.73	3.5	32.82	67.71	63.73
	-3.5+3.2	12.17	48.12	16.79	3.2	44.99	62.41	80.52
	-3.2+2.9	13.54	25.56	9.92	2.9	58.53	53.89	90.44
	-2.9+2.7	9.59	12.81	3.52	2.7	68.12	48.11	93.97
	Floats2.7	31.88	6.60	6.03		100	34.87	100
	Total	100.00	34.87	100.00				
-1.18+0.212mm	Sinks 3.5	38.58	61.68	68.94	3.5	38.58	61.68	68.94
	-3.5+3.2	10.78	43.51	13.59	3.2	49.36	57.71	82.53
	-3.2+2.9	17.26	25.68	12.84	2.9	66.62	49.41	95.37
	-2.9+2.7	4.33	9.13	1.14	2.7	70.95	46.95	96.51
	Floats2.7	29.05	4.14	3.49		100	34.51	100
	Total	100.00	34.51	100.00				

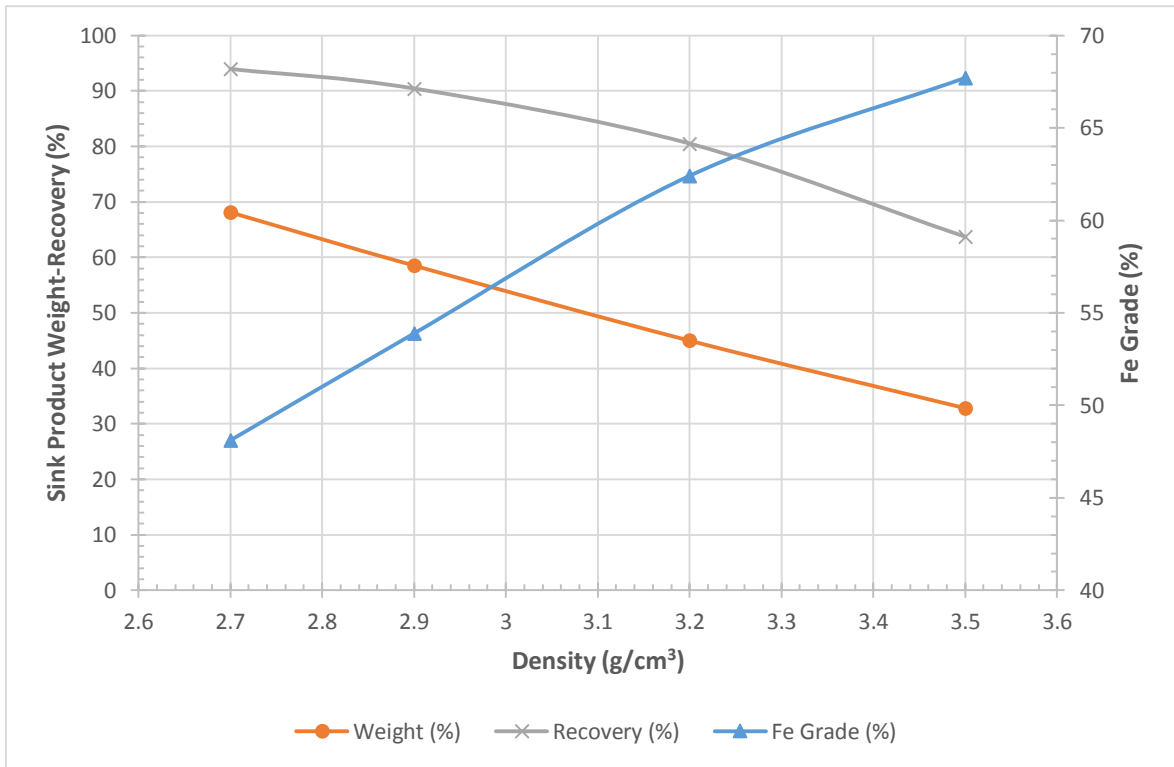


Figure 3.12. Heavy liquid density vs Fe grade (%), Fe recovery (%) and weight of the sink products (%) for -4.75mm+1.18mm size fraction

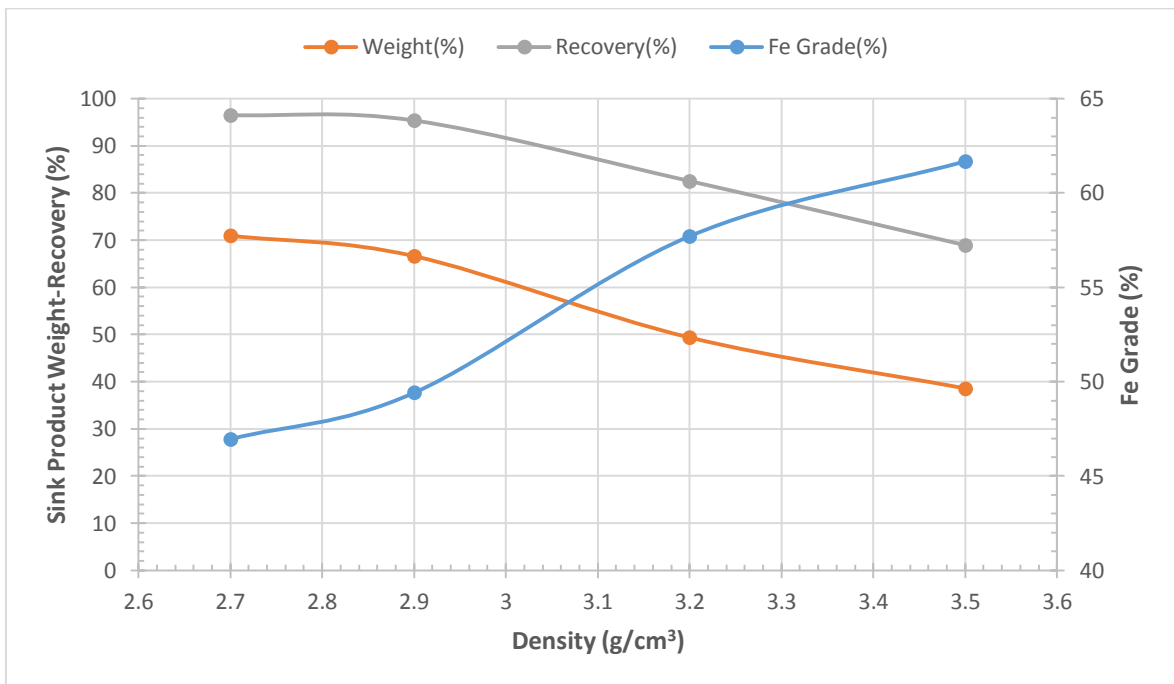


Figure 3.13. Heavy liquid density vs Fe grade (%), Fe recovery (%) and weight of the sink products (%) for -1.18mm+0.212mm size fraction

3.3.2 Manganese Ore

According to previous section, Crushed manganese ore was divided to -16mm+5mm, -5mm+1mm, -1+0.2mm and -0.2mm size fractions. The same sink float tests were done as iron ore. Table 3.4 shows the results of sink-float tests for manganese ore sample. Also the relationship between heavy liquid density, weight of sink products, recovery and grade for size fractions of -16+5mm, -5mm+1mm and -18mm+0.2mm are presented in Figures 3.14, 3.15 and 3.16 respectively.

Table 3.4. Sink-float results for three coarse size fractions of iron manganese sample

Size Fraction	Product	Weight (%)	Mn (%)	Recovery (%)	Cumulative to Sinks			
					Density (g/cm ³)	Weight (%)	Mn (%)	Recovery (%)
-16+5mm	Sinks 3.5	10.25	41.05	14.96	3.5	10.25	41.05	56.97
	-3.5+3.2	24.46	40.27	35.01	3.2	34.71	40.50	74.96
	-3.2+2.9	30.16	39.42	42.26	2.9	64.87	40.00	88.04
	-2.9+2.7	5.69	10.61	2.15	2.7	70.56	37.63	92.50
	Floats 2.7	29.44	5.37	5.62		100	28.13	100
	Total	100	28.13	100				
-5+1mm	Sinks 3.5	19.69	40.35	34.31	3.5	19.69	40.35	63.73
	-3.5+3.2	12.05	39.88	20.76	3.2	31.74	40.17	80.52
	-3.2+2.9	28.10	32.91	39.94	2.9	59.84	36.76	90.44
	-2.9+2.7	5.09	8.52	1.87	2.7	64.93	34.55	93.97
	Floats 2.7	35.07	2.06	3.12		100	23.15	100
	Total	100.00	23.15	100.00				
-1+0.2mm	Sinks 3.5	14.19	37.33	26.67	3.5	14.19	37.33	68.94
	-3.5+3.2	20.84	33.22	34.86	3.2	35.02	34.88	82.53
	-3.2+2.9	26.58	25.94	34.72	2.9	61.60	31.03	95.37
	-2.9+2.7	2.22	10.73	1.20	2.7	63.83	30.32	96.51
	Floats 2.7	36.17	1.40	2.55		100.00	19.86	100
	Total	100.00	19.86	100.00				

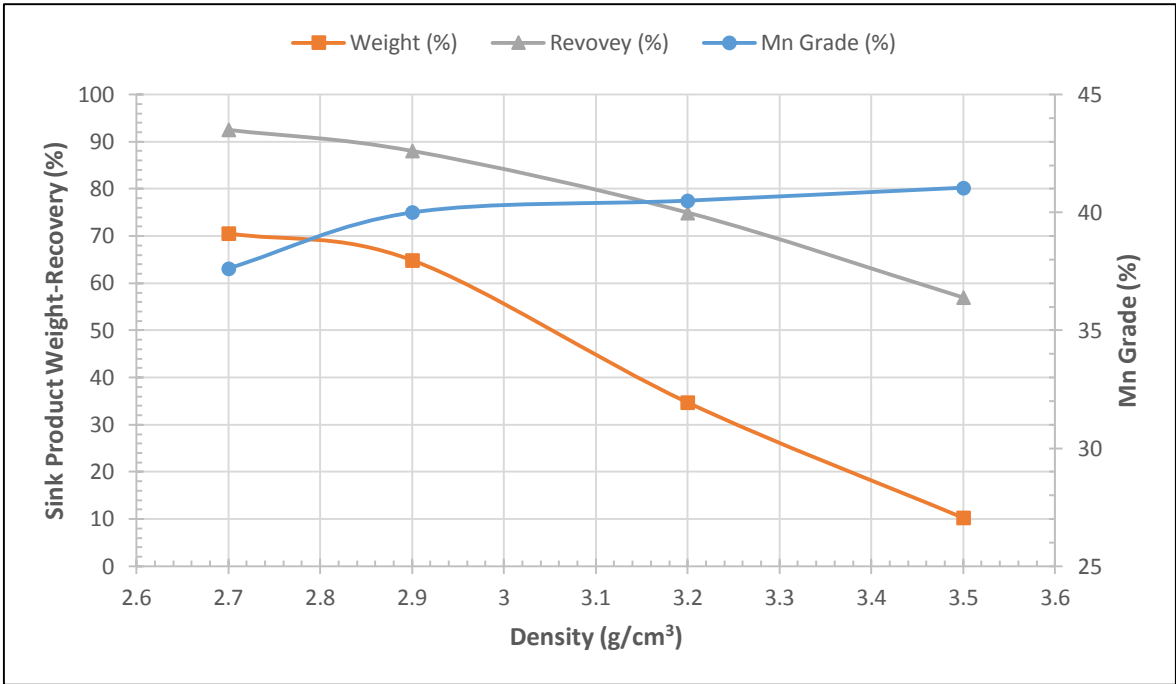


Figure 3.14. . Heavy liquid density vs Mn grade (%), Mn recovery (%) and weight of the sink products (%) for -16mm+5mm size fraction

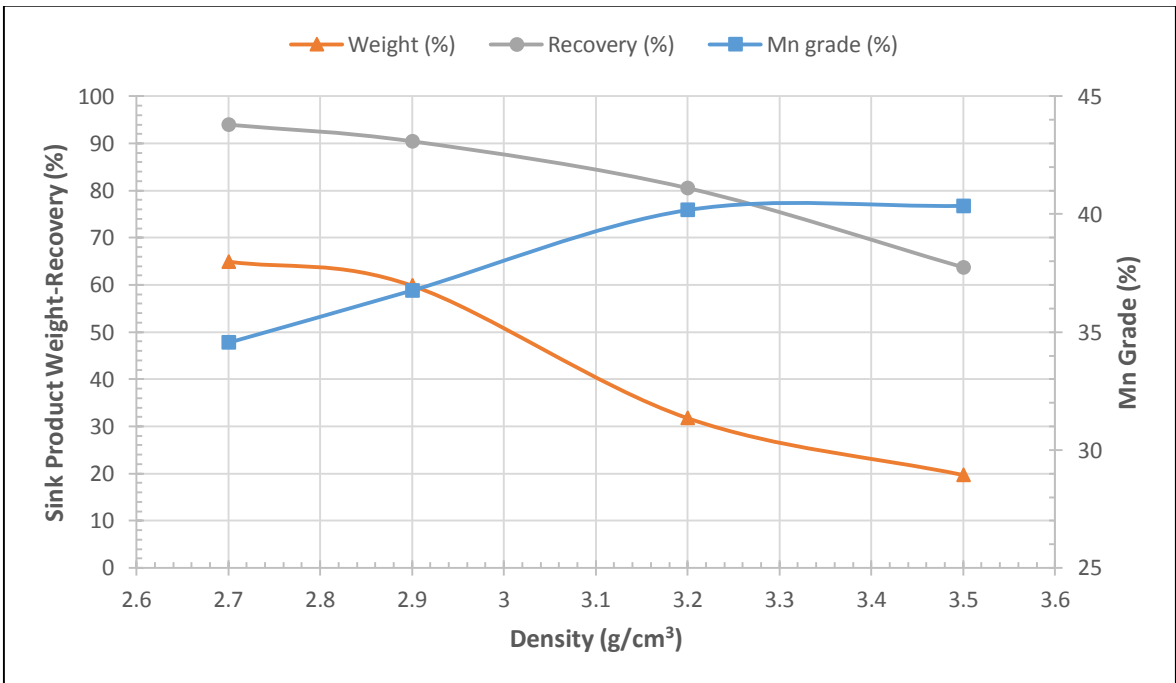


Figure 3.15. Heavy liquid density vs Mn grade (%), Mn recovery (%) and weight of the sink products (%) for -5.0mm+1.0mm size fraction

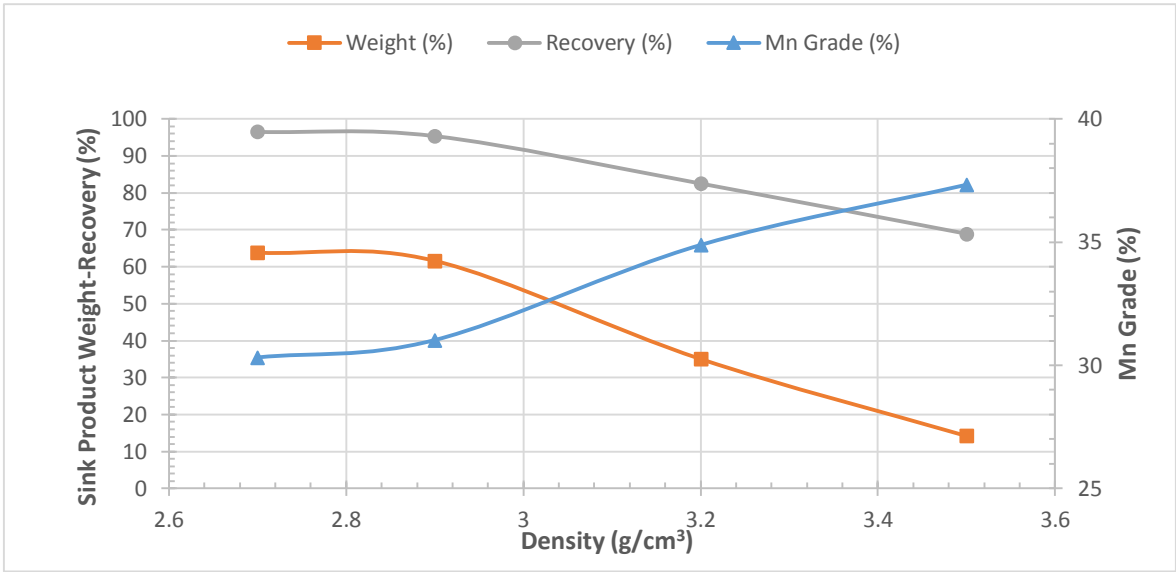


Figure 3.16. Heavy liquid density vs Mn grade (%), Mn recovery (%) and weight of sink products (%) for -1.0mm+0.2mm size fraction

3.3.3 Chromite Ore

After size distribution analysis for feed sample, some size fractions were combined together and sample was divided into three part (-1.18+0.425mm, -0.425+0.212mm and -0.212mm). Then sink-float tests were done for two coarse size fractions and photomicrography were taken from products of sink-float tests.

Table 3.5 presents the results of sink-float tests and relationship between liquid density vs grade, recovery and concentrate weight is shown in Figures 3.17 and 3.18.

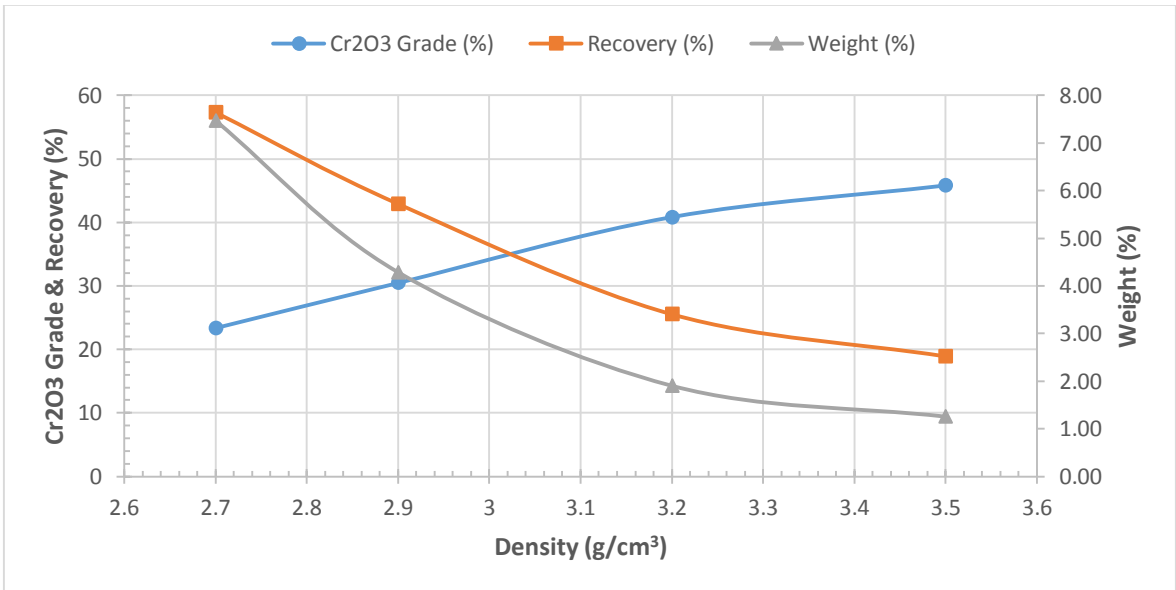


Figure 3.17. Heavy liquid density vs Cr₂O₃ grade (%), Cr₂O₃ recovery (%) and weight of sink products (%) for -1.18mm+0.425mm size fraction

Table 3.5. Sink-float results for three coarse size fractions of chromite ore sample

Size Fraction	Product	Weight (%)	Cr ₂ O ₃ (%)	Recovery (%)	Cumulative to Sinks			
					Density (g/cm ³)	Weight (%)	Cr ₂ O ₃ (%)	Recovery (%)
-1.18+0.425mm	Sinks 3.5	1.25	45.82	18.89	3.5	1.25	45.82	18.89
	-3.5+3.2	0.65	31.17	6.63	3.2	1.90	40.83	25.53
	-3.2+2.9	2.38	22.18	17.38	2.9	4.29	30.45	42.91
	-2.9+2.7	3.18	13.77	14.41	2.7	7.47	23.34	57.32
	Floats 2.7	92.53	1.40	42.68		100	3.04	100
	Total	100	3.04	100				
-0.425+0.212mm	Sinks 3.5	6.50	50.25	68.95	3.5	6.50	50.25	68.95
	-3.5+3.2	2.73	22.15	12.76	3.2	9.23	41.94	81.71
	-3.2+2.9	1.08	16.95	3.87	2.9	10.32	39.32	85.57
	-2.9+2.7	3.09	12.21	7.95	2.7	13.40	33.08	93.52
	Floats 2.7	86.60	0.35	6.48		100	4.74	100
	Total	100	4.74	100				

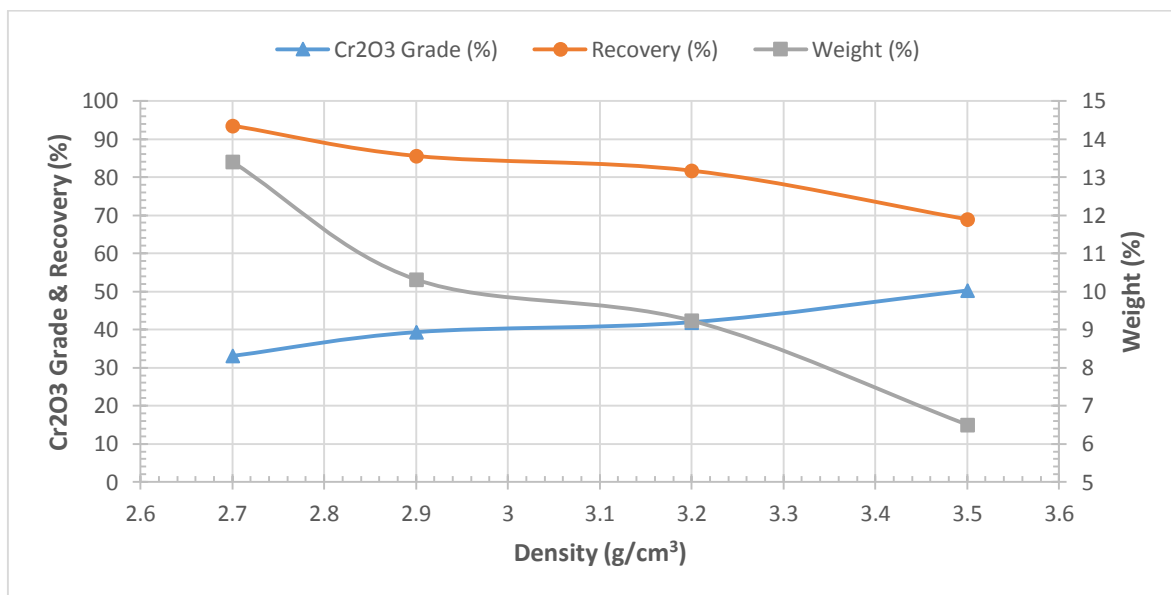


Figure 3.18. . Heavy liquid density vs Cr₂O₃ grade (%), Cr₂O₃ recovery (%) and weight of sink products (%) for -0.425mm+0.212mm size fraction

3.3.4 Zinc ore

Tetrabromoethane (TBE) and acetone combination was used for adjusting heavy liquids with 2.7 and 2.96 specific gravities and sink-float tests were done for two size fractions of two samples. Tables 3.6 and 3.7 show the results of the sink-float tests.

Table 3.6. Sink-float results for Zinc ore sample 1

Size Fractions	Product	Weight (%)	Zn (%)	Recovery (%)	Cumulative to Sinks			
					Density (g/cm ³)	Weight (%)	Zn (%)	Recovery (%)
-8+1.7mm	Sinks2.9	77.39	29.25	88.02	2.9	77.39	29.25	92.95
	-2.9+2.7	8.22	11.08	8.12	2.7	85.61	27.51	96.69
	Floats2.7	14.39	5.61	3.86		100	24.36	100
	Total	100.00	24.36	100				
-1.7+0.2mm	Sinks2.9	89.72	20.44	96.37	2.9	89.72	20.44	96.37
	-2.9+2.7	3.10	6.79	1.11	2.7	92.82	19.98	97.47
	Floats2.7	7.18	6.70	2.53		100	19.03	100
	Total	100	19.03	100				

Table 3.7. Sink-float results for zinc ore sample 2

Size Fractions	Product	Weight (%)	Zn (%)	Recovery (%)	Cumulative to Sinks			
					Density (g/cm ³)	Weight (%)	Zn (%)	Recovery (%)
-8+1.7mm	Sinks2.9	72.00	33.38	88.02	2.9	72.00	33.38	88.02
	-2.9+2.7	14.69	15.10	8.12	2.7	86.69	30.28	96.14
	Floats2.7	13.31	7.91	3.86		100	27.30	100
	Total	100.00	27.30	100				
-1.7+0.2mm	Sinks2.9	81.41	24.93	90.93	2.9	81.41	24.93	90.93
	-2.9+2.7	5.91	21.54	5.70	2.7	87.31	24.70	96.63
	Floats2.7	12.69	5.92	3.37		100	22.32	100
	Total	100	22.32	100				

4 Simulation Studies and Results

As discussed in Section 2, there are various approaches to predict the performance of heavy medium cyclones in the published literature. Most of the existing models are based on low density operations and specially coal washing plants. In the case of high density operations, Scott (1988) and Scott and Napier-Munn (1990) have published models to predict performance of heavy medium cyclones performance for pre-concentration of Lead-Zinc ore in Mount-Isa concentration plant.

Predicting partition number using separation density and operational parameters is the common factor between different models. Whiten equation (2.31) has been used as a basic foundation in most of these models.

$$(PN = \frac{100}{1+e^{1.099\left(\frac{\rho_{50}^A - \rho_d}{E_p d}\right)}})$$

Where ρ_{50} is the separation density and ρ_d is the particle density. According to the equation, having information about ore characteristics (ρ_d) and operational variables (ρ_{50} and E_p) it is possible to have a prediction about performance of heavy medium cyclone plant.

E_p value is the most important parameter in HMC plants modeling. Heavy medium's density and viscosity, cyclone's geometry and the mean size of the ore are variables that can affect the E_p . There is a simple equation in Scott and Napier-Munn (1990) [42] that shows the relationship between E_p and particle mean size for 400mm cyclone based on data from Argyle diamond plant :

$$E_p = (4 + 52d^{-1})/1000 \quad (\text{Where } d \text{ is mean particle size in mm}) \quad (4.1)$$

In this research Lave 1.0 program was used to simulate DM cyclone performance. This computer program has been developed at the Department of Mining Engineering of Hacettepe University by Orhan et al (2010) [58] and it uses JKMRC model based on Whiten equation (Equation 2.31).

Lave 1.0 is able to run with minimal information that listed below:

- Particle size distribution of feed
- Heavy liquid analysis on each size range
- Separation density
- Ecart probable of separation (E_p)

As mentioned above, separation E_p changes for different size fractions of the feed so we have to calculate it for each size fraction then import them to the simulator program. Equation (4.1) was used to calculate E_p values for different size fractions.

Figure 4.1 shows the principle of working with Lave 1.0 simulator.

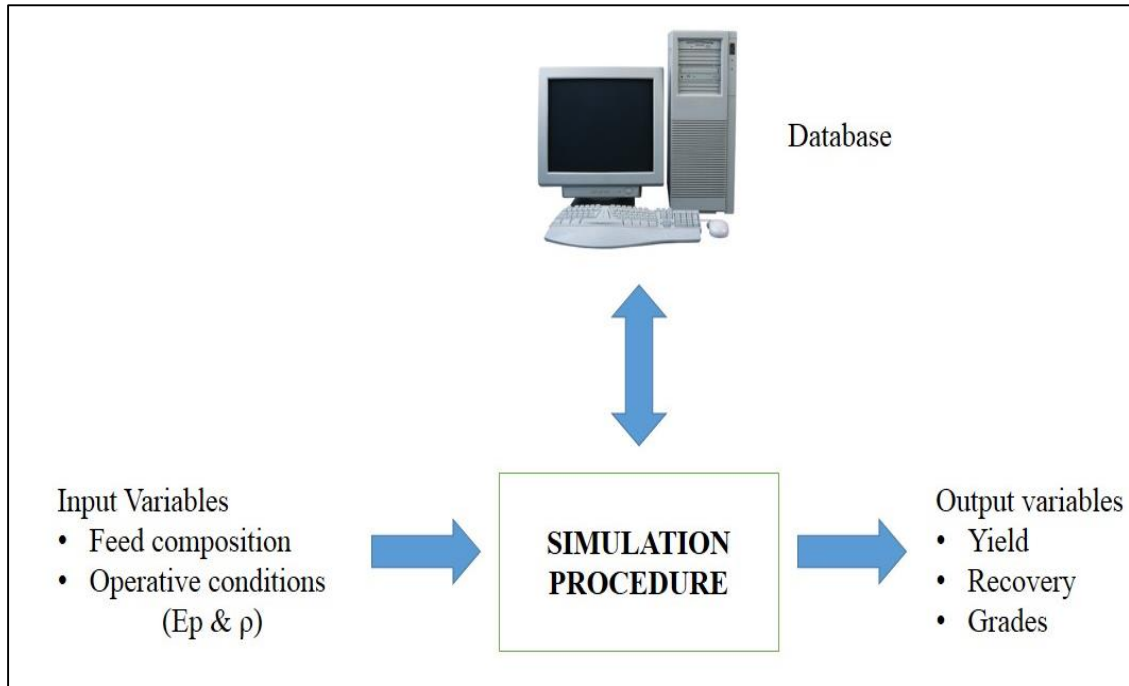


Figure 4.1. Principle of working with Lave 1.0 separator

Because of lack of information and relatively bad results of sink-float tests of zinc ore, this ore was not considered for simulations.

4.1 Simulation Study for Iron Ore Sample and Results

Using equation (4.1), E_p values were calculated for different size fractions and then these values were entered to Lave 1.0 simulator. As a second variable pulp densities from 2.5 gr/cm^3 to 3.5 gr/cm^3 were entered to the simulator and simulation outputs were listed. In order to select the best separation density (saleable concentrate grade with maximum recovery), grade-recovery and grade, recovery and concentrate percentage charts were drawn.

Table 4.1 shows calculated E_p values with equation 4.1 for different size fractions, Figures 4.2 shows grade and recovery relationship and Figure 4.3 illustrates the effect of separation density on grade, recovery and concentrate weight percentage.

It is concluded from the Table 4.1 that E_p value increase with decreasing the particle size especially for particles below 0.2mm. Therefore it is necessary to separate -0.2mm size

fraction from the cyclone feed. These particles can also affect heavy medium cyclone plant's performance because according to literature fine particles increase the medium's viscosity and reduce separation sharpness.

Table 4.1. Calculated E_p values for different size fractions

Size fractions (mm)	Mean Size (mm)	Calculated E_p
-9.5+5	7.25	0.009
-5+1	3	0.021
-1+0.2	0.6	0.091
-0.2	0.1	0.524

As we can see in Figure 4.2 and Figure 4.3, recovery and concentrate weight reduce with increasing concentrate grade and considering saleable iron concentrate, separation density of 3.1 gr/cm^3 is the most favorable density for the plant design. In this separation density it is possible to obtain concentrate with 60.45% Fe grade and 80% Fe recovery that contains 46% of the heavy medium plant's feed. Also we can reject 54% of the cyclone feed with 12.83% Fe grade at this separation density.

Figure 4.4 shows the simulated flowsheet for iron ore with 50 t/h feed capacity and separation density of 3.1 gr/cm^3 and figure 4.5 shows the used partition curves for simulation of heavy medium cyclone plant in mentioned separation density

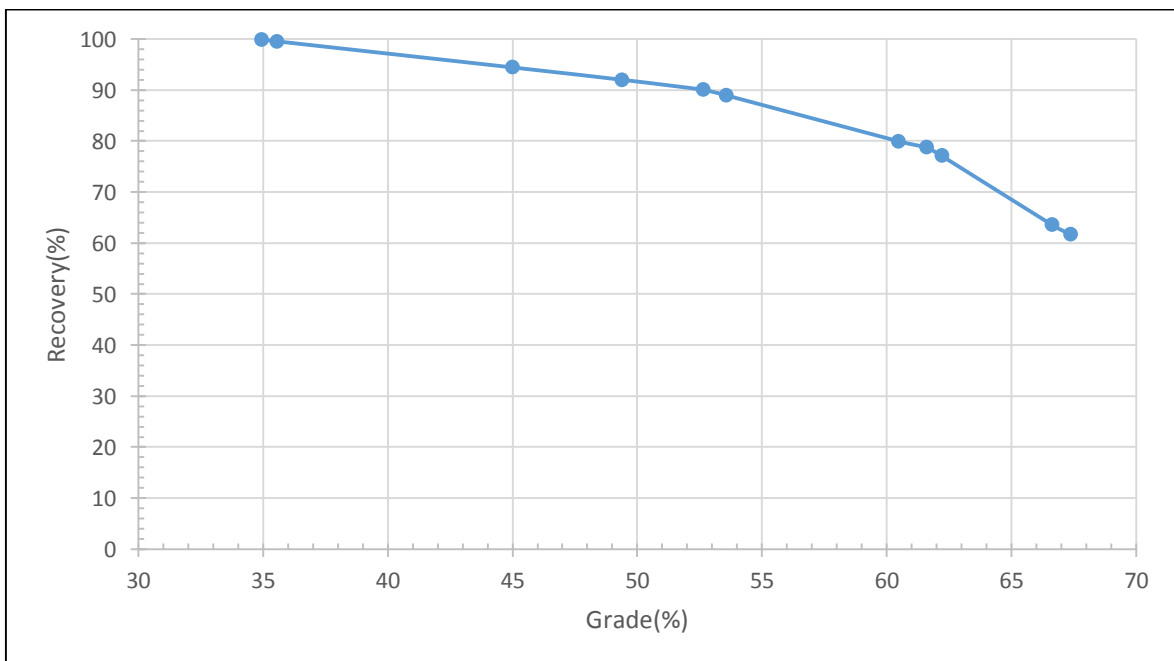


Figure 4.2. Grade-recovery relationship for iron ore sample

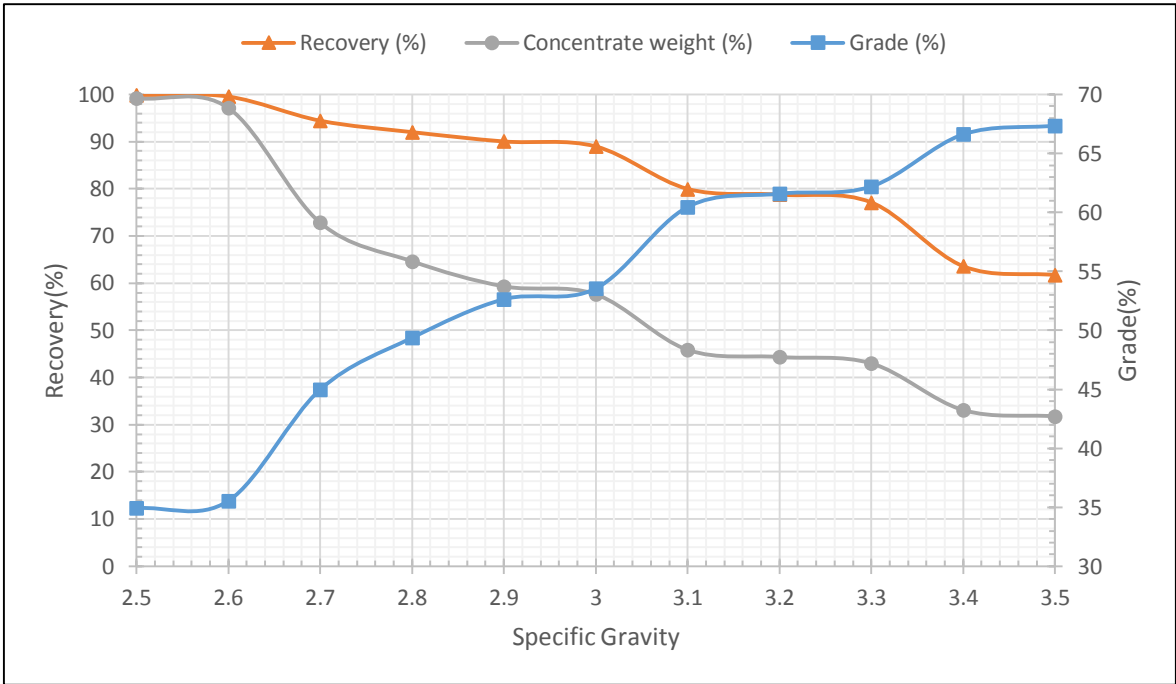


Figure 4.3. Grade, recovery and concentrate weight for different separation densities

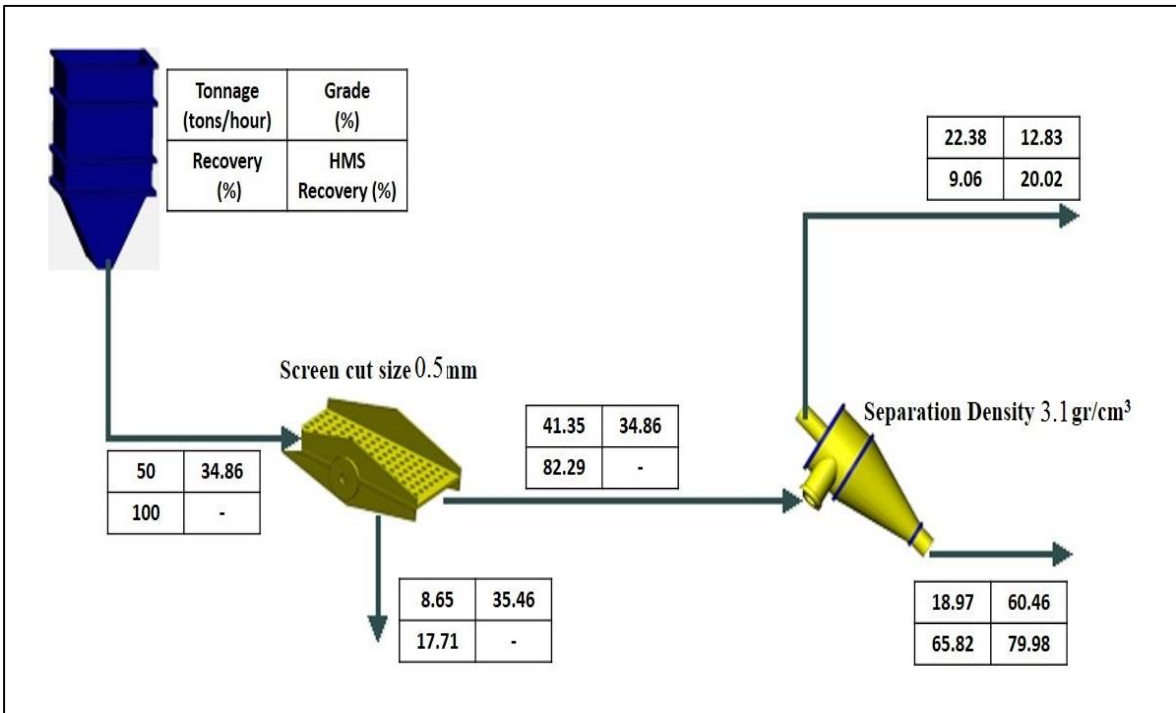


Figure 4.4. Schematic flowsheet of HMC plant for iron ore in separation density of 3.1 gr/cm³

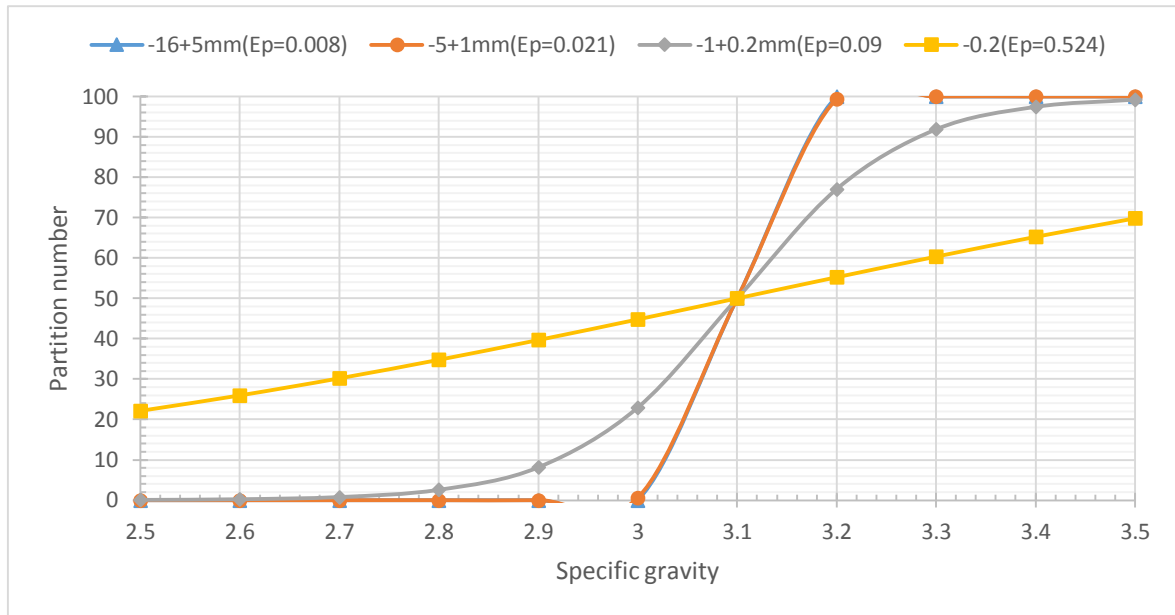


Figure 4.5. Partition curves used in the simulation of the heavy medium cyclone plant of the iron ore with the separation density of 3.1 g/cm³ (based on simulated data)

According to the simulation results, screen's undersize section (-0.5mm) is about 17% of the feed with approximately 36% Fe grade. This part of the feed can be beneficiated with spiral concentrator or shaking table which was not investigated because it is beyond the scope of this study.

4.2 Simulation Study for Manganese Ore Sample and Results

Using equation (4.1), E_p values were calculated for different size fractions of manganese ore sample and then these values were entered to Lave 1.0 simulator. As a second variable pulp densities from 2.5 gr/cm³ to 3.5 gr/cm³ were entered to the simulator and simulation outputs were listed. In order to select best separation density (saleable concentrate grade with maximum recovery), grade-recovery and grade, recovery and concentrate percentage charts were plotted.

Table 4.2 shows calculated E_p values for different size fractions, Figures 4.6 shows grade and recovery relationship and Figure 4.7 illustrates the effect of separation density on grade, recovery and concentrate weight percentage.

It is concluded from the Table 4.2 that E_p value increase with decreasing the particle size especially for particles below 0.2mm. So it is necessary to separate -0.2mm size fraction from the cyclone feed. These particles can also affect heavy medium cyclone plant's performance because according to literature fine particles increase the medium's viscosity and reduce separation sharpness.

Table 4.2. Calculated Ep values for different size fractions of manganese ore

Size fractions (mm)	Mean Size (mm)	Calculated Ep
-16+5	10.5	0.009
-5+1	3	0.021
-1+0.2	0.6	0.091
-0.2	0.1	0.524

As we can see in Figure 4.6 and Figure 4.7, recovery and concentrate weight reduce with increasing concentrate grade and considering salable manganese concentrate, separation density of 2.9 gr/cm³ is the most favorable density for the plant design. In this separation density we will have concentrate with 38.99% Mn grade and 92.96% Mn recovery that contains 63.18% of the heavy medium plant's feed. Also we can reject about 37% of the cyclone feed with 5.03% Mn grade in this separation density.

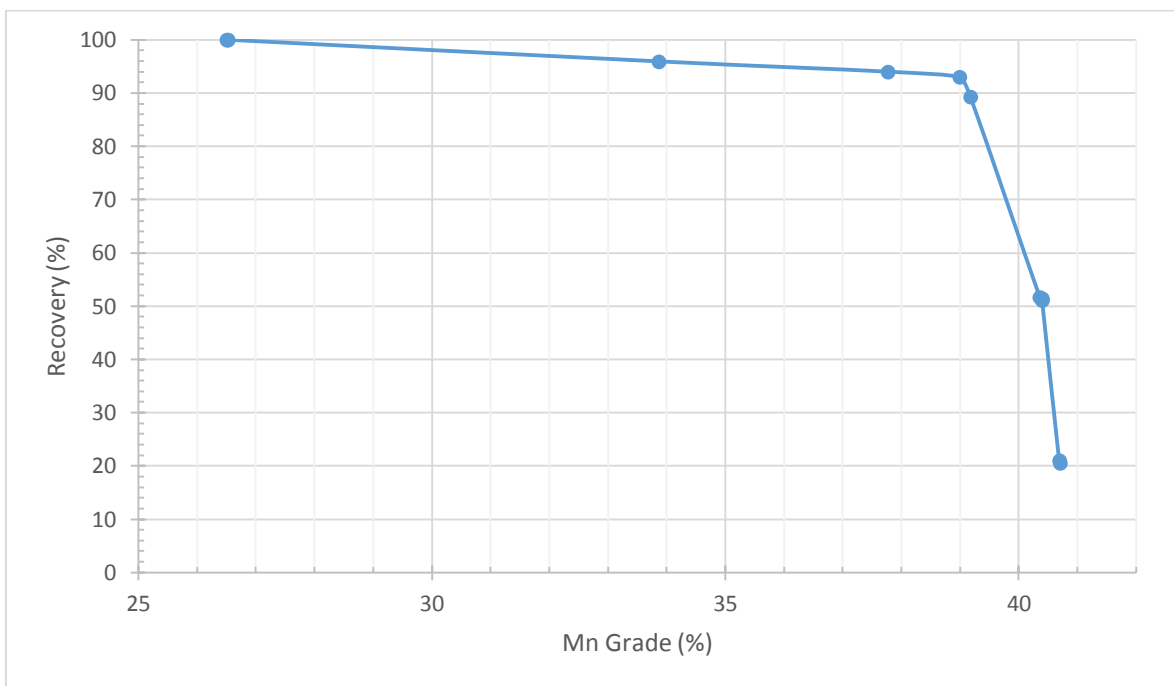


Figure 4.6. The relationship between Mn grade an recovery for manganese ore

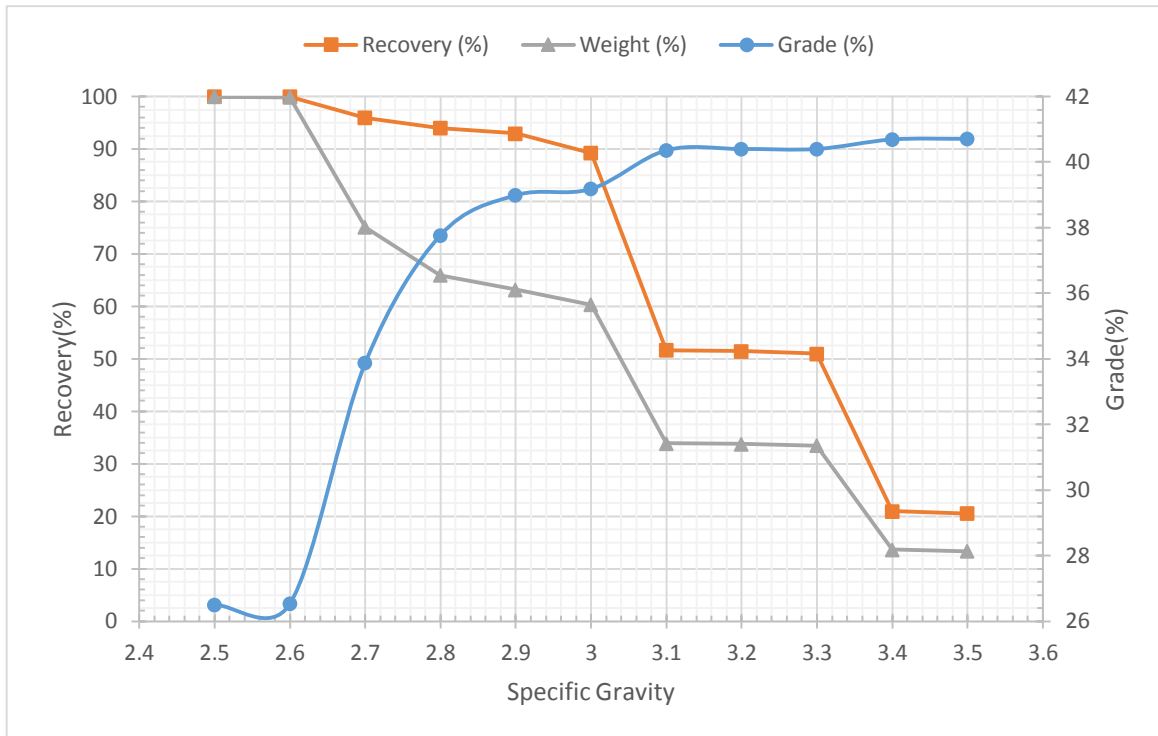


Figure 4.7. Effect of separation density in grade, recovery and concentrate weight of manganese ore sample (based on simulated data)

Figure 4.8 shows the simulated flowsheet for manganese ore with 20 t/h feed capacity and separation density of 2.9 gr/cm³ and Figure 4.9 shows the used partition curves for simulation of heavy medium cyclone plant in mentioned separation density

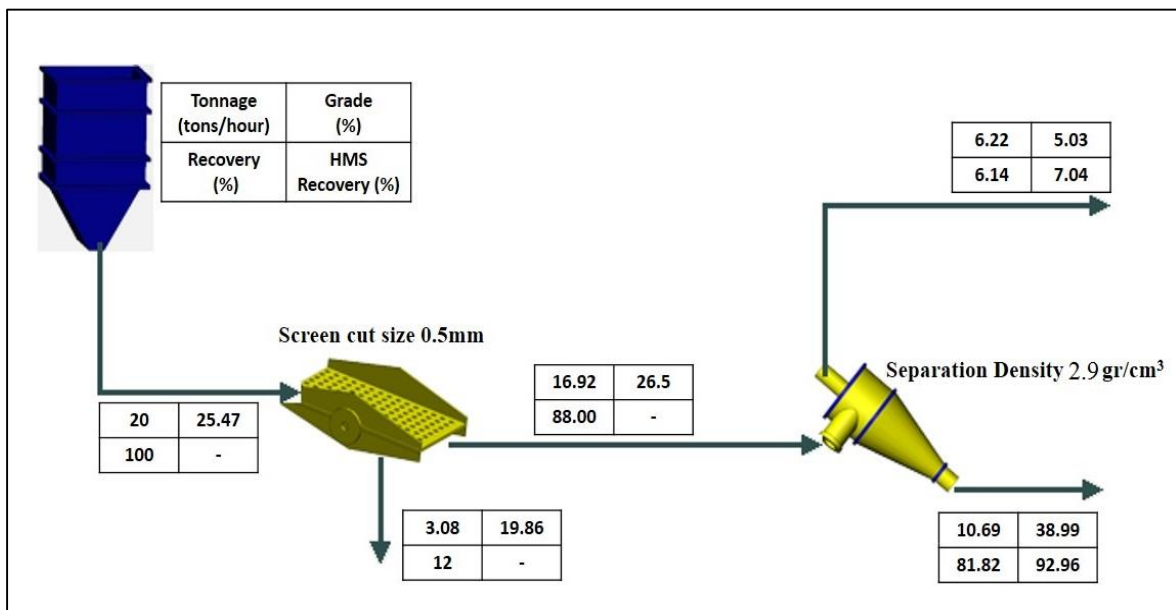


Figure 4.8. Schematic flowsheet of HMC plant for manganese ore

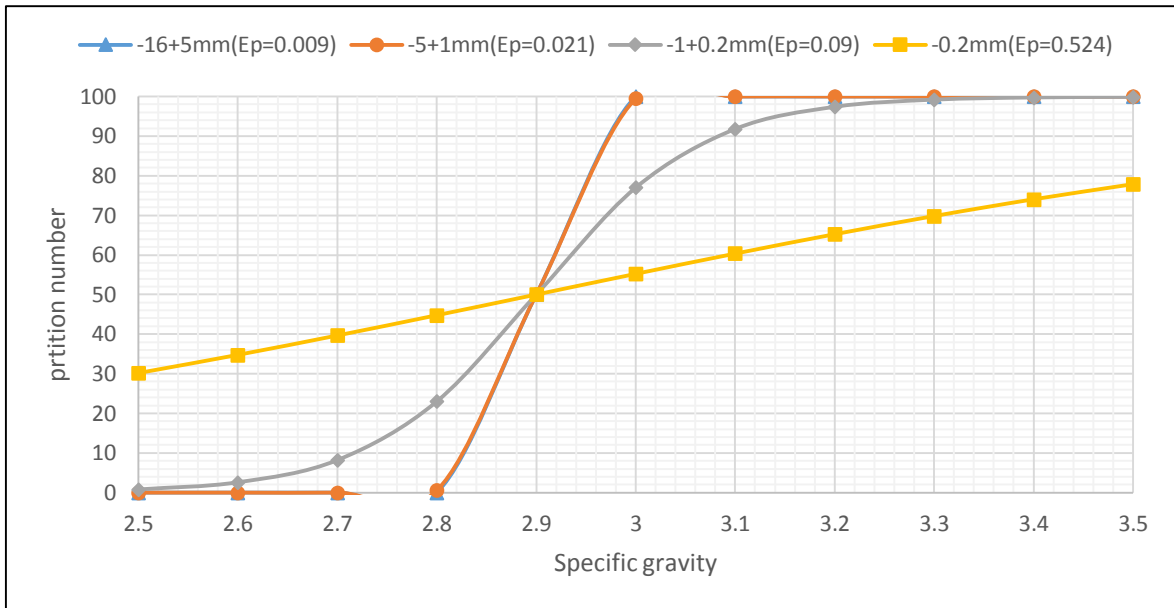


Figure 4.9. Partition curves used in the simulation of the heavy medium cyclone plant of the manganese ore with the separation density of 2.9 g/cm³

According to the simulation results, screen's undersize section (-0.5mm) is about 15.5% of the feed with approximately 20% Mn grade. This part of the feed can be beneficiated with spiral concentrator or shaking table which not investigated because it is beyond the scope of this study.

4.3 Simulation Study for Chromite Ore and Results

Using equation (4.1), Ep values were calculated for different size fractions of chromite ore sample and then these values were entered to Lave 1.0 simulator. As a second variable pulp densities from 2.5 gr/cm³ to 3.5 gr/cm³ were entered to the simulator and simulation outputs were listed. In order to select best separation density (saleable concentrate grade with maximum recovery), grade-recovery and grade, recovery and concentrate percentage charts were drawn.

Table 4.3 shows calculated Ep values for different size fractions, Figures 4.10 shows grade and recovery relationship and Figure 4.11 illustrates the effect of separation density on grade, recovery and concentrate weight percentage.

It is concluded from the Table 4.3 that Ep value increase with decreasing particle size especially for particles below 0.2mm. So it is necessary to separate -0.2mm size fraction from the cyclone feed. These particles can also affect heavy medium cyclone plant's performance because according to literature fine particles increase the medium's viscosity and reduce separation sharpness.

Table 4.3. Calculated E_p values for different size fractions of chromite ore

Size fractions (mm)	Mean Size (mm)	Calculated E_p
-1.18+0.425	0.80	0.069
-0.425+0.212	0.31	0.167
-0.212	0.1	0.495

As we can see in Figure 4.10 and Figure 4.11, recovery and concentrate weight reduce with increasing concentrate grade and considering saleable chromite concentrate, separation density of 3.5 gr/cm^3 is the most favorable density for the plant design. In this separation density we will have concentrate with 45% Cr_2O_3 grade and 51.43% Cr_2O_3 recovery that contains only 4.54% of the heavy medium plant's feed. Also we can reject about 96.5% of the cyclone feed with 2% Cr_2O_3 grade at this separation density.

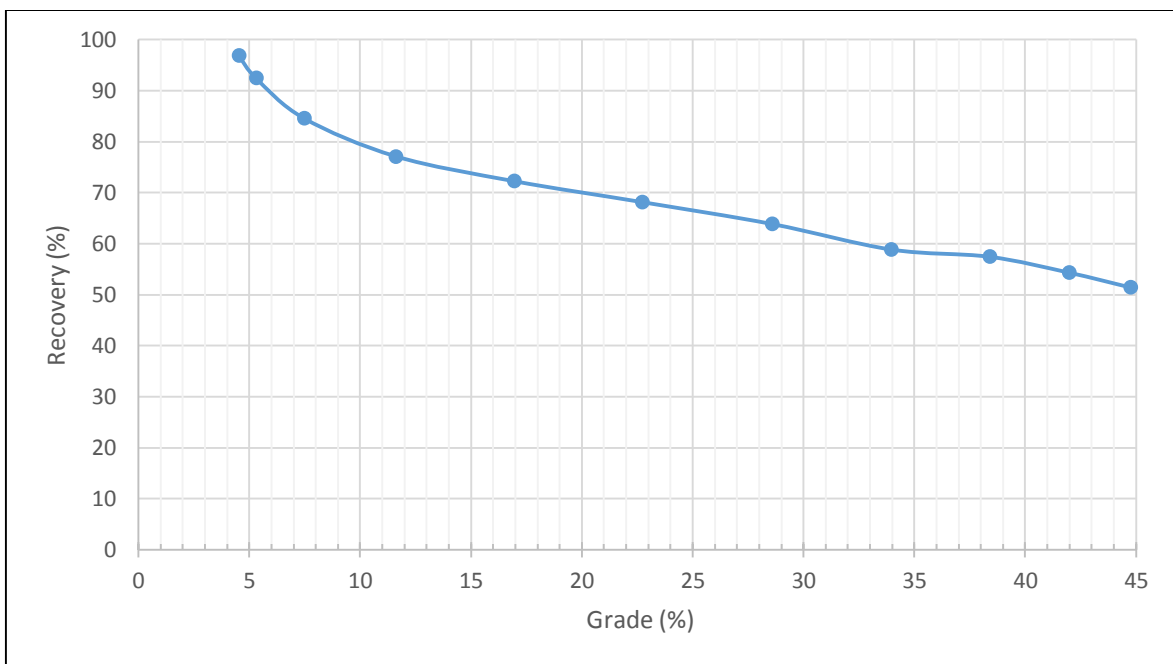


Figure 4.10. The relationship between Cr_2O_3 grade and recovery for chromite ore

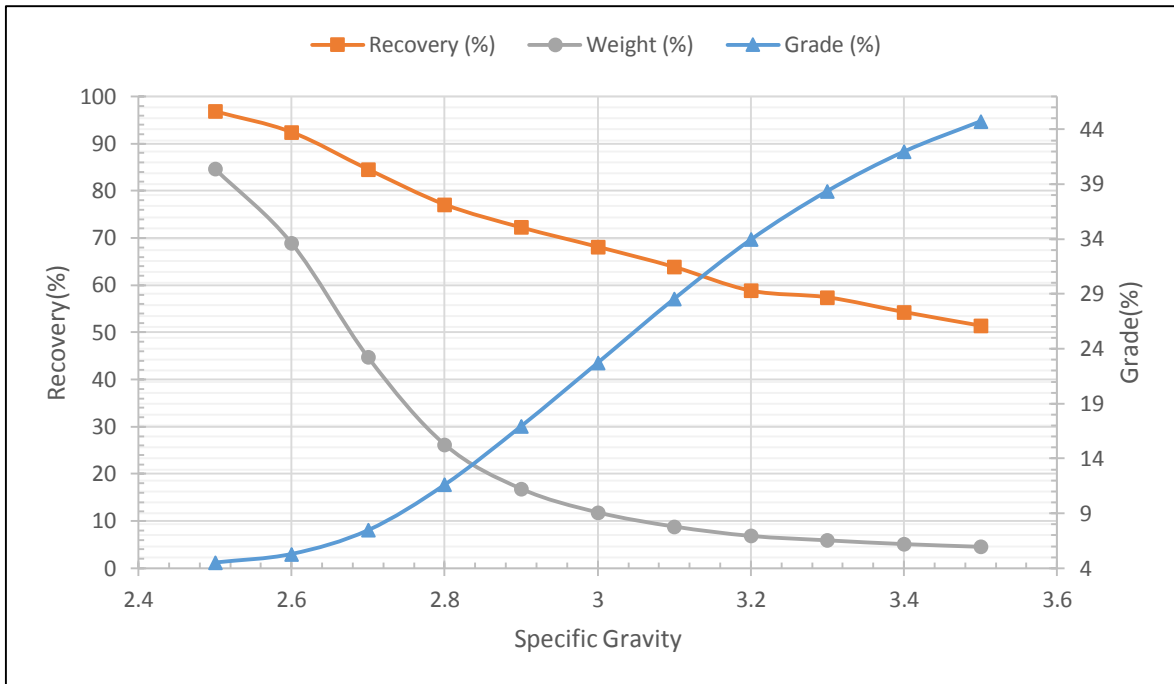


Figure 4.11. Effect of separation density in grade, recovery and concentrate weight of chromite ore sample (based on simulated data)

Figure 4.12 shows the simulated flowsheet for chromite ore with 10 t/h feed capacity and separation density of 3.5 gr/cm³ and Figure 4.13 shows the used partition curves for simulation of heavy medium cyclone plant in mentioned separation density.

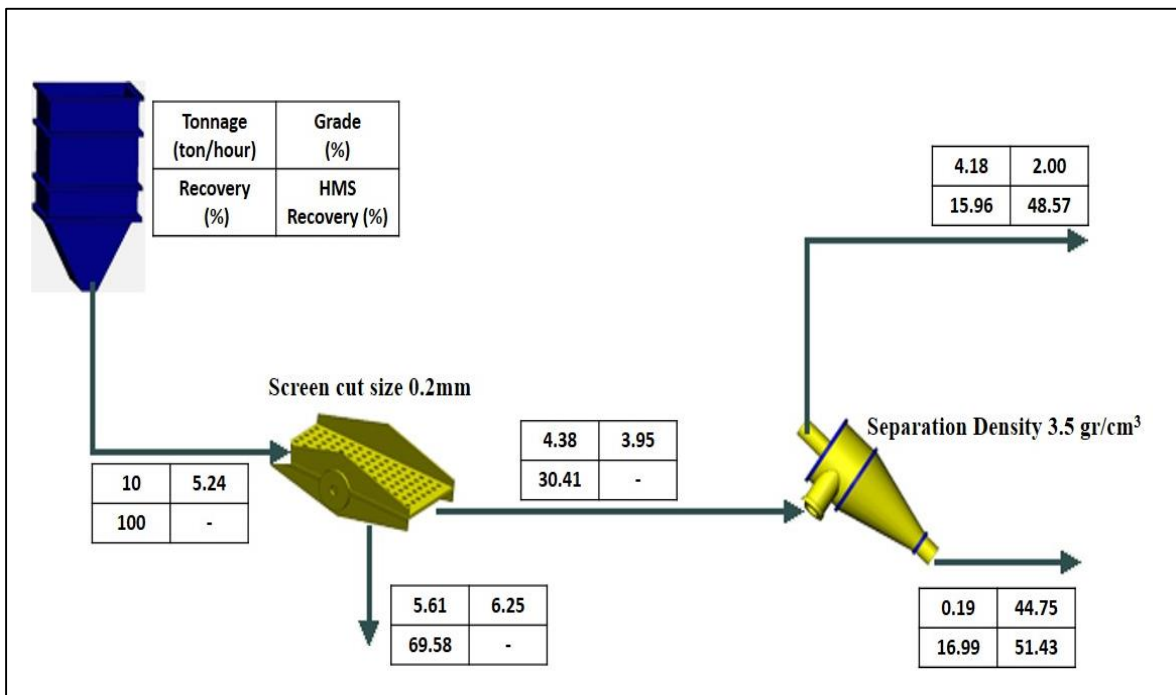


Figure 4.12. Schematic flowsheet of HMC plant for chromite ore

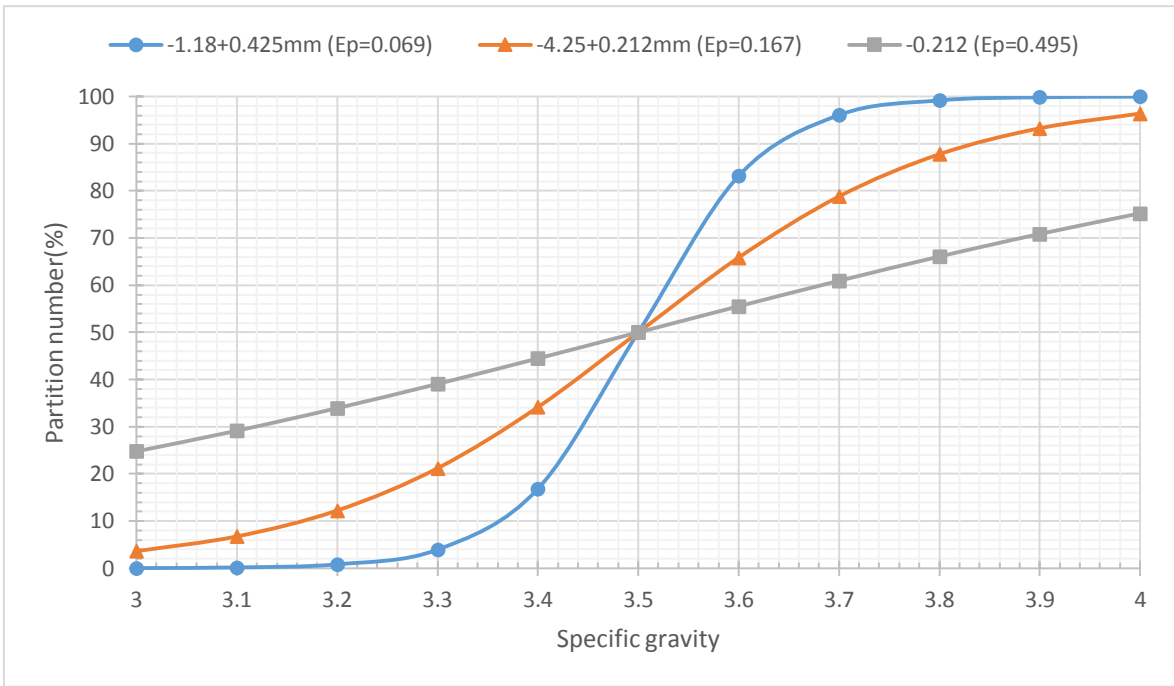


Figure 4.13. Partition curves used in the simulation of the heavy medium cyclone plant of the chromite ore with the separation density of 2.9 g/cm^3

5 Discussion of the Results

A comprehensive literature review about heavy medium cyclones showed that firstly this method has a lot of advantages the like ability to make sharp separation, ability to maintain controllable separation density, ability to handle a wide range of feed size, ability to remove products continuously, ability to change specific gravity of separation to meet varying market requirements and high capacity, comparing with other gravity separation methods. Second, although this method is limited to coal washing in Turkey, there are good examples of using heavy medium cyclones in none-coal applications all around the world. Third, there are well documented attempts to modelling heavy medium cyclones both empirically and mathematically. Although most of these models are about coal washing plants, there are some empirical models to predict heavy medium cyclones performance in high density separations like lead-zinc and iron ores.

The difficulty in gravity concentration processes can be evaluated using heavy liquid test results. according to Table 1.1 [4] when the amount of near gravity particles is higher than 10%, it is really hard to obtain good results with jigs, tables, spirals and other gravity methods and the only efficient gravity method is heavy medium separation. Table 5.1 shows the amount of near gravity particles for difference ores at different size fractions which calculated based on sink-float test results.

It is apparent from the Table 5.1 that, the amount of near gravity particles in all of these ores are more than 10% in most of the size fractions. therefore these ores are relatively problematic to beneficiate with mentioned gravity methods and using of heavy medium cyclone is inevitable for their beneficiation.

In this part of the thesis, the necessary calculation for the design of a heavy medium cyclone plant are given. The iron ore was considered for the design and all of the calculations were done according to method described in the literature as an example [20].

As described before iron ore sample was the tailing of low intensity magnetic separation plant which was designed to work with 250 t/h feed capacity and the flow-rate was calculated to be approximately 50 t/h. therefore heavy medium cyclone plant was considered to design with 50 t/h dry feed capacity.

Table 5.2 shows necessary information for the plant design which provided by feed characterization and simulation results.

Table 5.1. The amount of near gravity particles for different ores

Iron Ore	Size Fraction (mm)	Cum. Sinks Weight (%)		Difference
		- 0.1 of Separation Density	+0.1 of Separation Density	
	-9.5+4.75	51.5	40.78	10.63
	-4.75+1.18	54	45	9
	-1.18+0.212	61	49.36	11.64
Manganese ore	-16+5	69	55.4	13.6
	-5+1	63.75	51	12.75
	-1+0.2	64	53.5	10.5
Chromite Ore	-1.18+0.425	33.46	20.08	13.38
	-0.425+0.212	71.62	61.55	10.07

Table 5.2. Required information for plant design

	t/h Average	t/h maximum	sp.gr.	dm (mm)
Feed	50	50	3.17	3.5
Cyclone Feed	41.25	41.25	3.16	4.13
Overflow	22.23	50	2.78	4.33
Underflow	18.92	40	3.61	3.9
-0.5mm	10	10	3.22	

- **Desliming water requirements:**

The volume of solids is

$$50 \div 3.17 = 15.77 \text{ m}^3 / \text{h}$$

And required feed solids concentration for efficient sizing is 30% so total volume of slurry to sieve is

$$15.77 \div 0.3 = 52.57 \text{ m}^3 / \text{h}$$

Therefore water required for desliming is equal to

$$52.57 - 15.77 = 36.80 \text{ m}^3/\text{h}$$

- **Sieve bend**

Volume of -0.5mm solids:

$$10 \div 3.25 = 3.10 \text{ m}^3/\text{h}$$

Total volume to pass through the sieve bend:

$$3.10 + 36.80(\text{water}) = 39.90 \text{ m}^3/\text{h}$$

$$\text{Sieve capacity (1.5mm w/w profile)} = 112.5 \text{ m}^3/\text{h}/\text{m}^2$$

Therefore required sieve area is equal to:

$$39.90 \div 112.5 = 0.35 \text{ m}^2$$

- **Desliming Screen**

Maximum screen capacity was calculated according to following formula [20]:

$$\text{Screen Capacity} = 19((\text{dm})^2 \times (\text{sp.gr.})^2)^{0.33} \text{ (t/h/m)}$$

$$\text{Screen Capacity} = 103.53 \text{ t/h/m}$$

Hence required width is equal to (standard length is 4.88m):

$$41.25 \div 103.53 = 0.39 \text{ m}$$

- **Heavy medium cyclone**

According to simulations separation density is 3.1 gr/cm^3 which can be obtained with a medium with specific gravity of 2.9.

Medium to ore volumetric ratio is equal to 4:1

Considering this proportion, following calculations was done:

$$\text{Required ferrosilicon (sp.gr. 6.8) is equal to } 155 \text{ t/h (22.79 m}^3/\text{h)}$$

$$\text{Required clean water is equal to } 40 \text{ t/h}$$

$$\text{Volume of cyclone feed is equal to } 13.05 \text{ m}^3/\text{h}$$

Circulating medium volume is equal to

$$22.79 + 40 = \mathbf{62.79 \text{ m}^3/\text{h}}$$

According to literature [20] 400mm DSM standard cyclone can handle this capacity.

- **Overflow and Underflow sieve bend, drain and rinse screen**

The capacity of drain and rinse screens could be calculated with the following formula [20]:

$$\begin{aligned} \text{Capacity} &= 12 * ((dm)^2 * (sp. gr)^2)^{0.33} \text{ t/h/m} \\ &= 61.99 \text{ t/h/m} \end{aligned}$$

So required width is:

$$50 \div 61.99 = 0.8m \text{ (Standard length is 4.88m)}$$

Sieve to pass 80% of circulating medium

$$62.79 * 0.8 = 50.23 \text{ m}^3/h$$

Sieve capacity (1.5 mm w/w profile) is equal to 135 m³/h/m²

So required sieve area is equal to 0.37 m²

The same calculations were done for underflow drain and rinse screen and sieve bend to:

Required drain and rinse screen width: 0.58 m

Sieve area to handle 20% of circulating medium is equal to 0.1 m²

- **Medium Circuit**

The capacity of circulating medium pump in the worst condition can be calculated by:

capacity of circulating medium pump = circulating media volume + 25

$$= 62.79 + 25$$

$$= 87.79 \text{ m}^3/h$$

The minimum volume stored in the circulating media tank is:

$$2 \times (87.79 \div 60) = 2.92 \text{ m}^3$$

The diameter of pump tube calculated by following formula:

$$= 3.75 \times 1.25 \times (\text{circulating medium})^{0.5}$$

$$= 341.73 \text{ mm}$$

Spray water requirements:

Using a total of 32 m³/h/m width of screen:

Overflow spray water requirement = $0.8 * 32 = 25.6 \text{ m}^3/\text{h}$

underflow spray water requirement = $0.58 * 32 = 18.56 \text{ m}^3/\text{h}$

Total spray water requirement = $44.16 \text{ m}^3/\text{h}$

So the dilute medium's capacity has to be at least $70 \text{ m}^3/\text{h}$ ($44.16+25=69.16$) and the volume of dilute media tank calculated by:

$$2 \times (70 \div 60) = 2.33 \text{ m}^3$$

Primary separator selection:

According to literature [20], 2.13 m 2.18 wide x 914 mm diameter can handle $70 \text{ m}^3/\text{h}$ diluted medium pulp.

Thickening cyclone:

A cyclone with 250 mm diameter can handle the required capacity.

Secondary magnetic separator:

The cyclone overflow is directed to the primary spray water on the product drain and rinse screens (about 75% of cyclone feed capacity). Therefore the underflow capacity of the cyclone is equal to:

$70 \times 0.25 = 17.5 \text{ m}^3/\text{h}$ and this capacity can handle with a magnetic separator with 914mm wide and 914 mm diameter [20].

Figure 5.1 illustrates the schematic flowsheet of heavy medium cyclone plant which designed for iron ore.

6 Conclusions and Future Work

6.1 Conclusions

In view of the results obtained in this research the following conclusions are derived;

- In the case of iron ore, mineralogical analysis showed that hematite and goethite are the major iron minerals of the ore. Following sink-float tests, simulation results showed that obtaining a concentrate with up to 55% Fe grade and about 80% Fe recovery is possible for a heavy medium cyclone plant with 3.1 g/cm³ separation density, -9.5mm +0.5mm feed size and 50 t/h feed capacity.
- Manganese ore that contains Pyrolusite (MnO₂) as a major manganese mineral, was studied and simulation attempts showed that obtaining a concentrate with up to 38% Mn grade and about 92% Mn recovery is possible for a heavy medium cyclone plant with 2.9 g/cm³ separation density, -16mm +0.5mm feed size and 20 t/h feed capacity.
- In the case of chromite ore which contains of chromite (FeCr₂O₄) and magnesiochromite ((Mg.Fe)(Cr.Al)₂O₄) as major chromium minerals, simulation results showed that obtaining a concentrate with up to 45% Cr₂O₃ grade and about 52% Cr₂O₃ recovery is possible for a heavy medium cyclone plant with 3.5 g/cm³ separation density, -1.18mm +0.2mm feed size and 10 t/h feed capacity. It seems that low degree of liberation and existence of high amount of near gravity materials in the feed are the major reasons of low recovery.

6.2 Future Work

Obviously this research is the starting point to investigate the feasibility of using heavy medium cyclone plants for beneficiation of non-coal ores like iron, manganese, chromite and etc. in Turkey. Having precise and complete information about heavy medium circuit behavior, it is necessary to build both laboratory and pilot scale plants to test the validation of used models and this could be the future of this research.

REFERENCES

- [1] Aplan, F. F., Heavy media separations, *SME Mineral Processing Handbook Volume 1*, SME, 1–16, **1985**.
- [2] Kruttschnitt, J. and Road, I., Some causes of medium loss in dense medium plants, *Minerals Engineering*, vol. 8, no. 6, 659–678, **1995**.
- [3] Palowitch, E. R., Deurbrouck, A. W., Torak, E., and Akers, D. J., Wet coarse particle concentration, *Coal preparation*, 271–300, **1990**.
- [4] Wills, B. A. and Napier-Munn, T. J., *Mineral Processing Technology*. Elsevier Science & Technology Books, **2006**.
- [5] King, I., The Latest Developments in Iron Ore Processing, <http://www.mintek.co.za/Mintek75/Proceedings/K01-King.pdf>. (March, **2014**)
- [6] Mcculloch, W. E., Copper ore preconcentration by heavy media separation for reduced capital and operating costs, *Miner. Met. Mater. Society*, vol. 2, **1999**.
- [7] Bird, B. M., Mitchell, D. R., and Smith, F. E., *Dense-media Processes*. AIME, 458–496, **1943**.
- [8] Osborne, D., Global Challenge for Coal Technology - with the End User in Mind, *South African Coal Preparation Society Conference*, **2005**.
- [9] Chen, J., *Pc-based application od dense media cyclone fundamental simulations*, Master of science thesis, New south wales University, School of Materials Science and Engineering, **2010**.
- [10] Gupta, A. and Yan, D. S., Mineral Processing Design and Operations An Introduction, *Elsevier*, p. 693, **2006**.
- [11] Walker, M., A new method for the commercial separation of particles of differing densities using magnetic fluids, *XVth International Mineral Processing Congress*, 307–312, **1985**.
- [12] Rhodes, D., Hall, S., and Miles, N., Density separations in heavy inorganic liquid suspensions, *XVII International Mineral Processing Congress*, 375–377, **1993**.
- [13] Grobler, P., Production and application of ferrosilicon in the mining industry, *DMS and gravity concentration ;operations and technology in Sough Africa*, 153–162, **2006**.
- [14] Collins, B., Napier-Munn, T. J., and Sciarone, M., The production , properties , and selection of ferrosilicon powders for heavy-medium separation,”*Journal. South African Inst. Min. Metall.*, 103–115, **1974**.
- [15] Napier-Munn, T. J., Dunglison, M., and Shi, F., Rheology of ferrosilicon dense medium suspensions, *Miner. Process. Extr. Metall. Rev.*, vol. 20, 183–199, **1999**.
- [16] Bozatto, P., Bevilacqua, P., and Ferrara, G., Static and dynamic stability in dense medium separation processes,”*Miner. Process. Extr. Metall. Rev.*, vol. 20, 197–214, **1999**.
- [17] Grobler, J. D., Sandenbergh, R. F., and Pistorius, P. C., The stability of ferrosilicon dense medium suspensions, *Journal. South African Inst. Min. Metall.*, pp. 83–86, **2002**.

- [18] Robinson, F. P. and Du PLESSIS, D., Polarization and corrosion of ferrosilicon alloys for iron ore beneficiation media., *Corrosion*, vol. 22, 117–131, **1966**.
- [19] Schmeiser, K. and Uhle, K., Calculation of the magnetic condition of ferrosilicon powder in a heavy medium., *Erzmetall*, vol. 15, 247–251, **1962**.
- [20] Symonds, D. F. and Malbon, S., Selection and sizing of heavy media equipment, *Mineral Processing Plant Design, Practice, and Control Proceedings*, Volume 1, SME, 1011–1033, **2002**.
- [21] Chastont, I. R. M. and Napier-Munn, T. J., Design and operation of dense-medium cyclone plants for the recovery of diamonds in Africa, *Journal. South African Inst. Min. Metall.*, 120–121, **1974**.
- [22] Reeves, R., Types and characteristics of heavy-media separators and flowsheets, *Mineral Processing Plant Design, Practice, and Control Proceedings*, New York, 962–977, **2002**.
- [23] De Korte, J., Index of South African coal preparation plants. <http://www.sacoalprep.co.za/information.htm>. (February, **2014**).
- [24] Magwai, M. K., *Spigot Capacity of Dense Medium Cyclones*, Master of Engineering thesis, University of Pretoria, Pretoria, **2007**.
- [25] King, R. P. and Juckes, A.,leaning of fine coals by dense-medium hydrocyclone, *Powder Technol.*, vol. 40, 147–160, **1984**.
- [26] Svarovsky, L., *Hydrocyclones*, PA. Lancaster: Technomic Publishing Inc, **1984**.
- [27] Scott, I. A., Particle size effect in ore preconcentration using dense medium cyclones, Master of Science degree Thesis, Queensland University, Queensland, **1985**.
- [28] Bradley, D., *The Hydrocyclones*, 1st ed. Oxford, United Kingdom: Oxford, **1965**.
- [29] Schubert, H. and Neese, T., The role of turbulence in wet classification, *10th International Mineral Processing Congress*, 213–239, **1973**.
- [30] Napier-Munn, T. J., The influence of medium viscosity in on the density separation of minerals in cyclone, *INTERNATIONAL CONFERENCES OF HYDROCYCLONES*, 68–82, **1980**.
- [31] Michell, S. J., *Fluid and particle mechanics*, 1st ed. Oxford: Pergamon press, **1970**.
- [32] Bookless, T., Dense Medium Cyclone Geometry and Materials of Construction, *Tenth DMS Powders Conference*, 1–23, **2008**.
- [33] Koen, F., Cyclone Pressure Control at Namaqualand Mines, *Seventh Samancor Symposium on Dense Media Separation*, **2000**.
- [34] Napier-Munn, T. J., *Dense Medium Cyclones in Diamond Recovery*, University of the Witwatersrand, **1977**.
- [35] Engelbrecht, J., The effect of changes in design variables on Dense Medium Separation, *Fourth Samancor Symposium on Dense Media Separation*, **1990**.
- [36] Mengelers, J., The Influence of Cyclone Diameter on Separating Performance and Economy, *IX International Coal Preparation Congress*, **1982**.
- [37] Mular, A. L. and Jull, N., The Selection of Cyclone Classifiers, Pumps, and Pump Boxes for Grinding Circuits, *Mineral Processing Plant Design*, Mular, A. L. and Bhappu, B., Eds. AIME, **1978**.

- [38] Magwai, M. K. and Bosman, J., The effect of cyclone geometry and operating conditions on spigot capacity of dense medium cyclones, *Int. J. Miner. Process.*, vol. 86, no. 1–4, 94–103, **2008**.
- [39] Anon, Guide to the calculation of h.m. cyclone and w.o cyclone plants, *Stamicarbon bv, Dutch State Mines*, **1985**.
- [40] Bevilacqua, P. and Zanin, M., A simulation procedure for the design of the dense medium separation circuits, *The Eighth Samancor Symposium on Dense Media*, 1–13, **2002**.
- [41] Wood, C. J., *A performance model for coal-washing dense medium cyclones*, Ph.D Thesis, University of Queensland, Australia, **1990**.
- [42] Scott, I. A. and Napier-Munn, T. J., A dense medium cuclone model for simulation, **1990**.
- [43] Chu, K. W., Wang, B., Yu, a. B., Vince, a., Barnett, G. D., and Barnett, P. J., CFD–DEM study of the effect of particle density distribution on the multiphase flow and performance of dense medium cyclone, *Miner. Eng.*, vol. 22, no. 11, 893–909, **2009**.
- [44] Burt, R. O., *Gravity Concentration Technology*. Amesterdam-Oxford-New York-Tokyo: Elsevier, **1984**.
- [45] Anon, The Role of Heavy Media Separation- a Survey of Modern Applications, *Eng. Min. J*, vol. 164, no. 5, 80–87, **1963**.
- [46] Krige, J., Heavy medium separation at Iscor 's Sishen, *The AuslMM Southern Queensland Branch, Dense Medium Operators' Conference*, 65–73, **1987**.
- [47] Dardisl, K. A. and Mack, J., “The design and commissioning of the Argyly diamonds mines heavy medium, *The AuslMM Southern Queensland Branch, Dense Medium Operators' Conference*, 17–31, **1987**.
- [48] Nafziger, R. H., A review of the deposits and beneficiation of lower-grade chromite, *J. S. Afr. Inst. Min. Met.*, 205–226, **1982**.
- [49] Mousoulos, L. and Papadopoulos, M. Z., *Gravity concentration of Troodos chromites*, Cyprus, **1975**.
- [50] Ryan, P. J., A review of the fluorspar-mining industry in South Africa, *12th CMMI Congress*, 228–247, **1982**.
- [51] Anon, Buffalo fluorspar: Serving the strategic needs of western world, *South African Min. World*, vol. 5, 26–31, **1983**.
- [52] Ellison, T. D., “Manganese,” *Min. Annu. Rev.*, 67–69, **1983**.
- [53] Sassos, M. P., Manganese: Gemco Mines Huge Resources at Groote Eylandt, *Eng. Min. J*, 57–58, **1984**.
- [54] McNiel, M., Panasqueira - The largest mine in portugal, *World Min.*, 52–55, **1982**.
- [55] Overbeek, P. W., The development of Andalusite industry in South Africa, *12th CMMI Congress*, 505–513, **1982**.
- [56] Carroll, J. and Matthews, G. W., Silimanite minerals as raw materials for refractories, *Minerals in the refacractoriesnindustry - assessing the decade ahead*, 47–54, **1983**.
- [57] Koroznikova, L., Klutke, C., Knight, S. M. C., and Hall, S., The use of low-toxic heavy suspensions in mineral sands evaluation and zircon fractionation, *The 6th*

International Heavy Minerals Conference, The Southern African Institute of Mining and Metallurgy, **2007**.

- [58] Orhan, E., Gülsoy, Ö., and Ergün, L., *Coal Washing Plant Simulator*. Hacettepe University, Department of Mining Engineering, Ankara, Turkey, **2010**.

CIRRUCILUM VITAE

Credentials:

Name, Surname: AHAD AGHLMANDI HARZANAGH

Place of Birth: TABRIZ, IRAN

Marital Status: Married

E-mail: ahad.aghlmandi@gmail.com, ahad@hacettepe.edu.tr

Address: Eryaman, Şehit Osman Avcı Mahallesi, 48.sokak, Selvi Apt, No: 19

Education:

High School: Ferdosi, Tabriz

B.Sc. (2002-2006): UrmiaUniversity, Faculty of Engineering, Mining Division

M.Sc. (2012-2014): Hacettepe University, Faculty of Engineering, Mining Engineering
Department

Foreign Language:

English (Advanced)

Turkish (Advanced)

Persian (Advanced)

Arabic (Intermediate)

Professional Experience:

Geo-technical chief in ITP, Tehran, Iran (2008-2014)

Areas of Experiences: Mineral Processing, Mineral Economy, Applied Mineralogy and
Geo-technic

Development Projects from the Thesis:

-

Publications from the Thesis:

-

Presentation from the Thesis:

-